Calcium – Friend or Foe:

An investigation of stability and solubility properties of a recombinant *Bacillus halmapalus* α-amylase

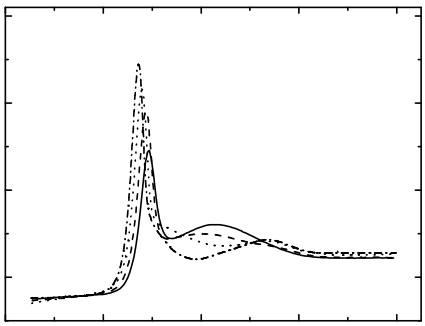

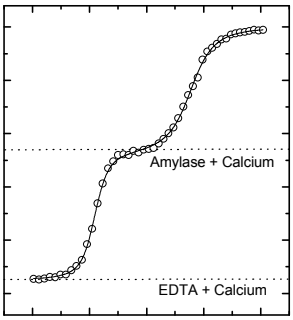

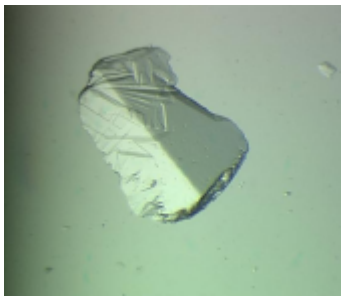

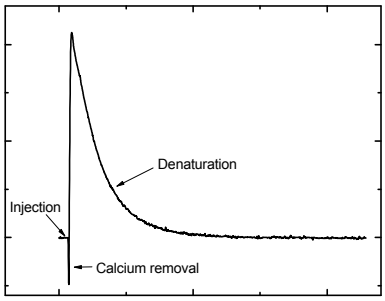

Anders Dybdal Nielsen
Ph.D. Thesis, 2003

Department of Life Sciences and Chemistry
Roskilde University, Denmark

Calcium – Friend or Foe:

An investigation of stability and solubility properties of a recombinant *Bacillus halmapalus* α-amylase

Anders Dybdal Nielsen
Ph.D. Thesis, 2003

This Ph.D. project has been carried out in collaboration with Novozymes A/S and Roskilde University (RUC) as an industrial Ph.D. project (EF 862) administered by the Committee on Industrial Ph.D. Fellowship under the Danish Academy of Technical Sciences (ATV) and supported by the Danish Agency for Trade and Industry.

Preface

This dissertation has been submitted for the partial fulfillment of the requirements for obtaining the Danish Ph.D. degree. The project has been carried out in collaboration with Novozymes A/S and Roskilde University (RUC) as an industrial Ph.D. project (EF 862) administered by the Committee on Industrial Ph.D. Fellowship under the Danish Academy of Technical Sciences (ATV) and supported by the Danish Agency for Trade and Industry. The experimental work of this project has been carried out at Department of Life Sciences and Chemistry, Roskilde University; Protein Biochemistry, Novozymes and Marshall Space Flight Center; NASA (USA), from April 2000 to March 2003, under supervision of Professor Peter Westh and Director Claus C. Fuglsang.

I am thankful to all the people who contributed with invaluable support, inspiration and assistance during this project. First of all, I wish to thank my supervisors Peter Westh and Claus C. Fuglsang, for their enthusiasm, continuous support and setting up a wide framework for my work. Several people at Novozymes have contributed to this project. In particular, the input and support from Kim Borch, especially during the startup of this project is highly appreciated. Throughout this project, I have had the excellent opportunity to obtain invaluable information about α-amylases from Dr. Svend Kaasgaard and Carsten Andersen. In addition, I would like to express my appreciation to all colleagues in Protein Chemistry for providing me with good working conditions. At RUC I would like to thank Bodil Larsen for excellent technical assistance and Karin Liltorp for support.

The solubility and circular dichroism studies in this project have been carried out during the three months I spent at Marshall Space Flight Center, NASA, Huntsville, USA. In this context, I am deeply indebted to Dr. Marc L. Pusey, who guided me into the field of protein solubility and crystallization and showed me exceptional hospitality during my stay. In addition, the people in his laboratory are thanked for their help and for making my stay in Hunstville perfect and unforgettable. In particular, I would like to thank Eva Bernhardsdottir, Boris Stanojev, Jennifer Dowell, Nicole Laxman and Dr. Marc van der Woerd.

Finally, I thank Charlotte Hubert for her never failing support and invaluable inputs.

Anders Dybdal Nielsen

Ballerup, April, 2003

Contents

Summary

α-amylases of *Bacillus* origin are widely used in diverse starch modifying processes, and the academic and industrial interest in these enzymes is reflected by the extensive literature. Like any other enzyme, successful industrial use of an α-amylase requires that it is sufficiently active, stable and soluble under relevant application conditions, e.g. at high temperatures and pH extremes. In this study, we characterize the stability and solubility of a recombinant *Bacillus halmapalus* α-amylase (BHA) for which published information at present is sparse. In addition, calorimetric methodologies to facilitate the characterization of proteins that bind metal ions have been developed and evaluated.

Determination of binding parameters for metal ions to proteins typically requires preceding steps to remove protein-bound metal ions. This removal of bound metal ions often leads to decreased stability and inactivation of the protein. Therefore, two isothermal titration calorimetric (ITC) procedures that eliminate separate metal ion removal steps have been developed. The concept of the procedures is to add either excess metal ion or chelator to a protein and subsequently titrate with chelator or metal ion, respectively. This makes it possible in a single experimental trial to obtain both chelator-metal ion and protein-metal ion binding parameters as a result of different thermodynamic "fingerprints" of chelator and protein. The binding models and corresponding regression routines have been created and evaluated on mixtures of calcium chelators and calcium ions, where they proved to account satisfactorily for the obtained binding isotherms. The procedures were used to study the calcium binding properties of BHA. An apparent affinity of 10^5-10^6 M^{-1} was obtained and the enthalpy and entropy changes upon binding suggested that a dehydration process contribute significantly to the binding.

The effect of temperature and calcium ions on the stability of BHA has been investigated using calorimetry and circular dichroism spectroscopy (CD). Differential scanning calorimetric (DSC) and CD data show that BHA denatures irreversibly and that the apparent denaturation temperature (T_m) depends considerably on the calcium ion activity. The latter is clearly demonstrated by a difference in T_m of up to 45°C between BHA in the presence of excess calcium chelator and calcium ions. The difference in thermal stability with and without calcium ions has been utilized to develop an ITC procedure that allows simultaneous determination of kinetic parameters and enthalpy changes of denaturation of calcium depleted enzyme. Combination of kinetic data and calcium binding constants at different temperatures

provided basis for estimation of the kinetic stability as a function of temperature and concentration of calcium ions. This has been done using a simple model for irreversible denaturation of BHA. The stabilizing effect of calcium ions was further studied by DSC measurements with different concentrations of calcium chelator. This provided information about the thermal stability of BHA with varying degrees of saturated calcium binding sites, i.e. the stability of different BHA:Ca complexes. Combined interpretation of these data and structural data on homologous *Bacillus* α-amylases suggested a model describing the mechanism of BHA inactivation in relation to temperature and number of bound calcium ions. The model accounts for the irreversible thermal denaturation of different BHA:Ca complexes, a temperature induced reversible structural change and calcium binding equilibria.

The study also addressed the solubility and crystallizing properties of BHA. A micro-column method, where columns were packed with protein crystals, was used to determine the equilibrium solubility of BHA. A low solubility and complex temperature dependence were observed. Thus, the lowest solubility (~0.2 mg/mL) was observed at 35-40°C but decrease or increase of the temperature resulted in increased solubility (~0.7 mg/mL). No pronounced effect of calcium ions, in the range 5-25 mM, on the solubility was found. However, calcium ions apparently enhance the rate of crystallization and the tendency of BHA to aggregate.

Finally, the concept of thermodynamic “fingerprinting” is discussed in general and in relation to the calorimetric procedures applied in this study. It is suggested that the concept has a great potential to expand the applicability of microcalorimetry in analysis of complex and multi-component systems.

Dansk resumé

α-amylaser af *Bacillus* oprindelse er meget brugt i forskellige stivelsesmodificerende processer og den akademiske og industrielle interesse i disse enzymer afspejles i den omfattende litteratur. Ligesom for ethvert andet enzym, kræver industriel anvendelse af en α-amylase, at denne er tilstrækkeligt aktiv, stabil og opløselig under anvendelsesrelevante betingelser, eksempelvis ved høj temperatur og pH ekstremer. I dette studie karakteriseres stabiliteten og opløseligheden af en rekombinant *Bacillus halmapalus* α-amylase (BHA), for hvilken publiceret information er sparsom på nuværende tidspunkt. Yderligere er der udviklet kalorimetriske metoder, som gør karakteriseringen af proteiner, som binder metalioner, simplere.

Bestemmelse af parametre for metalioners binding til proteiner kræver typisk indledende trin for at fjerne proteinbundne metalioner. Denne fjernelse af bundne metalioner fører ofte til sænket stabilitet og inaktivering af proteinet. Derfor er to isotermisk titrer kalorimetriske (ITC) procedurer udviklet, som gør det muligt at undgå forudgående trin til fjernelse af metalioner. Konceptet bag procedurerne er at tilsætte overskud af enten metalion eller chelator til et protein og efterfølgende titrere med henholdsvis chelator eller metalion. Dette gør det muligt i et enkelt eksperiment at opnå både chelator-metalion og protein-metalion bindingsparametre, på grund af de forskellige termodynamiske "fingeraftryk" for chelator og protein. Bindingsmodeller og tilhørende regressionsrutiner er blevet produceret og evalueret på blandinger af calciumchelatorer og -ioner, hvor de viste sig på tilfredsstillende måde at redegøre for de observerede bindingsisotermer. Procedurerne blev anvendt til at undersøge calciumbindings egenskaber for BHA. En tilsyneladende affinitet i størrelsesorden 10^5-10^6 M^{-1} blev fundet, og både ændringerne i enthalpi og entropi tydede på, at dehydrering er en vigtig del af bindingsprocessen.

Effekten af temperatur og calciumioner på stabiliteten af BHA er blevet undersøgt ved kalorimetri og cirkulær dikroisme spektroskopi (CD). Differentiel skanning kalorimetri (DSC) og CD data viste, at BHA denaturerer irreversibelt, og at den tilsyneladende denatureringstemperatur (T_m) afhænger betydeligt af calciumion aktiviteten. Sidstnævnte er tydeligt demonstreret ved en forskel i T_m på op til 45°C mellem BHA, ved tilstedeværelse af calciumchelator og -ioner i overskud. Forskellen i den termiske stabilitet med og uden calciumioner er blevet anvendt til at udvikle en ITC procedure, som giver mulighed for samtidig bestemmelse af kinetiske parametre og enthalpi ændringer ved denaturering af calcium "frit" enzym. Kombination af kinetiske data og calciumbindingskonstanter ved forskellige temperaturer gav

mulighed for at estimere den kinetiske stabilitet som funktion af temperatur og calciumionkoncentrationen. Dette er blevet gjort ved hjælp af en simpel model for irreversibel denaturering af BHA. Den stabiliserende effekt af calciumioner blev yderligere studeret gennem DSC målinger ved forskellige koncentrationer af calciumchelator. Dette gav information om den termiske stabilitet af BHA med varierende grad af mættede calciumbindingssites, det vil sige stabiliteten af forskellige BHA:Ca komplekser. Kombineret fortolkning af disse data og strukturelle data for homologe *Bacillus* α-amylaser blev anvendt til at foreslå en mekanisme for inaktivering af BHA i relation til temperatur og antallet af bundne calciumioner. Denne model redegør for irreversibel denaturering af forskellige BHA:Ca komplekser, en temperatur induceret reversibel strukturel ændring og calciumbindingsligevægte.

I dette studie er også opløseligheden og krystallisationsegenskaberne for BHA blevet undersøgt. En mikrokolonnemetode, hvor kolonner var pakket med protein krystaller, blev anvendt til at bestemme ligevægtsopløseligheden af BHA. En lav opløselighed og kompleks temperaturafhængighed blev observeret. Det vil sige, at den laveste opløselighed (~0,2 mg/mL) blev observeret ved 35-40°C, men sænkning eller forøgelse af temperaturen resulterede i en højere opløselighed (~0,7 mg/mL). Ingen tydelig effekt af calciumioner, i området 5-25 mM, på opløseligheden blev fundet. Dog øger calciumioner tilsyneladende krystallisationshastigheden og BHAs tilbøjelighed til at aggregere.

Endelig diskuteres termodynamisk fingeraftrykskonceptet alment og i relation til de kalorimetriske procedurer, anvendt i dette studie. Det foreslås, at konceptet har et stort potentiale for at udvide anvendelsen af mikrokalorimetri ved analyse af komplekse og multi-komponent systemer.

1

Introduction

1.1 Industrial use of enzymes

A limiting factor of successful use of industrial enzymes is that enzymes often are not sufficiently catalytically active, stable or soluble under the relevant conditions, of production, storage and application. The conditions are defined by parameters such as temperature, pH, salts and co-solutes. In search for an enzyme candidate one might screen microbial organisms, which live in environments similar to the application conditions, for useful enzymes (Marrs et al., 1999;Niehaus et al., 1999). Thus, if high thermal stability is the main requirement hyperthermophiles, i.e. organisms that are able to grow at temperatures up to 100°C, may be a possible source (Bertoldo and Antranikian, 2001), but also non-thermophiles express relatively stable enzymes and are therefore potential sources. Further optimization of the enzyme can be achieved by protein engineering. However, rational protein engineering requires detailed knowledge of the structural and physical properties, including the ability to interact with co-solutes.

The literature provides numerous examples how co-solutes, such as metal ions, salts and carbohydrates, influence the solubility and/or the stability of proteins (Schein, 1990;Timasheff, 1998;Baldwin, 1996). The complexity of the problem is illustrated by the effect of $MgCl_2$ on the solubility of globular proteins, since addition of the salt increases the solubility of bovine serum albumin (BSA) but reduces the solubility of lysozyme (Arakawa et al., 1990). The effect of specifically binding ligands, such as metal ions, is less ambiguous. Thus, binding of ligands, to sites that only exist in the native structure, increase the thermal stability of proteins. This is clearly demonstrated by the effect of calcium ions on the thermal stability of bovine α-lactalbumin where a ~40°C difference between the calcium depleted and non-depleted protein have been observed (Hendrix et al., 2000). Further stabilization (~15°C) could be achieved by adding excess calcium. Successful stabilization of proteins by construction or modification of metal ion binding sites, using protein engineering, has been reported for diverse protein systems (Muheim et al., 1993;Muller and Skerra, 1994;Braxton and Wells, 1992).

Thus, introduction of a calcium binding site in human lysozyme resulted in a significant structural stabilization corresponding to a ~9°C higher unfolding temperature compared to the wild-type lysozyme in the presence of excess calcium ions (Kuroki et al., 1989;Kuroki and Yutani, 1998). In addition, a two fold higher enzymatic activity towards glycol chitin at 40°C was obtained.

Combination of structural and thermodynamic information provide basis for a rational understanding of the mechanisms responsible for the effect of ligands and co-solutes on proteins. A better understanding provide basis for qualitative protein engineering and construction of models to predict the stability and solubility of a protein under relevant conditions.

1.2 α-amylases from *Bacillus* species

α-amylases (α-1,4 glucan-4-glucanohydrolase, EC 3.2.1.1) are amylolytic enzymes that are widely used in diverse industrial processes including bread improvement, alcohol production, textile desizing, starch liquefaction and detergent applications (Kirk et al., 2002;Vihinen and Mäntsälä, 1989;Guzmán-Maldonado and Paredes, 1995;van der Maarel et al., 2002). The processes take place under quite different physical and chemical, and often harsh, conditions and therefore, the required properties of an α-amylase depend on the specific application. One example is starch liquefaction, where the α-amylase is added to convert insoluble starch into more soluble maltodextrins for the subsequent saccharification process. This process is carried out at high temperature (95-105°C) and acidic pH (~6), where the enzyme must be active and stable for 1-2 h. Lowering the pH further to 4.5 is advantageous due to, e.g., reduced formation of by-products in the end of the entire process. Excess calcium is added to increase the protein stability (Bisgaard-Frantzen et al., 1999). Another example is the detergent industry, where α-amylases are used to remove starch containing stains on fabrics. This requires that the enzyme must be active and stable at alkaline pH (up to ~10.5) and at washing temperatures (typically 25-60°C). Furthermore, the α-amylase must tolerate presence of high levels of surfactants (denaturants), bleaching agents that may oxidize the enzyme and be independent of calcium because chelators are added to bind free calcium (Bisgaard-Frantzen et al., 1999).

The α-amylases from *Bacillus* species *licheniformis* (BLA), *amyloliquefaciens* (BAA) and *stearothermophillus* (BStA), and derived protein engineered variants, are among the most widely used industrially and studied α-amylases. These α-amylases are highly homologous with respect to primary and tertiary structure (Declerck et al., 2002). Hence, the sequence similarity between: BLA and BAA is 80%, BLA and BStA is 65% and BStA and BAA is 66% (Suvd et al., 2001;Yuuki et al., 1985). The tree-dimensional structure of the amylases is also predicted to be similar (Machius et al., 1995;Hwang et al., 1997). This is evident when the crystal structures of BLA and BStA are compared (see Fig. 1.1). Both structures are characterized by three distinct domains: a central core domain, termed domain A, containing a $(\beta/\alpha)_8$ barrel, domain B, a long complex loop protruding from the third strand and third helix of the barrel and the C-terminal, domain C, which contain a Greek key motif (Suvd et al., 2001;Machius et al., 1998;Hwang et al., 1997). The crystal structure of BAA is not yet available. However, the structure of a BAA/BLA chimera, constructed from the genes encoding for BAA (~60%) and BLA (~40%), is very similar to that of BLA (Fig. 1.1) (Brzozowski et al., 2000).

α-amylases require calcium to maintain their structural integrity (Vallee et al., 1959;Vihinen and Mäntsälä, 1989) and removal result in decreased thermostability and enzymatic activity (Violet and Meunier, 1989). All known α-amylases contain a conserved calcium binding site, CaI, which is located at the interface between the A and B domains (Boel et al., 1990;Machius et al., 1998;Machius et al., 1995). The binding affinity is high (Vallee et al., 1959) which is illustrated by a binding constant of $2 \cdot 10^{11}$ M^{-1} reported for pig pancreatic α-amylase (Levitzki and Steer, 1974). Two additional calcium binding sites have been identified in BLA (Machius et al., 1998) and BStA (Suvd et al., 2001). CaII is located in close proximity to CaI and the two calcium ions form a characteristic triad with one sodium ion (Ca-Na-Ca, see Fig. 1.1). Mutations in the region surrounding CaI and CaII resulted in collapse of the thermostability of BLA (Declerck et al., 2000;Declerck et al., 2002). A third calcium binding site (CaIII) is situated at the interface between domains A and C where it acts as a bridging ion (see Fig. 1.1). CaI and CaII were also identified in the BAA/BLA chimera where the residues involved originated from BAA (Brzozowski et al., 2000). A calcium binding site corresponding to CaIII was also identified as well as a fourth binding

site, which also likely binds calcium ions. The location of the calcium binding sites is illustrated in Fig. 1.1.

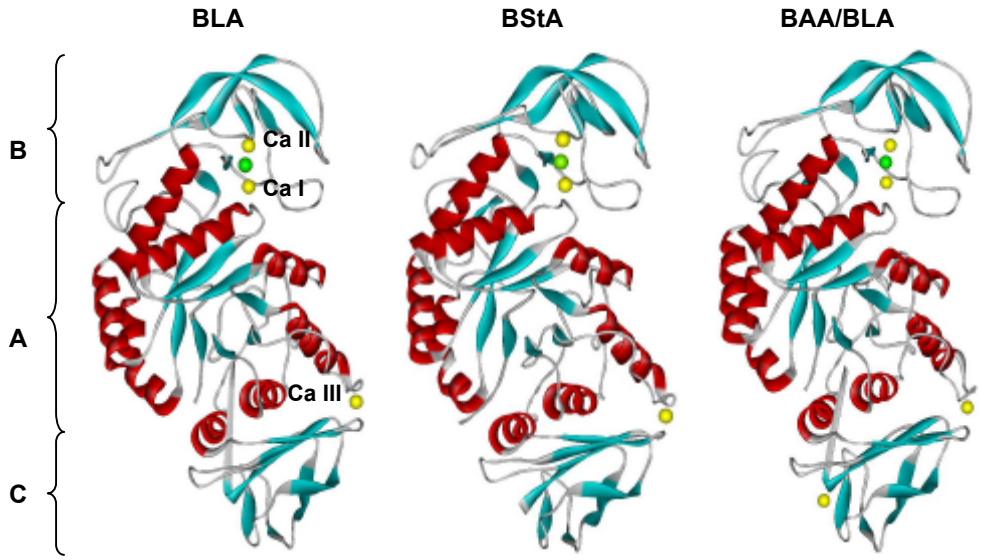

Fig. 1.1: Solid ribbon models of BLA, BStA and BAA/BLA chimera. The models have been constructed using WebLab VieverLite 4.0, Molecular Simulations Inc., using the files 1BLI (BLA with the following mutations N190F, Q264S and N265Y, (Machius et al., 1998)), 1HVX (BStA, (Suvd et al., 2001)) and 1E3X (BAA/BLA chimera, residues 1-300 of BAA and residues 301-483 of BLA, (Brzozowski et al., 2000)) from the Protein Data Bank. The yellow and green spheres represent the location of calcium (CaI, CaII and CaIII) and sodium ion binding sites, respectively. A, B and C indicates the location of the domains in the structure of the *Bacillus* α-amylases.

Despite the considerable homology between the *Bacillus* α-amylases, they possess quite diverse physio-chemical properties. For example they display significant differences in their thermal resistance, with half-lifes at 90°C of 2, 50 and 270 min. for BAA, BStA and BLA respectively (Tomazic and Klibanov, 1988b). It has been suggested that thermal inactivation of *Bacillus* α-amylases is a two step process, involving reversible unfolding followed by an irreversible conformational or covalent change (Tomazic and Klibanov, 1988a;Tomazic and Klibanov, 1988b;Violet and Meunier, 1989). Other models of thermal inactivation incorporate the effect of calcium ions, and it has been proposed that the first step includes a reversible dissociation of calcium ions from the native enzyme, followed

by irreversible denaturation at high temperatures (Lecker and Khan, 1998;Lecker and Khan, 1996;Tanaka and Hoshino, 2002;Bush et al., 1989).

1.3 Outline and purpose of the Thesis

Stability and solubility of a recombinant α-amylase from *Bacillus halmapalus* (BHA) are the themes of this Thesis. BHA is very homologous to BLA (Bisgaard-Frantzen et al., 1999), but published information is almost non-existing at present. The main purpose of this study is to elucidate the mechanisms responsible for the stability and solubility of BHA in relation to temperature and calcium ions. The acquired knowledge provide basis for discussion of thermal inactivation models. In addition, focus has been put on development and evaluation of methodology that facilitate characterization of physio-chemical properties of α-amylases in relation to metal ions.

The structure of the thesis is outlined in the following together with a short introduction to each chapter in relation to the purpose of this study.

Chapter 2

This chapter (Paper I) is a paper recently published in *Analytical Biochemistry*. The paper describes and evaluates isothermal titration calorimetric procedures to determine protein-metal ion binding parameters in the presence of excess metal ion or chelator. The procedures eliminate separate metal ion removal steps that usually are needed in studies of protein-metal ion binding, while the main scope is to investigate the potential of the methodology; BHA-calcium ions binding parameters, at different pH values, have been determined and discussed in relation to structural information about calcium binding sites in related *Bacillus* α-amylases.

Chapter 3

The chapter (Paper II) is a manuscript that is currently in press in *Biochemical Journal*. The study addresses the effect of calcium ions on the denaturation of BHA using differential scanning calorimetry (DSC) and isothermal titration calorimetry (ITC). An isothermal titration calorimetric

procedure that allows simultaneous determination of kinetic parameters and enthalpy changes of the denaturation of calcium depleted BHA is presented and evaluated. In addition, BHA-calcium binding parameters at various temperatures are determined. Combination of the kinetic data of denaturation and binding constants has been used to estimate the kinetic stability of BHA as a function of temperature and calcium ion concentration.

Chapter 4

This chapter (Paper III) is a manuscript submitted to *Biochimica et Biophysica Acta* (March, 2003). In this study, the thermal stability of BHA and the stabilizing effect of calcium ions have been further investigated using circular dichroism spectroscopy (CD) and DSC in order to elucidate the complex mechanism underlying BHA denaturation. Complex DSC thermograms of partially calcium depleted BHA were analyzed in terms of different populations of BHA:calcium complexes. Combination of the observations in the study with structural information of homologous *Bacillus* α-amylases is used to put forward a tentative molecular picture for the mechanism of thermal denaturation of BHA in relation to calcium ions.

Chapter 5

The topics of this chapter are solubility and precipitation properties of BHA. Crystallization of BHA is discussed and the solubility diagrams of BHA crystals determined using a micro-column method. The effect of calcium ions on the crystallization rate and solubility is explored. Another subject studied is mechanical perturbation in relation to precipitation of BHA.

Chapter 6

This chapter emphasizes trends and conclusions, which are general to the four experimental chapters.

2

Paper I

Isothermal titration calorimetric procedure to determine protein-metal ion binding parameters in the presence of excess metal ion or chelator

Analytical Biochemistry, **2003**, 314(2) 227-234

ACADEMIC PRESS

Available online at www.sciencedirect.com

SCIENCE DIRECT®

Analytical Biochemistry 314 (2003) 227–234

ANALYTICAL BIOCHEMISTRY

www.elsevier.com/locate/yabio

Isothermal titration calorimetric procedure to determine protein–metal ion binding parameters in the presence of excess metal ion or chelator

Anders D. Nielsen,[a,b] Claus C. Fuglsang,[b] and Peter Westh[a,*]

[a] *Department of Life Sciences and Chemistry, Roskilde University, P. O. Box 260, DK-4000 Roskilde, Denmark*
[b] *Novozymes A/S, Novo Allé, DK-2880 Bagsværd, Denmark*

Received 1 August 2002

Abstract

Determination of binding parameters for metal ion binding to proteins usually requires preceding steps to remove protein-bound metal ions. Removal of bound metal ions from protein is often associated with decreased stability and inactivation. We present two simple isothermal titration calorimetric procedures that eliminate separate metal ion removal steps and directly monitor the exchange of metal ions between buffer, protein, and chelator. The concept is to add either excess chelator or metal ion to the protein under investigation and subsequently titrate with metal ion or chelator, respectively. It is thereby possible in the same experimental trial to obtain both chelator–metal ion and protein–metal ion binding parameters due to the different thermodynamic "fingerprints" of chelator and protein. The binding models and regression routines necessary to analyze the corresponding binding isotherms have been constructed. Verifications of the models have been done by titrations of mixtures of calcium chelators (BAPTA, HEDTA, and EGTA) and calcium ions and they were both able to account satisfactorily for the observed binding isotherms. Therefore, it was possible to determine stoichiometric and thermodynamic binding parameters. In addition, the concept has been tested on a recombinant α-amylase from *Bacillus halmapalus* where it proved to be a consistent procedure to obtain calcium binding parameters.

Keywords: Isothermal titration calorimetry; Calcium binding; Binding models

Removal of tightly bound metal ions from biological macromolecules, such as proteins, without inactivation or denaturation is a common problem when trying to determine metal ion binding parameters. Several methods and procedures to remove metal ions from a protein have been devised. Dialysis against a chelating agent, such as ethylenediaminetetraacetic acid (EDTA), or chromatography using chelating resins, such as Chelex, are among the most frequently used. There are, however, several disadvantages associated with the metal ion removal procedures: (1) they can be time consuming, with the concomitant requirement of high protein stability during the removal process, (2) the removal may remain incomplete, and (3) the chelating molecule may contaminate the sample. We report here a titration calorimetry methodology which overcomes these limitations. While conventional isothermal titration calorimetry (ITC)[1] follows one of the removal procedures mentioned above, the current method utilizes the addition of excess metal ion or chelator.

ITC is a widely used technique to determine binding parameters for metal ions to proteins [1–4]. It is usually necessary to include steps to remove protein bound metal ions. The purpose of the present paper is to describe two simple procedures that eliminate separate metal ion removal steps. The concept of the procedures

* Corresponding author.
E-mail address: pwesth@ruc.dk (P. Westh).

[1] *Abbrevations used:* ITC, isothermal titration calorimetry; BAPTA, 1,2-bis(2-aminophenoxy)ethane-*N*,*N*,*N*′,*N*′-tetraacetic acid ethylenedioxybis(*o*-phenylenenitrilo)tetraacetic acid; HEDTA, *N*-(2-hydroxyethyl)ethylene diamine-*N*,*N*′,*N*′-triacetic acid; EDTA, ethylenediaminetetraacetic acid; EGTA, ethylene glycol bis(β-aminoethyl ether) *N*,*N*,*N*′,*N*′-tetraacetic acid; BHA, *Bacillus halmapalus* amylase; [PL], protein–ligand complex.

0003-2697/03/$ - see front matter © 2003 Elsevier Science (USA). All rights reserved.
doi:10.1016/S0003-2697(02)00655-3

is to add excess metal ion (or chelator) to the protein under investigation and then make a titration with a chelator (or metal ion).

ITC quantifies the change in protein–ligand complexes, Δ[PL], formed as a result of an increase in ligand concentration. Most other techniques allow one to determine only the total amount of protein–ligand complex, [PL], at a certain protein to ligand ratio. In the latter case, the change in complex formation must be derived form a small difference between two separate observations. Thus, ITC data relate to the slope of a binding isotherm while most techniques show the binding isotherm itself. As a consequence, it is possible in many cases to obtain a resolution high enough to clearly distinguish the two binding events of this methodology (protein–metal ion and chelator–metal ion). Extraction of thermodynamic binding parameters from ITC thermograms requires that relevant binding models and corresponding regression routines are available.

A commonly used model is the two-sites model that is used to describe binding of a ligand to two sets of binding sites on a macromolecule [5]. New models have been scarce, but recently Sigurskjold [6] presented a displacement model, which applies to systems including a molecule with a binding site to which two ligands with different affinity bind. This model extends the application of ITC to systems of both very low and very high binding constants.

To extract thermodynamic and stoichiometric parameters from the resulting thermograms we have developed the relevant binding models that can be used to analyze ITC experiments with systems involving two molecules that compete for the same ligand. Both models have been verified on systems consisting of calcium chelators and calcium ions. In addition, the models have been used to determine calcium binding affinity of a recombinant *Bacillus halmapalus* α-amylase (BHA).

Theory

Let us consider binding experiments that include two molecules, A and B, which have numbers of binding sites, n_A and n_B, for the same ligand, L,

$$A_{1-f_A} + L = AL_{f_A} \text{ and } B_{1-f_B} + L = BL_{f_B}, \tag{1}$$

where f_A and f_B are the fractional saturation of binding sites on A and B, respectively.

The equilibrium constants are given by

$$K_A = \frac{f_A}{[L](1-f_A)} \text{ and } K_B = \frac{f_B}{[L](1-f_B)}, \tag{2}$$

where

$$f_A = \frac{[AL]}{n_A[A]_0} \text{ and } f_B = \frac{[BL]}{n_B[B]_0}. \tag{3}$$

From mass conservation the total concentrations of A, B, and L ($[A]_0$, $[B]_0$, and $[L]_0$, respectively) are defined by

$$[A]_0 = [A] + [AL], \tag{4}$$

$$[B]_0 = [B] + [BL], \text{ and} \tag{5}$$

$$[L]_0 = [L] + n_A[AL] + n_B[BL], \tag{6}$$

where [A], [B], and [L] are the concentrations of A, B, and L, respectively.

Combination of Eqs. (2) and (3) and substitution into Eq. (6) gives

$$[L]_0 = [L] + \frac{n_A[A]_0K_A[L]}{1+K_A[L]} + \frac{n_B[B]_0K_B[L]}{1+K_B[L]}. \tag{7}$$

Solving Eq. (7) with respect to [L] yields a cubic equation of the form

$$[L]^3 + p[L]^2 + q[L] + r = 0, \tag{8}$$

where

$$p = \frac{1}{K_A} + \frac{1}{K_B} + n_A[A]_0 + n_B[B]_0 - [L]_0, \tag{9}$$

$$q = \frac{n_A[A]_0}{K_B} + \frac{n_B[B]_0}{K_A} - [L]_0\left(\frac{1}{K_A} + \frac{1}{K_B}\right) + \frac{1}{K_AK_B}, \tag{10}$$

$$\text{and } r = \frac{-[L]_0}{K_AK_B}. \tag{11}$$

The physically meaningful root of Eq. (8) [7,8] is

$$[L] = \frac{2\sqrt{p^2-3q}\cos(\Theta/3) - p}{3}, \tag{12}$$

where

$$\Theta = \arccos\frac{-2p^3 + 9pq - 27r}{2\sqrt{(p^2-3q)^3}}. \tag{13}$$

The heat evolved from each injection in an ITC experiment will be proportional to the changes in [AL] and [BL] and the corresponding molar binding enthalpies. The observed heat change, ΔQ, is then given by

$$\begin{aligned}\Delta Q &= V_0(\Delta H_A\Delta[AL] + \Delta H_B\Delta[BL]) \\ &= V_0(n_A\Delta f_A\Delta H_A[A]_0 + n_B\Delta f_B\Delta H_B[B]_0),\end{aligned} \tag{14}$$

where V_0 is the volume of the calorimeter cell.

In the following, it is assumed that B binds L more strongly than A and that there is a significant difference in molar binding enthalpy between A, ΔH_A, and B, ΔH_B. Furthermore it is assumed that the enthalpy of nonspecific A–B interactions is small compared to ΔH_A and ΔH_B. This is supported by the observation that the heat signal is always negligible at the end of the titration trial when all binding sites are saturated. Also, the perfect match of the enthalpies listed in Table 1 is in strong support for the lack of nonspecific effects (see below).

A/B-L system—titration of an A/B mixture with L

We consider first an ITC experiment where a mixture of A and B is titrated with L. In this case, the initial addition of L will lead to the formation of BL complexes. As B gradually saturates, additional L will bind to A. This can be exemplified by a system consisting of a calcium binding protein (A), EDTA (B), and calcium ions (L).

The analysis of the binding isotherm is somewhat similar to the treatment of a single ligand binding to two sets of independent sites on the same molecule [5]. However, the model must include ligand binding to two molecules instead of just one. As a consequence, it is necessary to take into account the concentration of three rather than two molecular species.

A/L-B system—titration of an A/L mixture with B

Consider the case when a mixture of A and L, where L is in excess, is titrated with B. By analogy to the A/B-L system, the initial injections will be dominated by the formation of BL complexes. When all free L molecules have been used to saturate B, additional B will lead to a displacement of A with B due the higher affinity of B.

In the analysis of the corresponding binding isotherm it is necessary to use a binding model that includes the displacement reaction. As mentioned above, this has recently been discussed by Sigurskjold [6], who described the binding of two ligands to the same site on a third molecule with the same stoichiometry. The model can be used to account for binding isotherms if A and B are considered ligands and L is the third molecule to which they bind. However, the model applies only to cases where the number of binding sites on A and B are equal ($n_A = n_B$).

To analyze A/B-L and A/L-B titration curves we have constructed nonlinear least-squares regression routines, which extend the displacement model to encompass the stoichiometric considerations discussed above. The nonlinear least-squares regression method for exact analysis of displacement titration calorimetric experiments [6] combined with the above-mentioned binding models have provided the basis for construction of new regression routines that make it possible to account for A/B-L and A/L-B systems.

Materials and methods

Recombinant BHA was expressed in *Bacillus licheniformis* and purified to 99.5% at Novozymes A/S, Bagsværd, Denmark. The protein was extensively dialyzed against one of the following buffers: 20 mM glycine (pH 10.0), 20 mM Tris (pH 9.0), or 20 mM Hepes (pH 8.0). All buffers used have passed through Chelex 100 columns to remove calcium ions. The following calcium chelators were used: ethylenediaminetetraacetic acid (EDTA) (>99%; Merck, Darmstadt, Germany); ethylene glycol bis(β-aminoethyl ether)*N*,*N*,*N*′,*N*′-tetraacetic acid (EGTA) (>97%; Sigma, St. Louis, MO, USA); 1,2-bis(2-aminophenoxy)ethane-*N*,*N*,*N*′,*N*′-tetraacetic acid ethylenedioxybis(*o*-phenylenenitrilo) tetraacetic acid (BAPTA) (>98%; Sigma); and *N*-(2-hydroxyethyl)ethylene diamine-*N*,*N*′,*N*′-triacetic acid (HEDTA) (>98%; Fluka, Buchs, Switzerland). Calcium sulfate, $CaSO_4$ (>99%; Fluka) was used as source of calcium ions. All glassware and plastic bottles used were washed with EDTA solutions and Chelex 100-treated Milli-Q water. Solutions were stored in plastic bottles.

The chelators and calcium sulfate were dissolved in buffer, homogenized through repeated stirring and ultrasound treatment, and kept at 5 °C until use. All calorimetric measurements were conducted on MCS-ITC (MicroCal Inc., Northampton, MA, USA) isothermal titration calorimetry equipment [9]. The reference cell was filled with water. In a typical experiment, the sample cell was loaded with a solution containing mixtures of chelators, calcium, and/or protein. The cell solution was titrated with 30–40 aliquots of 8 μL of either a chelator or a calcium solution. All solutions were degassed by stirring under vacuum before the experiments. The obtained heat signals from the ITC were integrated using the Origin software supplied by MicroCal Inc. to obtain binding isotherms. Regression routines were programmed using the same software package and used for fitting of the binding isotherms.

Results and discussion

Two regression methods to analyze multicomponent systems have been developed. They have both been verified and validated on simple systems including Ca^{2+} ions and chelators. One of the methods is used to analyze binding of a ligand to binding sites on two different molecules (A/B-L system). Examples of this type of system, where Ca^{2+} binds to mixtures of EGTA/HEDTA and EGTA/BAPTA, are presented in Fig. 1. Both cases result in clearly resolved binding curves, which can be readily accounted for by the nonlinear regression routine. The lowest plateau represents the enthalpy change for binding of Ca^{2+} to the stronger chelator EGTA, whereas the second plateau corresponds to the enthalpy change for the low-affinity chelators, HEDTA and BAPTA. The continuous lines on Fig. 1 are the best-fit curves when the model for binding of a ligand to two sets of sites on two molecules is used (A/B-L). It appears that the model accounts well for the data, since both binding isotherms show good correlation between the experimental data points and the fitted curve. Table 1 shows the obtained binding parameters.

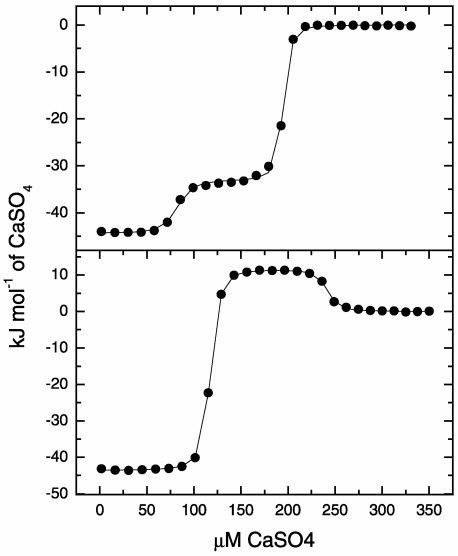

Fig. 1. (Top) Binding isotherm from titration of 95 μM EGTA/125 μM HEDTA with $CaSO_4$ at 19 °C. (Bottom) Binding isotherm from titration of 137 μM EGTA/140 μM BAPTA with $CaSO_4$ at 19 °C. Buffer: 20 mM glycin, pH 10. The continuous lines represent the results of the nonlinear least-squares fitting of the data points to the A/B-L binding model.

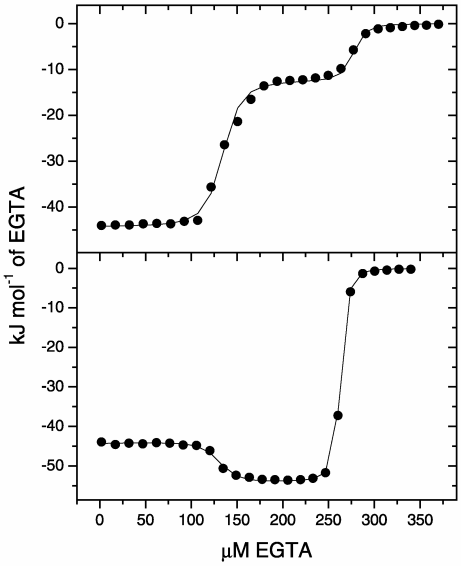

Fig. 2. (Top) Binding isotherm from titration of 320 μM $CaSO_4$/170 μM HEDTA with EGTA at 19 °C. (Bottom) Binding isotherm from titration of 315 μM $CaSO_4$/160 μM BAPTA with EGTA at 19 °C. Buffer: 20 mM glycin, pH 10. The continuous lines represent the results of nonlinear least-squares fitting of the data points to the A/L-B binding model.

The second method has been verified by analyzing the binding isotherms from titration of $CaSO_4$/HEDTA and $CaSO_4$/BAPTA mixtures with EGTA (Fig. 2). Again, we find well-resolved binding events, which are assigned as follows. The first plateau corresponds to the binding of EGTA to Ca^{2+} ions. When free Ca^{2+} ions are exhausted by EGTA further addition of EGTA will lead to displacement of HEDTA or BAPTA form HEDTA–Ca or BAPTA–Ca complexes, respectively. It is possible to account for the binding isotherm using the A/L-B model. This is illustrated by the continuous lines on Fig. 2, which represent the best-fit curves. The binding parameters are summarized in Table 1, together with parameters obtained from titration of the individual chelators with Ca^{2+} ions.

When the parameters from A/B-L and A/L-B experiments are compared a satisfactory correlation is observed. Furthermore, the obtained parameters correlate well with the corresponding parameters from titration of the individual chelators in simple binary systems. This shows that both the A/B-L and the A/L-B methods can

Table 1
Binding parameters of calcium to BAPTA, HEDTA, and EGTA at 18–19 °C (pH 10)

Chelator	A/B-L		A/L-B		Single
BAPTA					
ΔH (kJ/mol)		11.6 ± 0.1		11.1 ± 1.1	11.4 ± 0.2
K (M^{-1})		$(3.4 \pm 0.4) \cdot 10^6$		$(1.2 \pm 0.3) \cdot 10^6$	$(4.1 \pm 0.3) \cdot 10^6$
n		1.0 ± 0.1		1.0 ± 0.1	1.0 ± 0.1
HEDTA					
ΔH (kJ/mol)	-33.1 ± 0.2		-32.2 ± 0.8		-33.8 ± 0.1
K (M^{-1})	$(8.0 \pm 1.3) \cdot 10^6$		$(1.5 \pm 0.4) \cdot 10^6$		$(2.8 \pm 0.6) \cdot 10^7$
n	1.0 ± 0.1		1.0 ± 0.1		1.0 ± 0.1
EGTA					
ΔH (kJ/mol)	-44.5 ± 0.2	-43.7 ± 0.1	-44.4 ± 0.7	-44.3 ± 0.2	-44.2 ± 0.1
K (M^{-1})	$(1.5 \pm 0.5) \cdot 10^9$	$(2.9 \pm 0.4) \cdot 10^9$	$(1.3 \pm 0.9) \cdot 10^9$	$(3.6 \pm 1.1) \cdot 10^9$	$>10^8$
n	1.0 ± 0.1	0.9 ± 0.1	1.0 ± 0.1	1.0 ± 0.1	1.0 ± 0.1

A/B-L systems refer to experiments where a mixture of two chelators (A and B) is titrated with $CaSO_4$ (L); A/L-B systems refer to experiments where a mixture of chelator and $CaSO_4$ (A and L) is titrated with high-affinity chelator (B). Single systems correspond to experiments where a single chelator is titrated with $CaSO_4$.

be used to determine A-L and the B-L binding parameters.

Families of simulated binding isotherms indicate that satisfactory resolution of binding sites can be expected when the binding constants differ by at least one order of magnitude and that the difference in binding enthalpies is more than 25%. Similar results describing binding of a ligand to two sets of independent sites on a single molecule have previously been observed [10]. Alternatively, if the thermodynamic parameters are known for one of the sets of binding partners, only the restriction with different enthalpies applies.

The A/B-L and A/L-B methods have been used to determine binding parameters for binding of calcium to BHA. Titration of BHA in presence of excess EDTA with calcium ions gives rise to characteristic biphasic binding curves (Fig. 3). The first part corresponds to binding of calcium ions to EDTA, whereas the second part is the result of BHA–calcium binding. Similar biphasic titration curves are observed when BHA in the presence of excess calcium ions is titrated with EDTA (Fig. 4). The first part of the binding curve can be rationalized as binding of free calcium ions to EDTA. The second part involves dissociation of the BHA–Ca complex and concomitant formation of EDTA–Ca complexes. For both types of experiments, a clear separation of the BHA and EDTA binding is observed at pH 8–10. In the first type of experiments, it is therefore possible to use the A/B-L regression method to analyze the binding curves. Similarly, the second type of experiments can be analyzed by the A/L-B regression method. The actual concentration of Ca^{2+} ions is not known in the experiments because Ca^{2+} ions bound to BHA will contribute to the total concentration of Ca^{2+} ions. However, the EDTA–Ca stoichiometry is 1:1 and this allows for "calibration" of the concentration scale. Thus, a fixed stoichiometry of one, but a variable concentration of Ca^{2+} ions has been used in the regression analysis of titrations including BHA. In Figs. 3 and 4 the continuous lines are the best-fit curves when the A/B-L or A/L-B regression methods are used. The obtained BHA–Ca binding parameters are presented in Table 2 together with the EDTA–Ca binding parameters. A good correlation between the BHA–Ca and the

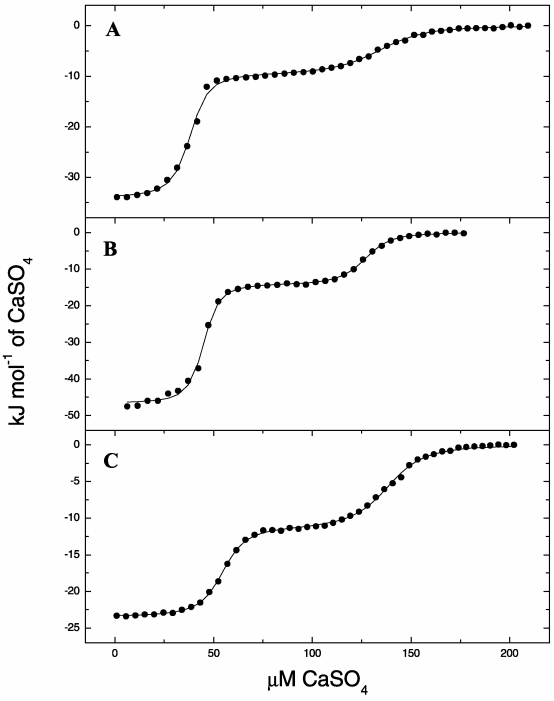

Fig. 3. (A) Binding isotherm from titration of 60 μM BHA/40 μM EDTA with $CaSO_4$ at 19 °C. Buffer: 20 mM glycin, pH 10. (B) Binding isotherm from titration of 65 μM BHA/50 μM EDTA with $CaSO_4$ at 18 °C. Buffer: 20 mM Tris, pH 9. (C) Binding isotherm from titration of 70 μM BHA/60 μM EDTA with $CaSO_4$ at 19 °C. Buffer: 20 mM Hepes, pH 8. The continuous lines represent the results of the non-linear least-squares fitting of the data points to the A/B-L binding model.

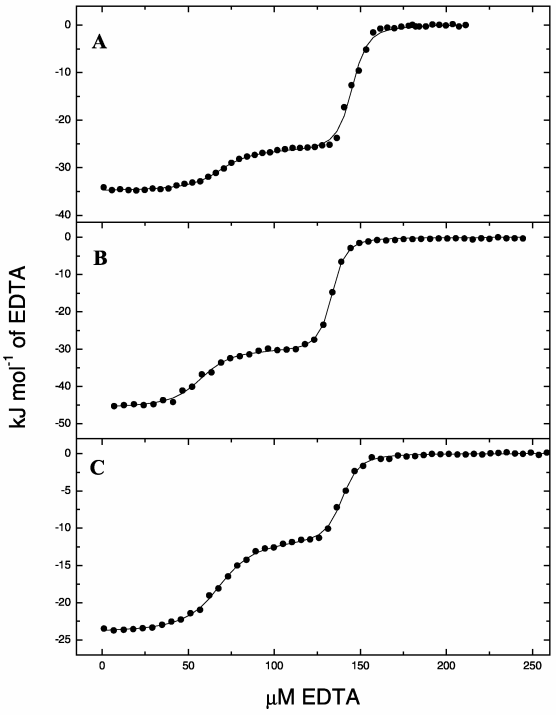

Fig. 4. (A) Binding isotherm from titration of 55 μM BHA/180 μM $CaSO_4$ with EDTA at 19 °C. Buffer: 20 mM glycin, pH 10. (B) Binding isotherm from titration of 55 μM BHA/150 μM $CaSO_4$ with EDTA at 18 °C. Buffer: 20 mM Tris, pH 9. (C) Binding isotherm from titration of 60 μM BHA/160 μM $CaSO_4$ with EDTA at 19 °C. Buffer: 20 mM Hepes, pH 8. The continuous lines represent the results of the non-linear least-squares fitting of the data points to the A/L-B binding model.

Table 2
BHA–calcium and EDTA–calcium binding parameters at 18–19 °C (pH 8–10)

Binding	Titration with $CaSO_4$ (pH)			Titration with EDTA (pH)		
	8	9	10	8	9	10
BHA–Ca						
ΔH (kJ/mol)	-11.5 ± 0.1	-14.2 ± 0.3	-9.7 ± 0.2	-12.3 ± 0.2	-15.4 ± 0.4	-8.6 ± 0.5
K (M^{-1})	$(7.6 \pm 0.6) \cdot 10^5$	$(1.6 \pm 0.3) \cdot 10^6$	$(5.4 \pm 0.9) \cdot 10^5$	$(6.6 \pm 0.6) \cdot 10^5$	$(9.9 \pm 0.2) \cdot 10^5$	$(8.9 \pm 3.2) \cdot 10^5$
ΔG^0 (kJ/mol)	-32.9 ± 0.2	-34.4 ± 0.5	-32.0 ± 0.4	-32.5 ± 0.2	-33.4 ± 0.1	-33.3 ± 1.2
$-T\Delta S^0$ (kJ/mol)	-21.4 ± 0.3	-20.2 ± 0.6	-22.3 ± 0.6	-20.2 ± 0.4	-18.0 ± 0.5	-24.7 ± 1.6
N	1.4 ± 0.1	1.4 ± 0.1	1.9 ± 0.1	1.5 ± 0.1	1.5 ± 0.1	1.7 ± 0.1
EDTA–Ca[a]						
ΔH (kJ/mol)	-23.5 ± 0.1	-46.8 ± 0.3	-34.1 ± 0.2	-24.0 ± 0.1	-45.8 ± 0.2	-34.9 ± 0.3
K (M^{-1})	$(1.1 \pm 0.1) \cdot 10^8$	$(4.5 \pm 1.0) \cdot 10^8$	$(1.1 \pm 0.2) \cdot 10^8$	$(2.4 \pm 0.3) \cdot 10^8$	$(6.1 \pm 1.0) \cdot 10^8$	$(4.2 \pm 1.4) \cdot 10^8$

[a] The EDTA–Ca stoichiometry has been fixed at 1 during the fitting sessions.

EDTA–Ca binding parameters obtained by the two methods is observed. Furthermore, the obtained EDTA–Ca parameters agree well with previous values determined by ITC [11]. The determined BHA–Ca binding affinity is in the range 10^5–10^6 M^{-1} and the binding enthalpy is between −9 and −15 kJ/mol. Apparently, there is little or no dependence of the binding constant on pH, in the range 8–10. It should be noted, however, that the binding affinity and enthalpy appear to be slightly higher at pH 9. For binding reactions involving proton release it is expected that the observed binding enthalpy will depend on the ionization enthalpy of the buffer used [12]. Tris, which is used at pH 9, has a large ionization enthalpy compared to Hepes and glycine, and this is presumably the reason for the slightly different values observed at pH 9. The effect of the high buffer ionization enthalpy is more obvious for binding of EDTA to calcium where the enthalpy is −46 to −47 kJ/mol at pH 9 compared to −24 and −34 to −35 kJ/mol at pH 8 and 10, respectively. The highest affinity is also observed at pH 9. It has previously been shown that proton release is involved in binding of calcium to EDTA [11].

The crystal structure of the structurally similar *B. licheniformis* α-amylase has revealed three calcium binding sites [13]. If we presume that BHA also contains three binding sites it is not unexpected to observe a Ca–BHA stoichiometry higher than one. Thus, the results suggest that it is possible to remove an average of 1.4–1.5 calcium ions from BHA with EDTA at pH 8 and 9. When pH is raised to 10 a slightly higher stoichiometry (1.7–1.9) is observed. A likely explanation is that the ratio between the BHA–Ca and the EDTA–Ca affinity decreases at high pH.

The observations suggest that BHA has one binding site with $K_{BHA\text{–}Ca} < K_{EDTA\text{–}Ca}$, one site with $K_{BHA\text{–}Ca} \approx K_{EDTA\text{–}Ca}$, and possibly one site with $K_{BHA\text{–}Ca} > K_{EDTA\text{–}Ca}$.

As can be seen from Table 2 both the enthalpy and the entropy contribute favorably to the binding of calcium to BHA. The positive ΔS value suggests that a dehydration process is involved in the binding of calcium to BHA.

Table 3 summarizes binding parameters found in this study and in the literature. Literature data under experimental conditions exactly matching the current measurements are generally not available and the specifics of each value are listed at the bottom of the table. For the purpose of validating the two new procedures it

Table 3
Obtained binding constants compared with literature values[a]

Chelator	K (M^{-1})	
	This study	Literature
BAPTA	$3.4 \cdot 10^{6}$[b] $1.2 \cdot 10^{6}$[c] $4.1 \cdot 10^{6}$[d]	$6.0 \cdot 10^{6}$[g]
HEDTA	$8.0 \cdot 10^{6}$[b] $1.5 \cdot 10^{6}$[c] $2.8 \cdot 10^{7}$[d]	$1.1 \cdot 10^{8}$[h]
EGTA	$1.5 \cdot 10^{9}$[b] $2.9 \cdot 10^{9}$[b] $1.3 \cdot 10^{9}$[c] $3.6 \cdot 10^{9}$[c] $>10^{8}$[d]	$9.3 \cdot 10^{10}$[i]
EDTA	$1.1 \cdot 10^{8}$[b] $2.4 \cdot 10^{8}$[c]	$2.0 \cdot 10^{8}$[j]
Amylase	$7.6 \cdot 10^{5}$[e] $6.6 \cdot 10^{5}$[f]	$3.5 \cdot 10^{5}$[k]

[a] The reported values are obtained in 20 mM glycin, pH 10.0, at 19 °C if nothing else is indicated.
[b] A/B-L titration.
[c] A/L-B titration.
[d] Single titration.
[e] A/B-L titration (20 mM Hepes, pH 8.0, 19 °C).
[f] A/L-B titration in (20 mM Hepes, pH 8.0, 19 °C).
[g] From [14] (I = 0.1 M, 25 °C).
[h] From [15] (I = 0.1 M, 25 °C).
[i] From [16] (I = 0.1 M, 20 °C).
[j] From [11] (10 mM Tris, pH 7.5, 25 °C).
[k] Reported for *Bacillus amyloliquefaciens* α-amylase (25 mM Tris, pH 7.0, 45 °C), from [17].

is particularly important that the results for the A/B-L and A/L-B titrations concur with results from the well-established (two-component) receptor/ligand ITC trials at exactly matching conditions. Also, the current results are generally in good accordance with previously published data for the association of calcium ions to chelators and, more importantly, the binding of Ca^{2+} to a *Bacillus* α-amylase [17]. An exception, however, is found for Ca–EGTA where the current binding constants are smaller than the published values. This discrepancy probably reflects the fact that the upper range for tight binding measured by ITC is about $10^{-8}\,M^{-1}$ [9] and hence that ITC data for this system provide only estimates of minimum values.

A common problem associated with metal ion removal procedures is contamination of the sample by chelating molecules. This problem is overcome in the current procedures and the A/B-L concept relies on excess chelator in the sample. Furthermore, excess chelator is used as a calibration of the calcium concentration scale. Handling solutions of chelators requires precautions to avoid contamination by divalent metal ions from glassware, for example. However, a minor contamination of the chelator by divalent metal ions is easily handled in the A/B-L procedure by fixing the chelator stoichiometry and setting the total concentration of chelator as a variable during the fitting session.

In summary, two new concepts to determine parameters of protein–metal ion binding to in the presence of excess chelator or metal ion have been presented. A great advantage of the procedures is that they do not require time-consuming procedures to remove protein-bound metal ions and storage of destabilized metal-free protein. Metal ion removal procedures may result in incomplete removal of protein-bound metal ions or contaminate the sample with chelating molecules. Neither of the current procedures requires information about the amount of bound metal ions. Chelator contamination is not a problem when using the A/B-L concept, which requires excess chelator in the sample.

The relevant binding models and ITC regression routines have been constructed and proven to be robust against the simple system of calcium ions and chelators. In all cases, the models were able to account for the observed binding curves satisfactorily and thereby to obtain all relevant binding parameters. In addition, both concepts have been used to determine calcium binding parameters for BHA.

The two concepts presented in this paper should be applicable to other metal–ion binding systems. It requires a metal–ion chelator that binds the relevant ion with sufficiently high affinity. However, if the number of binding sites is known, it is possible to determine whether some of the sites have an affinity that is higher relative to the chelator. Chelators such as EDTA and EGTA may also be useful in other systems containing divalent metal–ion binding sites. The models and regression routines are, however, not limited to metal–ion binding systems and it should be possible to use them to extract binding parameters in other multicomponent binding systems.

Acknowledgments

This work was supported by the Danish Academy of Technical Sciences and the Carlsberg Foundation. Insightful comments on this work by Dr. Bent W. Sigurskjold, University of Copenhagen, are appreciated.

References

[1] Y.V. Griko, D.P. Remeta, Energetics of solvent and ligand-induced conformational changes in alpha-lactalbumin, Protein Sci. 8 (1999) 554–561.
[2] R. Gilli, D. Lafitte, C. Lopez, M. Kilhoffer, A. Makarov, C. Briand, J. Haiech, Thermodynamic analysis of calcium and magnesium binding to calmodulin, Biochemistry 37 (1998) 5450–5456.
[3] B. Gopal, C.P. Swaminathan, S. Bhattacharya, A. Bhattacharya, M.R.N. Murthy, A. Surolia, Thermodynamics of metal ion binding and denaturation of a calcium binding protein from Entamoeba histolytica, Biochemistry 36 (1997) 10910–10916.
[4] H. Gusman, U. Lendenmann, J. Grogan, R.F. Troxler, F.G. Oppenheim, Is salivary histatin 5 a metallopeptide?, Biochim. Biophys. Acta 1545 (2001) 86–95.
[5] L.-N. Lin, A.B. Mason, R.C. Woodworth, J.F. Brandts, Calorimetric studies of the binding of ferric ions to ovotransferrin and interaction between binding sites, Biochemistry 30 (1991) 11660–11669.
[6] B.W. Sigurskjold, Exact analysis of competition ligand binding by displacement isothermal titration calorimetry, Anal. Biochem. 277 (2000) 260–266.
[7] Z.X. Wang, An exact mathematical expression for describing competitive-binding of 2 different ligands to a protein molecule, FEBS Lett. 360 (1995) 111–114.
[8] Z.X. Wang, R.F. Jiang, A novel 2-site binding-equation presented in terms of the total ligand concentration, FEBS Lett. 392 (1996) 245–249.
[9] T. Wiseman, S. Wiliston, J.F. Brandts, L.-N. Lin, Rapid measurement of binding constants and heats of binding using a new titration calorimeter, Anal. Biochem. 179 (1989) 131–137.
[10] A.D. Nielsen, K. Borch, P. Westh, Thermochemistry of the specific binding of C12 surfactants to bovine serum albumin, Biochim. Biophys. Acta 1479 (2000) 321–331.
[11] Y.V. Griko, Energetics of Ca2+-EDTA interactions: Calorimetric study, Biophys. Chem. 79 (1999) 117–127.
[12] H. Fukada, K. Takahashi, Enthalpy and heat capacity changes for the proton dissociation of various buffer components in 0.1 M potassium chloride, Proteins 33 (1998) 159–166.
[13] M. Machius, N. Declerck, R. Huber, G. Wiegand, Activation of Bacillus licheniformis alpha-amylase through a disorder–order transition of the substrate-binding site mediated by a calcium-sodium-calcium metal triad, Structure (London) 6 (1998) 281–292.
[14] A. Yuchi, A. Tanaka, M. Hirai, T. Yasui, H. Wada, G. Nakagawa, Complexation equilibria and fluorescent properties

of chelating reagents derived from ethylene-glycol bis(beta-aminoethylether)-n, n,n′,n′ tetraacetic acid, Bull. Chem. Soc. Jpn. 66 (1993) 3377–3381.

[15] J.J. Christensen, R.M. Izatt, Handbook of metal ligand heats and related thermodynamic quantities, Marcel Dekker Inc., New York, 1983.

[16] G. Anderegg, Komlexone XXXVI. Reaktionsenthalpie und entropie bei der bildung der metallkomplexe der hoheren EDTA-homologen, Helv. Chim. Acta 47 (1964) 1801–1814.

[17] A. Tanaka, E. Hoshino, Calcium-binding parameter of Bacillus amyloliquefaciens alpha-amylase determined by inactivation kinetics, Biochem J. 364 (2002) 635–639.

3

Paper II

The effect of calcium ions on the irreversible denaturation of a recombinant *Bacillus halmapalus* a-amylase – a calorimetric investigation

Anders D. Nielsen [a,b], Claus C. Fuglsang [b], Peter Westh [a]

[a] Department of Life Sciences and Chemistry, Roskilde University
P.O.Box 260, DK-4000 Roskilde, Denmark

[b] Novozymes A/S, Novo Allé, DK-2880 Bagsværd, Denmark

Biochemical Journal, **2003**, In press (doi:10.1042/BJ20030220)

3.1 Abstract

The effect of temperature and calcium ions on the denaturation of a recombinant α–amylase from *Bacillus halmapalus* (BHA) have been studied using calorimetry. It was found, that thermal inactivation of BHA is irreversible and that calcium ions have a significant effect on the stability. Thus, an apparent denaturation temperature (T_m) of 83°C in the presence of excess calcium ions was observed, while T_m decreased to 48°C when calcium was removed. The difference in thermal stability with and without calcium ions has been used to develop an isothermal titration calorimetric (ITC) procedure that allows simultaneous determination of kinetic parameters and enthalpy changes of the denaturation of calcium depleted BHA. An activation energy (E_A) of 101 kJ/mol was found for the denaturation of calcium depleted BHA. The data supports a kinetic denaturation mechanism where the calcium depleted amylase denatures irreversibly at low temperature and if calcium ions are in excess, the amylase denatures irreversible at high temperature. The two denaturation reactions are coupled through the calcium binding equilibrium between calcium bound and depleted amylase. Combination of the kinetic denaturation data and calcium binding constants, determined by ITC, has been used to estimate the kinetic stability, e.g. expressed as the half-life, of BHA as a function of temperature and free calcium ion concentration. Thus, it is estimated that the apparent E_A can be increased to approximately 123 kJ/mol by increasing the free calcium concentration.

Keywords: α-amylase, denaturation, calcium binding, calorimetry, activation energy, thermodynamics

Abbreviations used: BHA, *Bacillus halmapalus* α-amyalse; BLA, *Bacillus licheniformis* α-amylase; BAA, *Bacillus amyloliquefaciens* α-amylase; ITC, isothermal titration calorimetry; DSC, differential scanning calorimetry; EDTA, ethylenediaminetetraacetic acid; EGTA, ethylene glycol-bis[β-aminoethyl ether] *N,N,N',N'*-tetraacetic acid

3.2 Introduction

α-amylases (EC 3.2.1.1:1,4-α-D-glucan glucanohydrolase) are enzymes that catalyze the hydrolysis of the internal α-1,4-glucosidic bond in starch. The enzymes have several important industrial applications, particularly in food and detergent industry [1-3]. Successful industrial use of amylases requires that they are sufficiently stable and active at application conditions, e.g. at high temperatures in starch liquefaction processes. Besides the parameters, temperature and pH the influence of divalent metal ions are important in this context. Elucidation of the stabilization mechanisms involved may provide valuable tools to predict the stability under relevant conditions.

A characteristic feature of α-amylases is their requirement of calcium ions for activity and structural stability [4-9]. Vallee *et al.* [5] has previously shown that addition of excess EDTA to *Bacillus subtilis* amylases result in 40% decrease in activity in 2 hours at 25°C. However, complete reactivation after 2 hours was achieved upon addition of excess calcium ions. A similar decrease in activity at 37°C only required 40 min. and it was not possible to obtain complete reactivation upon addition of calcium ions. It has been suggested that irreversible inactivation of α–amylase follows a two stage process [9-11], where the first process involves a reversible dissociation of bound calcium ions from the amylase. This is followed by a second process where the amylase undergoes an irreversible denaturation.

All known α-amylases contain a structurally conserved calcium binding site [12;13], but one or more additional calcium binding sites have been identified dependent on the α-amylase origin. The X-ray structures of the α-amylases from the *Bacillus* species *licheniformis* and *subtilis* have revealed three calcium ion [14;15]. The objective of the present study is to investigate the interrelationships between calcium binding and the irreversible inactivation of a recombinant *Bacillus halmapalus* α–amylase (BHA). In previous investigations on the effect of calcium ions on the inactivation of amylase, the preferred method has been hydrolytic activity measurements. In this study, we have chosen a different approach, based on calorimetric methods. More specifically, we utilize the thermodynamic "fingerprint", i.e. the characteristic time course of heat flow from a certain reaction to resolve the rate of this reaction in a multi-component system. This requires that the fingerprint of each process can be identified and that they are

significantly different. This turned out to be the case for the ligand binding and protein denaturation studied here.

In this paper, we utilize a novel calorimetric methodology to determine both thermodynamic and kinetic parameters associated with irreversible denaturation of calcium depleted α-amylase. The methodology utilizes both scanning and titration calorimetry, and is based on the difference in thermostability of the α-amylase with and without bound calcium ions. Hence, if an experiment is performed at a temperature where the protein is mainly in the folded state when metal ions are bound removal of these ions will destabilize the protein. The calorimetric response will therefore include heat changes associated with the metal ion removal process and the subsequent denaturation process. This allows one to determine both the rate and enthalpy of denaturation at a specific temperature in a single experimental trial.

In the present study we have used a combination of data from denaturation kinetics, calcium binding and thermal stability to elucidate the denaturation mechanism of a recombinant α-amylase and how calcium ions are involved.

3.3 Materials and methods

3.3.1 Enzyme and chemicals

Recombinant BHA was expressed in *Bacillus licheniformis* and purified to >95%, determined by SDS/PAGE, at Novozymes A/S, Bagsvaerd, Denmark. The protein was extensively dialyzed, at 5°C, against one of the following buffers: 20 mM HEPES, 40 μM $CaSO_4$, pH 8.0 or 20 mM HEPES, 60 μM EGTA, pH 8.0. The following chemicals were used: 4-(2-Hydroxyethyl)piperazine-1-ethanesulfonic acid, HEPES (>99.5%, Sigma, St. Louis, MO, USA), ethylenediaminetetraacetic acid, EDTA (>99%, Merck, Darmstadt, Germany), ethylene glycol-bis[β-aminoethyl ether] *N,N,N',N'*-tetraacetic acid, EGTA (>97%, Sigma, St. Louis, MO, USA) and calcium sulfate, $CaSO_4$ (>99%, Fluka, Buchs, Switzerland).

3.3.2 Thermostability

DSC experiments were performed with a MicroCal VP-DSC (Northampton, MA) [16]. All enzyme solutions were dialyzed against the desired buffer, and the dialyzate was used as reference. Prior to scanning all solutions were degassed by stirring under vacuum. To determine if the denaturation of BHA was reversible a second scan was performed after cooling the samples. Furthermore, scans were performed at scan rates from 10 to 90 °C h^{-1} in order to determine if the BHA denaturation process is scan rate dependent. In all experiments, a BHA concentration of 20 μM was used and buffer scans were subtracted from BHA scans. The DSC data was analyzed using the Origin software from MicroCal, Inc. supplied with the calorimeter. Molar excess heat capacities (C_p) were obtained by normalizing with the BHA concentration and the volume of the calorimeter cell. Apparent denaturation temperatures (T_m) were determined as the temperature corresponding to maximum C_p. The denaturation enthalpy was determined by integration after subtraction of a cubic baseline. However, it was not possible to determine the denaturation enthalpy in the presence of calcium ions due to exothermic aggregation effects.

3.3.4 Chelator induced denaturation

Consider a protein (P) with a denaturation temperature of X °C in the presence of a ligand (L). When L is removed the denaturation temperature decreases to Y °C (i.e. Y < X). L can be removed by addition in excess of a molecule, B, with high affinity towards L (eqn (1)). If L is removed from the protein at a temperature between, X and Y the protein will begin to denature (eqn (2)). The following reactions take place upon addition of B:

$$\begin{aligned} L + B &= BL \\ PL + B &= P + BL \end{aligned} \qquad (1)$$

$$P \xrightarrow{k} D \qquad (2)$$

where D is the denatured state of the protein and k is a first-order rate constant. Both process (1) and (2) will generate or absorb heat. Therefore, the processes can be monitored as the heat flow ($\Delta q/\Delta t$) from a solution of PL upon injection of B. Initially the heat flow will be dominated by the heat released upon displacement of B with P (eqn (1)). Subsequently, the protein will begin to unfold (eqn (2)) and hence generate an endothermic heat flow.

The output of ITC is:

$$\frac{\Delta q}{\Delta t}(t) \tag{3}$$

and the heat flow generated during a first-order irreversible denaturation process is given by

$$\frac{\Delta q}{\Delta t} = k \cdot Q \cdot x(t) \tag{4}$$

Where Q is the total heat adsorbed during the denaturation process and $x(t)$ is the time dependent fraction of folded protein in the solution:

$$x(t) = \frac{[\mathrm{P(t)}]}{[\mathrm{P}]_0} \tag{5}$$

where $[P]_0$ is the initial concentration of folded protein.

According to first-order rate kinetics [P(t)] is

$$[\mathrm{P(t)}] = [\mathrm{P}]_0 \cdot e^{-k \cdot t} \tag{6}$$

Q is related to the enthalpy of denaturation (ΔH_{den}) by the following equation:

$$Q = \Delta H_{\mathrm{den}} \cdot [\mathrm{P}]_0 \cdot V_{\mathrm{cell}} \tag{7}$$

where V_{cell} is the volume of the calorimeter cell.

The following equation for the heat flow can be obtained by substitution of eqn (5)-(7) into eqn (4):

$$\frac{\Delta q}{\Delta t} = k \cdot \Delta H_{den} \cdot V_{cell} \cdot [P]_0 \cdot e^{-kt} \quad (8)$$

ΔH_{den} and k can then be determined by non-linear least squares regression of the ITC data using eqn (8). ΔH_{den} can also be determined, independent of any model, by integration of the thermogram from t_0, and thus provides an easy way to verify the value obtained from regression analysis. Other authors have derived equations similar to eqn (8) and discussed the applicability of isothermal heat conduction microcalorimetry to studies of slow reactions such as drug degradation [17]

Before a regression analysis is performed, it is necessary to account for the part of the thermogram corresponding to the initial removal of ligand (eqn (1)) and define time zero (t_0) for the denaturation process. For the current systems, the reaction rates are sufficiently different for t_0 to be determined by the linear extrapolations illustrated in the inset of Fig. 3.2. The shift from the binding process (eqn (1)) to the denaturation process (eqn (2)) is associated with a rapid change in heat flow. Due to the response time of the calorimeter, it is therefore necessary to ignore the initial heat flow of the denaturation process. The time required to reach a consistent heat flow is defined as the lag time (t_{lag}) and is disregarded in the regression analysis (see inset of Fig. 3.2).

All isothermal denaturation experiments were conducted on an MCS-ITC (MicroCal Inc., Northampton, MA, USA) isothermal titration calorimetry equipment [18]. Prior to titration, all solutions were degassed by stirring under vacuum. In a typical experiment, the sample cell was loaded with a solution of 20 μM BHA with 40μM $CaSO_4$. One aliquot of 50 μL EDTA solution was added (giving a 10:1 molar ratio of EDTA:BHA in the calorimeter cell) and the heat flow was recorded. The dilution heat was determined by making a second injection of the same volume after the protein had been completely denatured. Analysis of the thermograms was done using the Origin 7.0 software package, OriginLab

Corporation (Northampton, MA). All the reported uncertainties represent the standard deviations of regression analysis of three experiments.

3.3.5 Calcium binding

Calcium binding parameters of BHA were determined using ITC. The reference cell was filled with water. In a typical experiment, the sample cell was loaded with a solution containing a mixture of 60 μM EGTA and 30 μM BHA. The cell solution was titrated with 40 aliquots of 5 μL of 1.25 mM $CaSO_4$ solution. All solutions were degassed by stirring under vacuum before the experiments. The resulting binding isotherms showed a biphasic behavior reflecting the binding of Ca^{2+} to EGTA and, when the chelator had been saturated, to BHA. Binding isotherms were analyzed using a multi-component binding model as previously described [19]. A non-linear least squares minimization routine was used to obtain the maximum likelihood values of binding constants (K), enthalpies (ΔH) and stoichiometry (n). Changes in standard free energy ($\Delta G°$) and entropy ($\Delta S°$) were determined as $\Delta G°=-RT\ln K$ and $T\Delta S°=\Delta H-\Delta G°$ (under the assumption that $\Delta H=\Delta H°$). All the reported uncertainties represent three standard deviations of the regression analysis.

3. 4 Results and discussion

The denaturation of respectively BHA and calcium depleted BHA determined by DSC is illustrated in Fig. 3.1. In the presence of two fold excess calcium ions (2:1 $CaSO_4$:BHA) T_m was found to be 83°C. It was difficult to determine the precise value due to irreversible aggregation upon denaturation, and the reported value should therefore be regarded as a minimum value. T_m decreases to 48°C when EDTA is in excess (8:1 EDTA:BHA), and the denaturation was also found to be irreversible. The T_m values are scan rate dependent due to the irreversibility of the processes. Therefore, all scans were recorded at low scan rate (10 °C h^{-1}) to obtain T_m values approaching isothermal conditions. Increasing the scan rate to 90 °C h^{-1} resulted in approximately 10 °C higher T_m values for both processes. The obtained

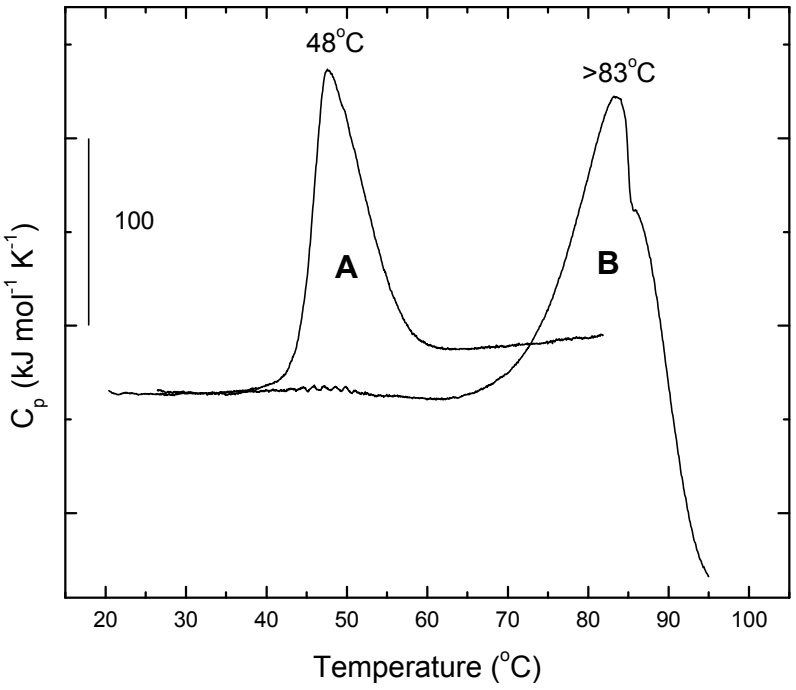

Fig. 3.1: DSC thermograms of 20 μM BHA denaturation in 20 mM HEPES, pH 8.0 in the absence and presence of calcium ions. (A) Calorimetric trace obtained in 8 times excess EDTA. (B) Calorimetric trace obtained in two times excess $CaSO_4$. The exothermic signal following denaturation in the presence of calcium ions reflects precipitation in the calorimeter cell. The apparent denaturation temperatures are listed above the curves.

DSC results support a kinetic inactivation mechanism similar to the one recently proposed for *Bacillus amyloliquefaciens* α-amylase (BAA) [11]:

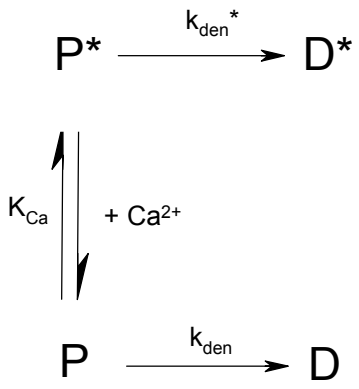

Scheme 1: Proposed mechanism for inactivation of BHA with and without calcium ions.

In scheme 1 P and D, represent the native and denatured conformations of the amylase respectively. The asterisk denotes calcium-depleted amylase. K_{Ca} is the calcium binding constant and k_{den} and k_{den}* corresponds to the rate constant for denaturation of calcium-bound and calcium-depleted amylase respectively. It is not known if D and D* are different. However, it is irrelevant in the analysis of the data in this study.

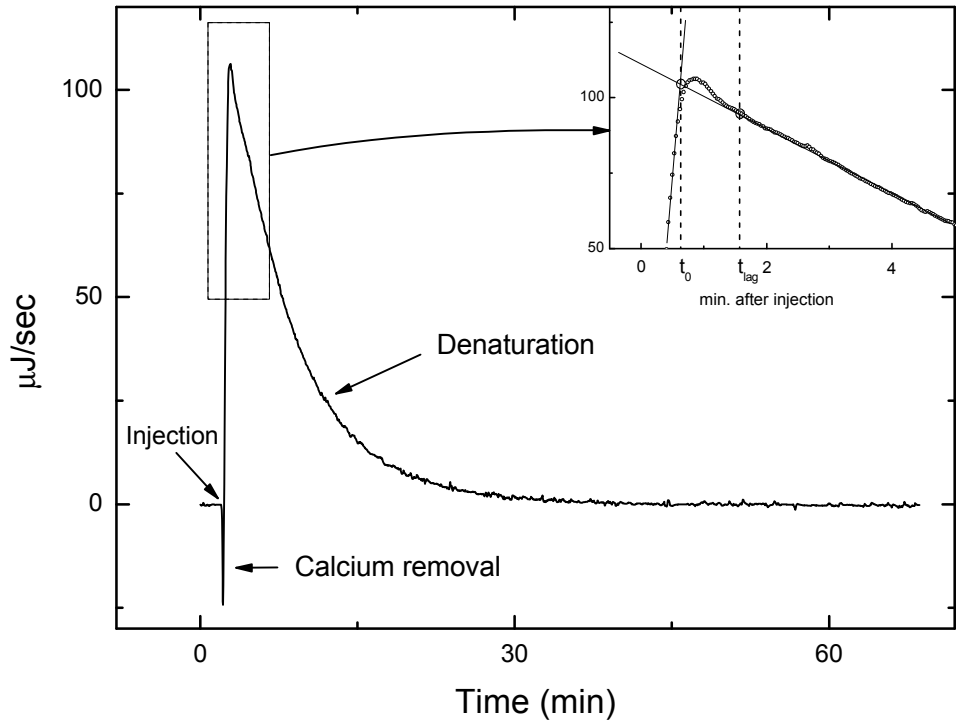

Fig. 3.2: Denaturation of BHA upon calcium depletion followed by ITC in 20 mM HEPES, pH 8.0 at 60°C. The thermogram was obtained by injection of 50 µL 5.2 mM EDTA into a 20 µM BHA, 40 µM $CaSO_4$ solution. The initial exothermic part of the thermogram corresponds to displacement of calcium ions from BHA to EDTA. This is followed by a large endothermic heat flow due to denaturation of calcium depleted BHA. The inset shows the initial part of the denaturation process. t_0 defines the time at which the denaturation process initiates and it can be determined graphically by drawing a straight line through the data points obtained before the denaturation process and a second line through the points obtained during the beginning of the denaturation process as indicated. t_{lag} defines the time required to reach a consistent heat flow upon initiation of the denaturation process.

The difference in T_m with and without calcium ions has been used to study the kinetics of denaturation upon calcium depletion. Injection of the calcium chelator EDTA into a solution of BHA/$CaCl_2$ at 60°C results in characteristic thermograms that allow a clear separation of the initial binding reaction (binding and displacement of calcium ions to EDTA, see eqn (1)) and the subsequent denaturation of the protein (Fig. 3.2). Initially the binding reaction generates an exothermic heat flow that is observed as a sharp peak. It has previously been observed that the displacement reaction is in fact exothermic [19]. Secondly, a positive heat flow is generated due to the endothermic denaturation of BHA. Thermograms obtained at temperatures from 50 to 70°C share the same characteristics (see Fig. 3.3). However, when the temperature is increased, the heat flow at the beginning of the denaturation is increased and the heat flow approaches the baseline faster. If a similar experiment is performed at 40°C only the initial binding reaction is observed. This is in accordance with the observation (Fig. 3.1) that the temperature is well below the T_m of calcium depleted BHA. Spectroscopic studies on BAA have indicated that the protein undergoes a conformational change upon removal of bound calcium ions [8]. Unfortunately, the experimental temperature of the work was not given by the authors.

As a first step in the thermogram analysis, t_0 and t_{lag} have been determined as described in the theory section (see inset in Fig. 3.2). t_0 remained close to 25 seconds at all temperatures, while t_{lag} varied from 280 s at 50°C to 40 s at the highest temperatures. Secondly, non-linear least squares regression using eqn (8) was used to obtain the maximum likelihood values for the parameters k and ΔH_{den}. The obtained k and ΔH_{den} values from 50 – 70 °C are listed in Table 3.1. The correlation coefficient for the regression analysis is higher than 0.998 in all experiments and the ability of eqn. (8) to account for the data is illustrated in Fig. 3.4. Furthermore, the method proved to be highly reproducible and the average standard deviation is 3%. The dilution heat was found to be approximately 5% of the denaturation enthalpy. Plotting ln ($\Delta q/\Delta t$) vs. t provides a simple test to determine if the observed process is of first-order [17], since a linear correlation is only expected for first order processes. These types of plot (data not shown) were indeed linear. This is in agreement with recent studies on BAA which indicated that inactivation is a one step irreversible process [11]. However, it should be noted

that a previous study on *Bacillus licheniformis* α-amylase concluded that the inactivation proceeds as a two step process [6].

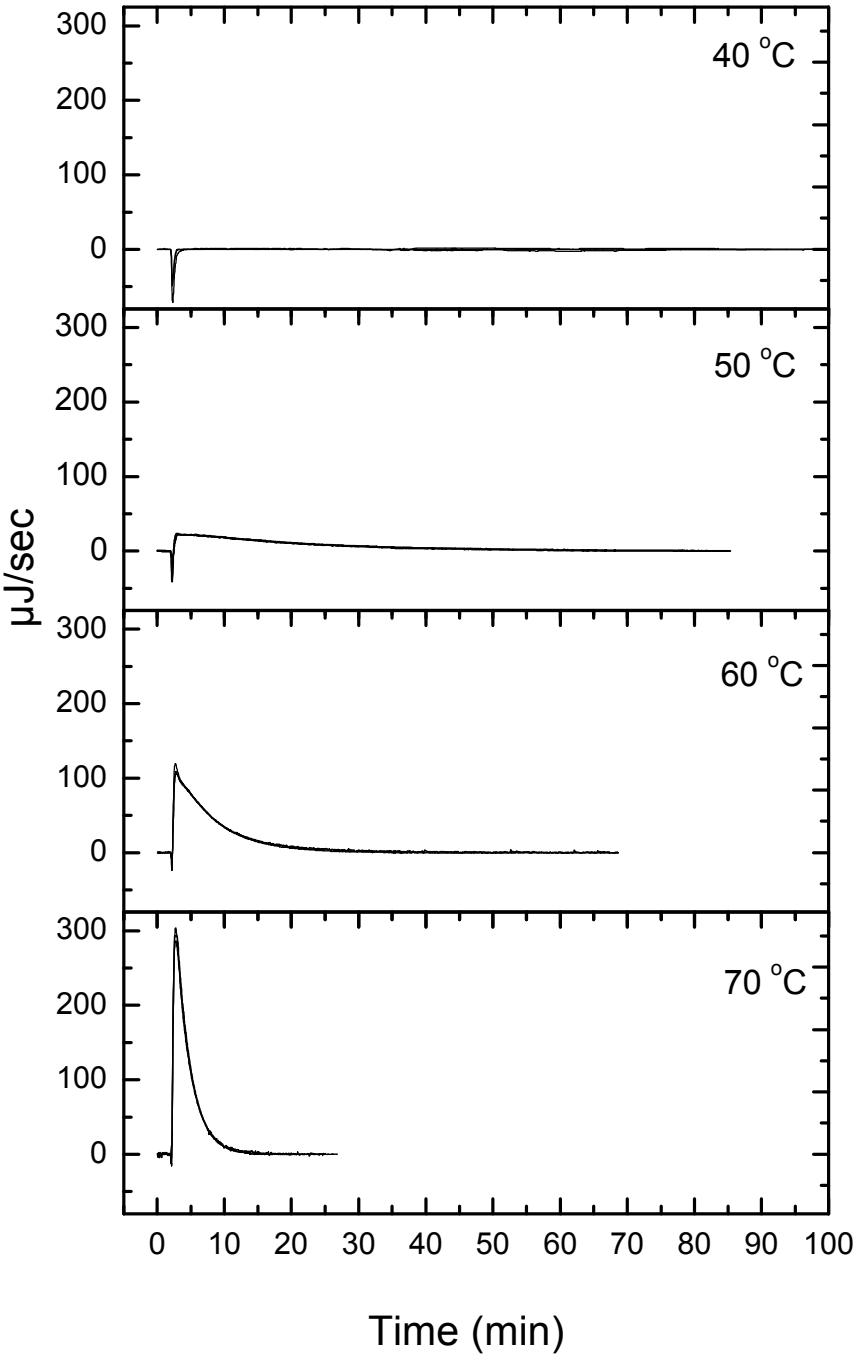

Fig. 3.3: Denaturation thermograms at 40-70°C obtained as described in Fig. 3.2. At each temperature, three thermograms are presented. At 40°C no significant denaturation appear to take place, since only an exothermic heat flow is observed.

Table 3.1: Rate constants and unfolding enthalpies for thermal inactivation of calcium depleted BHA in 20 mM HEPES, pH 8.0.

Temperature (°C)	ΔH_{AREA} (kJ/mol)[a]	ΔH_{FIT} (kJ/mol)[b]	k x 10^4 (s^{-1})[b]	$t_{1/2}$ (min)
50	1066 ± 55	1139 ± 43	9.23 ± 0.59	12.5
55	1476 ± 31	1474 ± 26	15.0 ± 0.2	7.7
60	1683 ± 63	1692 ± 20	27.4 ± 0.3	4.2
65	1761 ± 43	1747 ± 50	47.2 ± 1.6	2.4
70	1797 ± 76	1768 ± 67	80.6 ± 1.7	1.4

[a] obtained by integration

[b] obtained by regression analysis using Eq. (8)

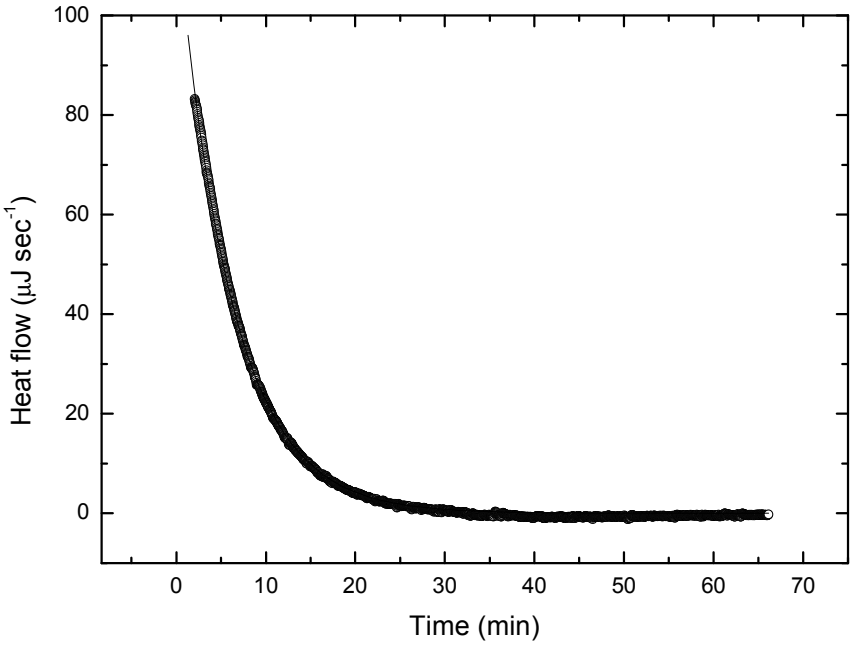

Fig. 3.4: Analysis of the denaturation thermogram at 60°C (see Fig. 3.2). The data points correspond to the heat flow. Non-linear least squares regression using eqn (8) has been used to determine the denaturation rate and enthalpy.

The ΔH_{den} values obtained by regression analysis are in good agreement with the values determined by integration (see Fig. 3.5). ΔH_{den} increases with temperature from approx. 1100 kJ/mol at 50°C to almost 1800 kJ/mol at 70°C. The correlation

is not linear and the enthalpy seems to become practically temperature independent above 65°C. The enthalpy changes measured by ITC are further supported by the value (1310 kJ/mol at 48°C) determined by DSC.

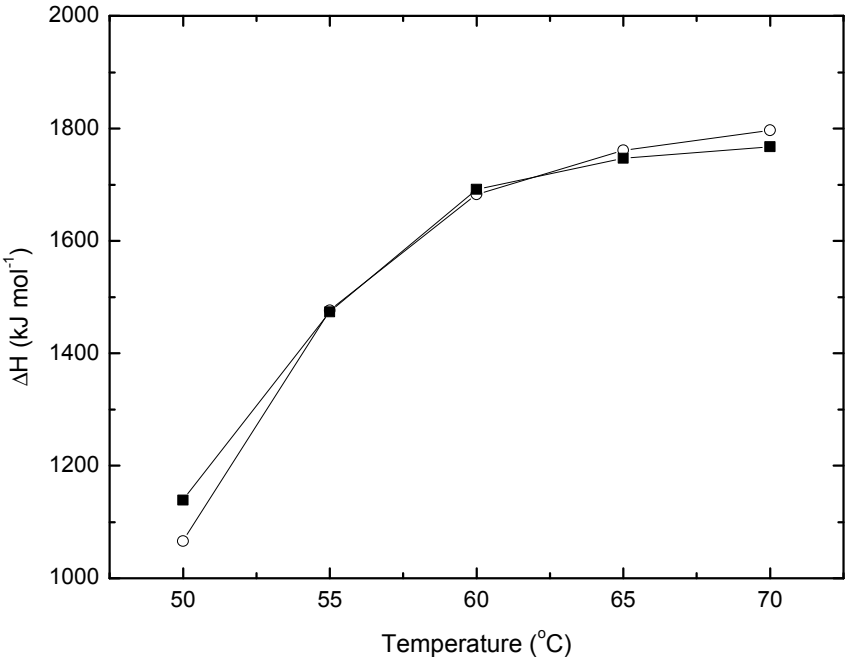

Fig. 3.5: Correlation of denaturation enthalpies (Table 3.1) obtained by integration (circles) and by fitting using eqn (8) (filled squares).

An Arrhenius plot was used to calculate the activation energy (E_A) of denaturation of calcium depleted BHA (see Fig. 3.6) and found to be 101 kJ/mol. This value is comparable with a previously reported E_A value of 113 kJ/mol for the inactivation of for *Bacillus licheniformis* α-amylase (BLA) in the presence of excess EDTA [10]. However, Violet & Meunier [6] has found an E_A value of 53.1 kJ/mol for inactivation of BLA without added calcium ions. The temperature dependent rate constant can, according to transition-state theory, be used to calculate the activation enthalpy ($\Delta H^{\neq}$) and entropy ($\Delta S^{\neq}$) of a thermoinactivation process [20]:

$$k = \frac{k_B T}{h} \exp\left(\frac{-\Delta H^{\neq}}{RT}\right) \exp\left(\frac{\Delta S^{\neq}}{R}\right) \tag{9}$$

where k_B is the Boltzmann's constant and h is Planck's constant. $\Delta H^{\neq}$ and $\Delta S^{\neq}$ were determined using the above equation to be 100 kJ/mol and 6,9 J mol^{-1} K^{-1}, respectively. Previously $\Delta H^{\neq}$ and $\Delta S^{\neq}$ values of 105 kJ/mol and 22,1 J mol^{-1} K^{-1}, respectively, have been reported for the irreversible thermal inactivation of BAA in 2 μM $CaCl_2$ at pH 7.0 [11].

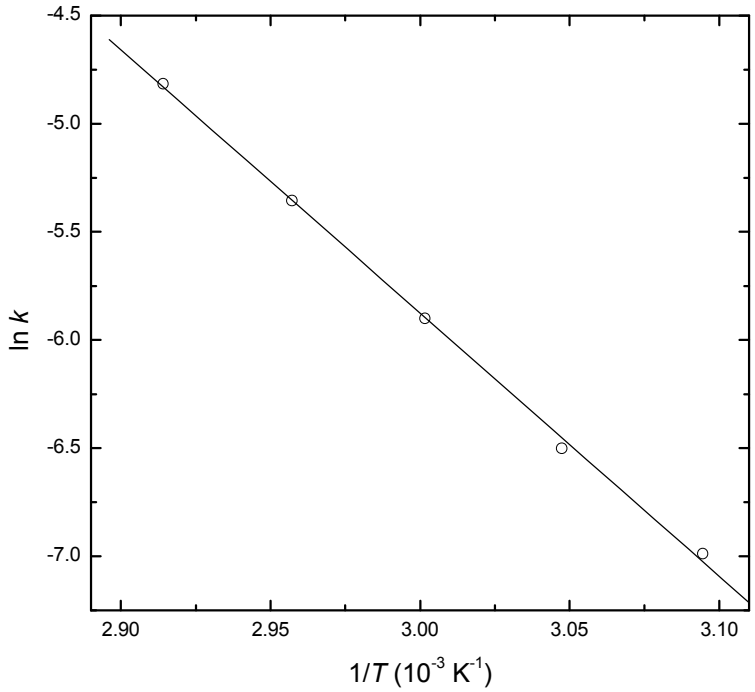

Fig. 3.6: Arrhenius plot of the denaturation rate constants (Table 3.1) of calcium depleted BHA in 20 mM HEPES, pH 8.0.

BHA calcium binding parameters have been determined by isothermal calorimetric titration of BHA/EGTA mixtures with $CaSO_4$ in the temperature range from 24 to 40°C. The latter temperature was chosen since the DSC and kinetic results indicate that no significant denaturation takes place below 40°C. Table 3.2 summarizes the obtained binding parameters. The binding affinity is in the order of 10^5 M^{-1} in the studied temperature range and decreases approximately linearly with temperature. An apparent stoichiometry of 1.4 is observed. The crystal structure of the structurally related BLA has revealed three calcium binding sites [14]. Under the assumption that BHA also contains three binding sites it is not unexpected to observe a stoichiometry higher than one. The observed stoichiometry provides

information about the ratio between the calcium affinity of BHA and EGTA and suggests, that BHA has one binding site with lower affinity than EGTA, one site with an affinity comparable to EGTA and possibly one site with an affinity higher than EGTA [19]. EGTA binds calcium with an affinity of 10^7-10^8 M^{-1} under the current experimental conditions (see Table 3.2). Hence, the observed stoichiometry indicate that BHA has one calcium site with an affinity of about 10^5 M^{-1} and one site with an affinity of about 10^7-10^8 M^{-1}.

Table 3.2: Calcium binding parameters of BHA and EGTA in 20 mM HEPES, pH 8.0 buffer.

Binding	BHA-Ca						EGTA-Ca	
Temperature (°C)	ΔH (kJ/mol)	K_{Ca} (M^{-1})	$\Delta G°$ (kJ/mol)	$-T\Delta S°$ (kJ/mol)	$\Delta S°$ (J/(mol K))	Apparent stoichiometry	ΔH (kJ/mol)	K (M^{-1})
19*	-11.5±0.1	$(7.6±0.6) \cdot 10^5$	-32.9±0.2	-21.4±0.3	73.3±1.0	1.4±0.1		
24	-11.3±0.3	$(7.3±0.2) \cdot 10^5$	-33.4±0.1	-22.1±0.4	74.4±1.3	1.3±0.1	-29.9±0.6	$(1.2±0.1) \cdot 10^8$
27	-11.1±0.2	$(6.8±0.8) \cdot 10^5$	-33.5±0.3	-22.4±0.5	74.6±1.7	1.4±0.1	-30.0±0.4	$(8.4±2.0) \cdot 10^7$
33	-11.0±0.1	$(5.7±0.4) \cdot 10^5$	-33.7±0.2	-22.7±0.3	74.1±1.0	1.4±0.1	-30.9±0.3	$(7.0±0.3) \cdot 10^7$
40	-10.8±0.3	$(5.1±0.3) \cdot 10^5$	-34.2±0.1	-23.4±0.4	74.7±1.3	1.3±0.1	-31.8±0.6	$(5.3±2.0) \cdot 10^7$

*: Values at 19°C from [19]

Both the binding enthalpy (ΔH=-11.1 kJ/mol at 27°C) and the changes in standard entropy ($T\Delta S°$=22.4 kJ/mol at 27°) contribute favorably to the binding. $T\Delta S°$ accounts for approximately 2/3 of the change in standard free energy ($\Delta G°$=-33.5 kJ/mol). The large positive ΔS value suggests that a dehydration process is involved in the binding of calcium to BHA. One such contribution may arise from the release of 6 coordinated water molecules around the calcium ion [21] upon binding to BHA. Furthermore, release of water molecules from the calcium binding site may contribute to increase in entropy upon calcium binding. Another possible source of entropy increase is dehydration of non-polar surfaces upon calcium binding either at the binding site or as a result of coupled conformational changes in the protein. Changes in the heat capacity function, C_p, can be used to estimate the significance of hydrophobic effects and it has been reported that dehydration of non-polar surfaces results in negative change in C_p which scales with the dehydrated surface area [22;23]. Apparently ΔH increases slightly with temperature corresponding to a small positive change in heat capacity of approximately 30 J/(mol K). Therefore, it seems unlikely that dehydration of non-polar surfaces contribute significantly in the calcium binding process.

Tanaka & Hoshino [11] have estimated the thermodynamic calcium binding parameters of BAA by inactivation kinetics at 45-65°C. The estimated van't Hoff $\Delta H°$ and $\Delta S°$ values were -149 kJ/mol and -360 J/(mol K) respectively. However, the authors note that their values may include contributions from both calcium binding and structural changes in the protein. In contrast, our reported ΔH values are not expected to contain significant contributions from structural changes in the protein, since both the DSC and kinetic results indicate no significant structural changes in both calcium-bound and -depleted amylase below 40°C where all binding experiments were performed. When the obtained K_{Ca} values in table 2 are introduced into a van't Hoff plot $\Delta H°$ and $\Delta S°$ values respectively -16±2 kJ/mol and 60±5 J/(mol K) are obtained (See Fig. 3.7). Thus, the van't Hoff values are in good agreement with the calorimetric values listed in Table 3.2. Furthermore, our binding enthalpy values compare well with a reported ΔH value of -16 kJ/mol (at 27°) for BAA calcium binding, which have been determined using microcalorimetry [24].

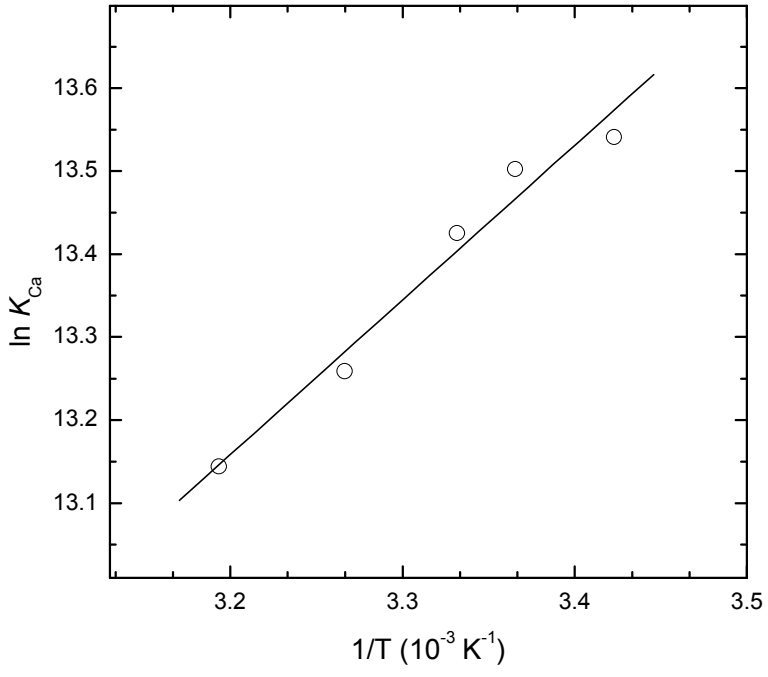

Fig. 3.7: van't Hoff plot of the obtained BHA-calcium binding constants (Table 3.2).

Combination of kinetic denaturation data and calcium binding constants can be used to predict the combined effect of free calcium and temperature on the apparent inactivation rate constant (k_{app}) for BHA. According to scheme 1, k_{app} can be determined using the following equation, which is based on pre-equilibrium approximations [11]:

$$k_{app} = \frac{k_{den*} + K_{Ca} k_{den} [Ca^{2+}]}{K_{Ca} [Ca^{2+}] + 1} \quad (10)$$

Calculation of k_{app} thus requires knowledge of both inactivation rate constants of calcium bound and depleted BHA and also the calcium binding constant. At low temperature the contribution from denaturation of calcium bound BHA is insignificant, since inactivation proceeds almost exclusively as denaturation of calcium depleted BHA. Based on the DSC thermograms (Fig. 3.1) it is expected that the denaturation of calcium bound BHA is negligible below 65°C. Hence, eqn (10) reduces to:

$$k_{app} = \frac{k_{den*}}{K_{Ca} [Ca^{2+}] + 1} \quad (11)$$

, where only knowledge of the inactivation constant of calcium depleted BHA and the calcium binding constant is required. In the absence of free calcium ions ($[Ca^{2+}]=0$) eqn (11) further reduces to simply state that $k_{app} = k_{den*}$.

Using the Arrhenius equation and the E_A value of calcium depleted BHA we have estimated k_{den*} values at temperatures from 20 to 60°C. Extrapolation of the van't Hoff plot (Fig. 3.7) has been used to estimate K_{Ca} values in the same temperature range.

k_{app} values of the calcium depleted BHA were estimated using eqn (11) and the corresponding half-lifes ($t_{1/2}$) calculated. The estimated values are listed in table 3.3. Similarly, apparent $t_{1/2}$ values at free calcium concentration up to 100 μM were estimated. Fig. 3.8 illustrates the increase of $t_{1/2}$ upon increasing the free calcium concentration at temperatures from 20 to 60°C. At 20°C the free calcium concentration has a major effect on the half-life of BHA. Thus, increasing the free calcium concentration from 0 to 100 μM increases the apparent half-life from

approximately 10 to 750 hours. At 60°C a similar increase in the free calcium concentration increases $t_{1/2}$ from 4 min. to 2 hours. To obtain an apparent half-life of 10 hours at 60°C a free calcium concentration of more than 500 μM is required.

Table 3.3: Kinetic unfolding and calcium binding parameters of BHA at 20-60°C in 20 mM HEPES, pH 8.0 buffer.

Temperature (°C)	$k_{unf^*} \cdot 10^5$ (s^{-1})	$K_{Ca} \cdot 10^{-5}$ (M^{-1})	$t_{1/2}$ (min)
20	2.0[#]	7.6[§]	590
30	7.7[#]	6.3[§]	150
40	28[#]	5.0[§]	42
50	92[¤]	3.8[*]	13
60	290[¤]	2.5[*]	4.0

[#]: extrapolated value from Arrhenius plot (Fig. 3.6)
[¤]: interpolated value from Arrhenius plot (Fig. 3.6)
[§]: interpolated value from van't Hoff plot (Fig. 3.7)
[*]: extrapolated value from van't Hoff plot (Fig. 3.7)

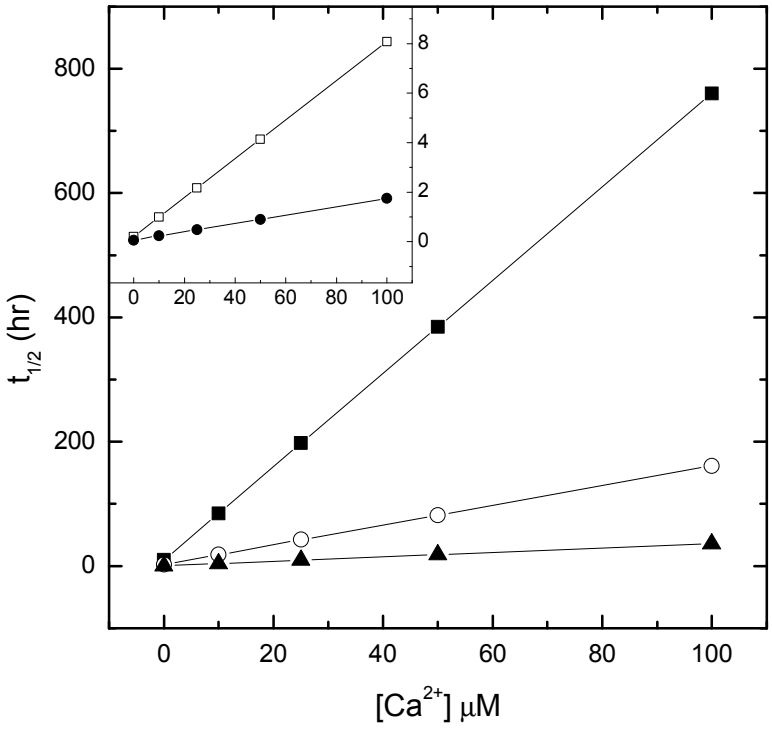

Fig. 3.8: Correlation between free calcium concentration and estimated apparent half-life of BHA in 20 mM HEPES, pH 8.0 at the following temperatures: 20 (filled squares), 30 (open circles), 40 (filled triangles), 50 (open squares) and 60°C (filled circles).

The estimated k_{app} values have also provided basis for construction of Arrhenius plots at different concentrations of free calcium ions. Hence, it has been possible to estimate apparent E_A values as a function of free calcium concentration (see Fig. 3.8). At low calcium concentration even small changes has a notable effect on E_A. For example, increasing the free calcium concentration form 0 to 2 μM increases E_A from 101 to 112 kJ/mol. Only minor increases in E_A are observed at higher calcium concentrations, and the E_A appear to asymptotically approach a value of 123 kJ/mol at high calcium concentrations (see Fig. 3.9). The data suggests that it is possible to increase the apparent E_A almost 22 kJ/mol by increasing the free calcium concentration. Violet & Meunier has previously found an E_A value of 155.4 kJ/ml for BLA in the presence of 5 mM $CaCl_2$ [6].

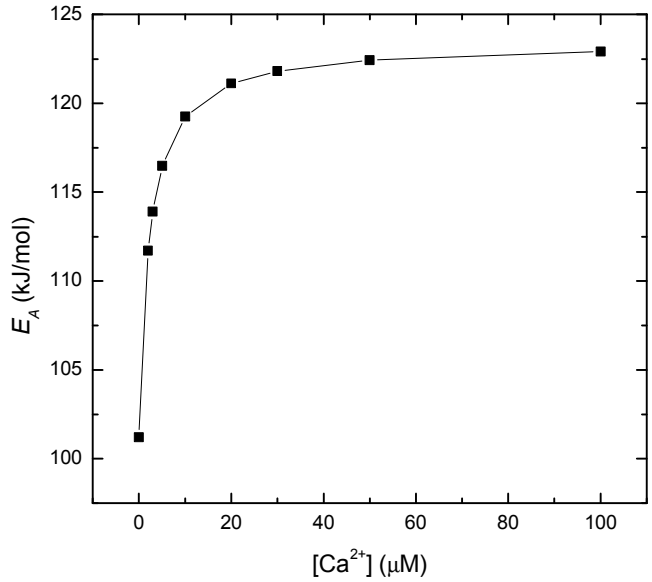

Fig. 3.9: Estimated apparent activation energy of BHA denaturation as a function of free calcium concentration in 20 mM HEPES, pH 8.0 at temperatures below 65°C where only denaturation of calcium depleted BHA takes place.

In summary, it was found that calcium ions have significant effect on the thermal stability of BHA. Thus, removal of calcium ions from a BHA solution leads to an apparent decrease in stability of approximately 35°C. This calcium dependent difference in thermal stability has been used to investigate the irreversible denaturation of BHA upon calcium depletion. The data support the kinetic denaturation mechanism proposed by Tanaka & Hoshino [11]. In this model, the calcium depleted enzyme unfolds irreversibly at low temperature. When calcium

ions are in excess the enzyme unfold irreversibly at high temperature. Therefore, the two denaturation reactions are coupled through the calcium binding equilibrium. This equilibrium has been quantified in this work and used, together with the kinetic data to estimate the half-life of BHA as function of temperature and free calcium ion concentration.

The calorimetric approach developed in this study appears to be a robust method in investigation of the effect of temperature and calcium ions on the stability of amylase. Hence, relatively few experimental trials are needed to obtain detailed kinetic and thermodynamic information. It seems likely that the procedures used in this study could be applicable to other protein systems where calcium ions or other divalent metal ions have significant effect on the thermal stability. As an example it has been reported that removal of calcium ions from bovine α-lactalbumin decrease the thermostability about 40°C [25].

3.5 Acknowledgements

This work was supported by the Danish Academy of Technical Sciences and the Carlsberg Foundation. The skillful technical assistance of Bodil Larsen is greatly acknowledged.

3.6 References

1 Guzmán-Maldonado, H. and Paredes, L. (1995) Amylolytic enzymes and products derived from starch: a review. Crit. Rev. Food Sci. Nutr. **35**, 373-403

2 Vihinen, M. and Mäntsälä, P. (1989) Microbial amylolytic enzymes. Crit. Rev. Biochem. Mol. Biol. **24**, 329-418

3 Nielsen, J. E. and Borchert, T. V. (2001) Protein engineering of bacterial α-amylases. Biochem. Biophys. Acta **1543**, 253-274

4 Buisson, G., Duée, E., Haser, R., and Payan, F. (1987) Three dimensional structure of porcine pancreatic alpha-amylase at 2.9 a resolution. Role of calcium in structure and activity. EMBO J. **6**, 3909-3916

5 Vallee, B. L., Stein, E. A., Sumerwell, W. N., and Fischer, E. H. (1959) Metal content of amylases of various origins. J. Biol. Chem. 234, 2901-2905

6 Violet, M. and Meunier, J. C. (1989) Kinetic study of the irreversible thermal denaturation of *Bacillus-licheniformis* alpha amylase. Biochem. J. **263**, 665-670

7 Declerck, N., Machius, M., Wiegand, G., Huber, R., and Gaillardin, C. (2000) Probing structural determinants specifying high thermostability in *Bacillus licheniformis* alpha-amylase. J. Mol. Biol. **301**, 1041-1057

8 Oh, H. S., Kim, K. H., Suh, S. W., and Choi, M. (1991) Spectroscopic and electrophoretic studies on structural stability of alpha amylase from *Bacillus-amyloliquefaciens*. Korean Biochem. J. **24**, 158-167

9 Bush, D. S., Sticher, L., van Huystee, R., Wagner, D., and Jones, R. L. (1989) The calcium requirement for stability and enzymatic activity of two isoforms of barley aleurone alpha-amylase. J. Biol. Chem. **264**, 19392-19398

10 Lecker, D. N. and Khan, A. (1996) Theoretical and experimental studies of the effects of heat, EDTA, and enzyme concentration on the inactivation rate of alpha-amylase from bacillus sp. Biotechnol. Prog. **12**, 713-717

11 Tanaka, A. and Hoshino, E. (2002) Calcium-binding parameter of *Bacillus amyloliquefaciens* alpha-amylase determined by inactivation kinetics. Biochem. J. **364**, 635-639

12 Boel, E., Brady, L., Brzozowski, A. M., Derewenda, Z., Dodson, G. G., Jensen, V. J., Petersen, S. B., Swift, H., Thim, L., and Woldike, H. F. (1990) Calcium binding in alpha-amylases: an x-ray diffraction study at 2.1- some resolution of two enzymes from *Aspergillus*. Biochemistry **29**, 6244-6249

13 Machius, M., Wiegand, G., and Huber, R. (1995) Crystal structure of calcium-depleted *Bacillus licheniformis* alpha-amylase at 2.2 a resolution. J. Mol. Biol. **246**, 545-559

14 Machius, M., Declerck, N., Huber, R., and Wiegand, G. (1998) Activation of *Bacillus licheniformis* alpha-amylase through a disorder - order transition of the substrate-binding site mediated by a calcium-sodium-calcium metal triad. Structure **6**, 281-292

15 Fujimoto, Z., Takase, K., Doui, N., Momma, M., Matsumoto, T., and Mizuno, H. (1998) Crystal structure of a catalytic-site mutant alpha-amylase from *Bacillus subtilis* complexed with maltopentaose. J. Mol. Biol. **277**, 393-407

16 Plotnikov, V. V., Brandts, J. M., Lin, L., and Brandts, J. F. (1997) A new ultrasensitive scanning calorimeter. Anal. Biochem. **250**, 237-244

17 Willson, R. J., Beezer, A. E., Mitchell, J. C., and Loh, W. (1995) Determination of thermodynamic and kinetic-parameters from isothermal heat-conduction microcalorimetry - applications to long-term-reaction studies. J. Phys. Chem. **99**, 7108-7113

18 Wiseman, T., Wiliston, S., Brandts, J. F., and Lin, L.-N. (1989) Rapid measurement of binding constants and heats of binding using a new titration calorimeter. Anal. Biochem. **179**, 131-137

19 Nielsen, A. D., Fuglsang, C. C., and Westh, P. (2003) Isothermal titration calorimetric procedure to determine protein-metal ion binding parameters in the presence of excess metal ion or chelator. Anal. Biochem. **314**, 227-234

20 Eyring, H. (1935) The activated complex and the absolute rate of chemical reactions. Chem. Rev. **17**, 65-77

21 Enderby, J. E. (1981) Ions in aqueous solutions. Science Progress **67**, 553-574

22 Spolar, R. S., Ha, J.-H., and Record, T. R. Jr. (1989) Hydrophobic effect in protein folding and other noncovalent processes involving proteins. Proc. Nat. Acad. Sci. U.S.A. **86**, 8382-8385

23 Mirejovsky, D. and Arnett, E. M. (1983) Heat capacity of the solution for alcohols in polar solvents and the new view of hydrophobic effects. J. Am. Chem. Soc. **105**, 1112-1117

24 Saboury, A. A. and Karbassi, F. (2000) Thermodynamic studies on the interaction of calcium ions with alpha-amylase. Thermochim. Acta **362**, 121-129

25 Hendrix, T., Griko, Y. V., and Privalov, P. L. (2000) a calorimetric study of the influence of calcium on the stability of bovine alpha-lactalbumin. Biophys. Chem. **84**, 27-34

4

Paper III

A proposed mechanism for the thermal denaturation of a recombinant *Bacillus halmapalus* a-amylase – the effect of calcium ions

Anders D. Nielsen [a,b], Marc L. Pusey [c], Claus C. Fuglsang [b], Peter Westh [a]

[a] Department of Life Sciences and Chemistry, Roskilde University
P.O.Box 260, DK-4000 Roskilde, Denmark

[b] Novozymes A/S, Novo Allé, DK-2880 Bagsværd, Denmark

[c] Biophysics SD48, NASA/Marshall Space Flight Center, Huntsville, Alabama 35812, USA

Biochimica et Biophysica Acta, **2003**, In press (doi:10.1016/j.bbapap.2003.08.002)

4.1 Abstract

The thermal stability of a recombinant α-amylase from *Bacillus halmapalus* α-amylase (BHA) has been investigated using circular dichroism spectroscopy (CD) and differential scanning calorimetry (DSC). This α-amylase is homologous to other *Bacillus* α-amylases where crystallographic studies have identified the existence of 3 calcium binding sites in the structure. Denaturation of BHA is irreversible with a T_m of approximately 89°C and DSC thermograms can be described using a one-step irreversible model. A 5°C increase in T_m in the presence of 10 fold excess $CaCl_2$ was observed. However, a concomitant increase in the tendency to aggregate was also observed. The presence of 30-40 fold excess calcium chelator (EDTA or EGTA) results in a large destabilization of BHA, corresponding to about 40°C lower T_m as determined by both CD and DSC. Ten fold excess EGTA reveals complex DSC thermograms corresponding both reversible and irreversible transitions, which probably originate from different populations of BHA:calcium complexes. Combined interpretation of these observations and structural information on homologous α-amylases, forms the basis for a suggested mechanism underlying the inactivation mechanism of BHA. The mechanism includes irreversible thermal denaturation of different BHA:calcium complexes and the calcium binding equilibria. Furthermore, the model accounts for a temperature induced reversible structural change associated with calcium binding.

Keywords: Protein-ligand interaction; calcium binding; calorimetry; circular dichroism; α-amylase; denaturation mechanism

Abbreviations: BHA, *Bacillus halmapalus* α-amyalse; BLA, *Bacillus licheniformis* α-amylase; BAA, *Bacillus amyloliquefaciens* α-amylase; BStA, *Bacillus stearothermophillus*; ITC, isothermal titration calorimetry; DSC, differential scanning calorimetry; CD, circular dichroism spectroscopy; EDTA, ethylenediaminetetraacetic acid; EGTA, ethylene glycol-bis[β-aminoethyl ether] *N,N,N',N'*-tetraacetic acid

4.2 Introduction

α-amylases (α-1,4 glucan-4-glucanohydrolase, EC 3.2.1.1) are amylolytic enzymes which catalyze the hydrolysis of internal α-1,4-glycosidic linkages in amylose and amylopectin. The enzymes are industrially important and widely used in the food and detergent industries [1-4]. The α-amylases from *Bacillus* species *licheniformis*, *amyloliquefaciens* and *stearothermophillus* are among the most widely studied amylases. These α-amylases are highly homologues with respect to primary and tertiary structure [5]. Thus, the sequence similarity between α-amylase from: *Bacillus licheniformis* (BLA) and *Bacillus amyloliquefaciens* (BAA) is 80% and BLA and *Bacillus stearothermophillus* (BStA) is 65% [6]. Furthermore, it is also expected that the three-dimensional structure of the amylases are very similar [7;8]. This is evident from the crystal structures of BLA and BStA. The structures are characterized by three distinct domains: a central core domain, termed domain A, containing a $(\beta/\alpha)_8$ barrel, domain B, a long complex loop protruding from the third strand and third helix of the barrel and the C-terminal, domain C, which contain a Greek key motif [8-10].

A characteristic feature of α-amylases is their requirement for calcium to maintain their structural integrity [1;11] and removal of calcium leads to decreased thermostability and enzymatic activity [12]. All known α-amylases contain a conserved calcium binding site, CaI, which is located at the interface between domain A and B [7;10;13]. The binding affinity is high [11] which is illustrated by a binding constant of $2 \cdot 10^{11}$ M^{-1} reported for pig pancreatic α-amylase [14]. Two additional calcium binding sites have been identified in α-amylases of the *Bacillus* species *licheniformis* [10] and *stearothermophillus*.[9]. CaII is located in close proximity to CaI and the two calcium ions form a triad with one sodium ion. Mutations in the region surrounding CaI and CaII resulted in collapse of the thermostability of BLA [5;15]. Another calcium binding site (CaIII) is located at the interface between domains A and C where it acts as a "bridging" ion. The three dimensional structure of BAA is not yet available. However, the structure of a chimeric protein constructed from the genes encoding for BAA and BLA [16] provides information on the calcium bindings sites in BAA. CaI and CaII were identified in the chimera where the residues involved originated from BAA. A calcium binding site corresponding to CaIII was also identified as well as a site

which also likely binds a calcium ion. Despite the structural similarities between the present amylases they display significant differences in their thermal resistance, with half-lifes at 90°C of 2, 50 and 270 min. for BAA, BStA and BLA respectively [17]. It has been suggested that thermal inactivation of *Bacillus* α-amylases is a two step process, involving reversible unfolding followed by an irreversible conformational or covalent change [12;17;18]. Other models include the role of calcium ions in connection to thermal inactivation. Thus, it has been proposed that the first step includes a reversible dissociation of calcium ions from the native enzyme, followed by irreversible denaturation at high temperatures [19-22].

In this study, we propose a mechanism for the thermal denaturation of a recombinant α-amylase from *Bacillus halmapalus* (BHA) and the role of calcium ions. The mechanism is based on calorimetric and spectroscopic observations of the thermal stability of BHA and the effect of calcium ions combined with structural information from *Bacillus* α-amylases that are homologous to BHA [23].

4.3 Materials and methods

4.3.1 Materials

Recombinant BHA was expressed in *Bacillus licheniformis* and purified to >95%, determined by SDS/PAGE, at Novozymes A/S, Bagsvaerd, Denmark. The protein was extensively dialyzed, at 5°C, against 10 mM borate buffer with pH of 8.0, 9.0 or 10.0 for use in spectroscopic experiments or 20 mM borate, pH 8.0 for calorimetric experiments. All buffers were passed through Chelex 100 columns to remove excess calcium ions. The calcium concentration was adjusted by addition of $CaCl_2$, EDTA or EGTA. The following chemicals were used: boric acid (>99.8%, Merck, Darmstadt, Germany), ethylenediaminetetraacetic acid, EDTA (>99%, Merck, Darmstadt, Germany), ethylene glycol-bis[β-aminoethyl ether] *N,N,N',N'*-tetraacetic acid, EGTA (>97%, Sigma, St. Louis, MO, USA) and calcium chloride, $CaCl_2$ (>99%, Merck, Darmstadt, Germany).

4.3.2 Circular dichroism spectroscopy

Spectra of BHA in the far-UV region (185-260 nm) were recorded on an OLIS-DSM 1000 CD spectropolarimeter. The light path of the cuvette was 1 mm and a protein concentration of 2.7 – 3.4 μM was used. Spectra were recorded at selected temperatures in the range 20 – 95°C using an external circulating water bath. The protein solution was allowed to equilibrate 7 min. at each temperature before recording was initiated. Each spectrum is an average of at least 10 scans. All spectra were background corrected, smoothed and transformed into mean residue ellipticity [θ]. A value of 114.7 g/mol was used as a mean residue weight for BHA. Titration experiments, with EDTA, were carried out using the automatic titrator supplied by OLIS.

4.3.3 Differential Scanning Calorimetry

DSC experiments were performed with a MicroCal VP-DSC (Northampton, MA) [24]. All enzyme solutions were dialyzed against the desired buffer, and the dialyzate was used as reference. Prior to scanning all solutions were degassed by stirring under vacuum. A pressure of 2 atm was applied over the cells during scanning. The concentration of BHA was 20-26 μM and buffer scans were subtracted from BHA scans. DSC data was analyzed using the Origin software from MicroCal, Inc. supplied with the instrument. Molar excess heat capacities (C_p) were obtained by normalizing with the BHA concentration and the volume of the calorimeter cell. Thermograms were analyzed using a model for irreversible unfolding [25] or using the successive annealing procedure [26]. A cubic baseline was subtracted prior to analysis. Apparent denaturation temperatures (T_m) values were determined as the temperature corresponding to maximum C_p.

4.4 Results and discussion

The main purpose of this work is to test the validity of a simple molecular model for the thermal inactivation of a recombinant *Bacillus halmapalus* α-amylase. As mentioned above previous work on homologous *Bacillus* α-amylases suggested that thermal inactivation is a two step process of reversible followed by an

irreversible unfolding step. Other models include a reversible calcium ion dissociation followed by irreversible denaturation. However, the previous models do not fully account for the observations in the present study, which motivated the search for a relevant mechanism. Before turning to a direct discussion of the proposed model, we examine the structural, kinetic and thermodynamic results retrieved here and in related work.

4.4.1 CD

Comparing the spectra of BHA at pH 8, 9 and 10, reveals no large differences. This indicates that there are only minor structural differences if any between the conformations of BHA over this pH range (Fig. 4.1).

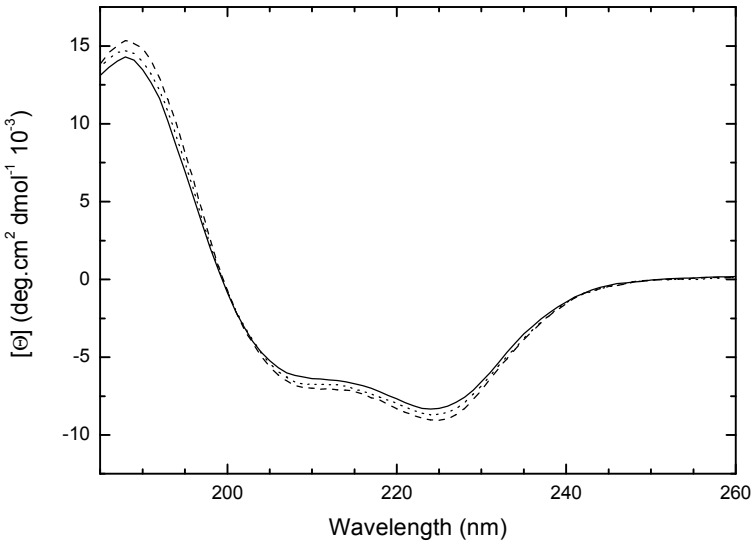

Fig. 4.1: CD spectra in the far-UV region of BHA (3.1-3.4 μM) in 10 mM borate buffer at pH 8.0 (—), pH 9.0 (---) and pH 10.0 (…) at 25°C.

The effect of calcium ions on the thermal denaturation of BHA has been studied by recording of CD spectra as a function of temperature with and without added EDTA. Fig. 4.2 illustrates the disruption of secondary structural elements upon increasing the temperature from 25°C to approximately 90°C at pH 8. Comparison of the spectra recorded without added EDTA and in the presence of 30 fold excess (molar ratio) EDTA reveals significantly different denaturation patterns. The

different denaturation patterns become obvious when the temperature dependence of the ellipicity at 222 nm is plotted (see insets in Fig. 4.2). The apparent denaturation temperature is approximately 48°C, corresponding to the temperature at the inflection point (inset in Fig. 4.2A), in the presence of excess EDTA. However, it is more difficult to determine the denaturation temperature of BHA without added EDTA, since the protein apparently is not completely denatured at the highest experimental temperature. It is thus estimated that the denaturation temperature is higher than 80°C. Previous CD results on BAA and BLA, at pH 7.5 without added calcium ions, provided T_m values of 72 and 85 °C, respectively [27].

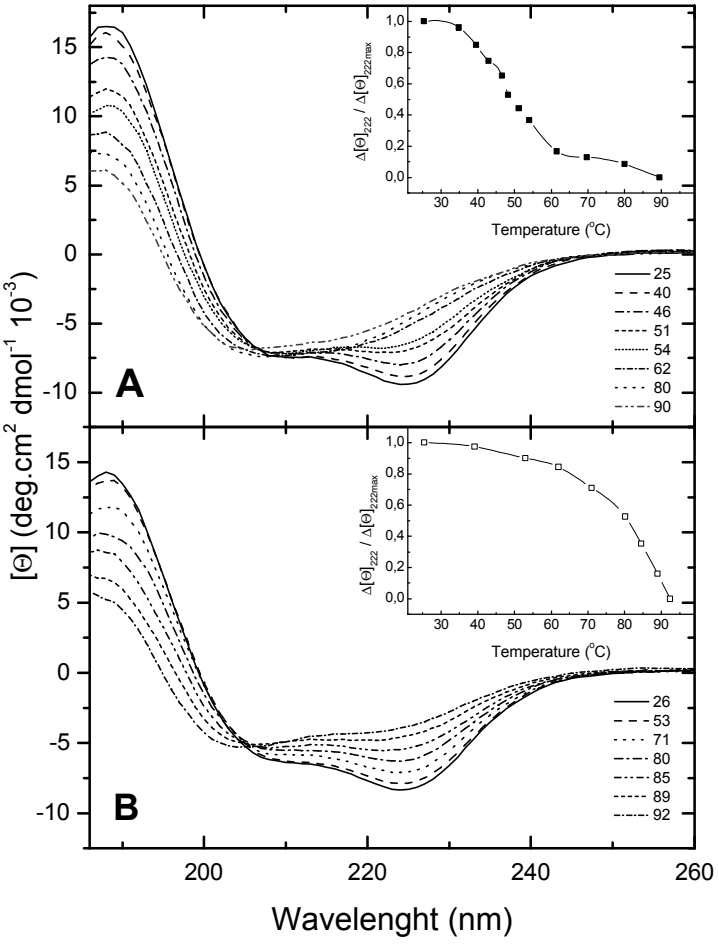

Fig. 4.2: CD spectra in the far-UV region of BHA in 10 mM borate, pH 8.0 buffer – the effect of temperature and calcium chelator. (A) Spectra of 3.1 μM BHA in the presence of 100 μM EDTA at temperatures between 25 and 90°C (se legend). (B) Spectra of 3.4 μM BHA without chelator at temperatures between 26 and 92°C (se legend). The insets illustrate the relative change in ellipicity at 222 nm vs. temperature.

Titration of BHA with EDTA up to a molar ratio of 10 at 25°C indicates only minor changes in the secondary structure (Fig. 4.3). Above 215 nm no significant changes in the spectra is observed. However, a visible increase in ellipicity in the region about 190 nm is observed at a molar ratio of 10. This shift in ellipicity may reflect minor local changes in the secondary structure around calcium binding sites upon calcium removal. In contrast, CD titration of BAA have revealed that even small amounts of calcium ions (corresponding to a molar ratio of less than 2) induces distinct differences in the UV region 200-220 nm [28].

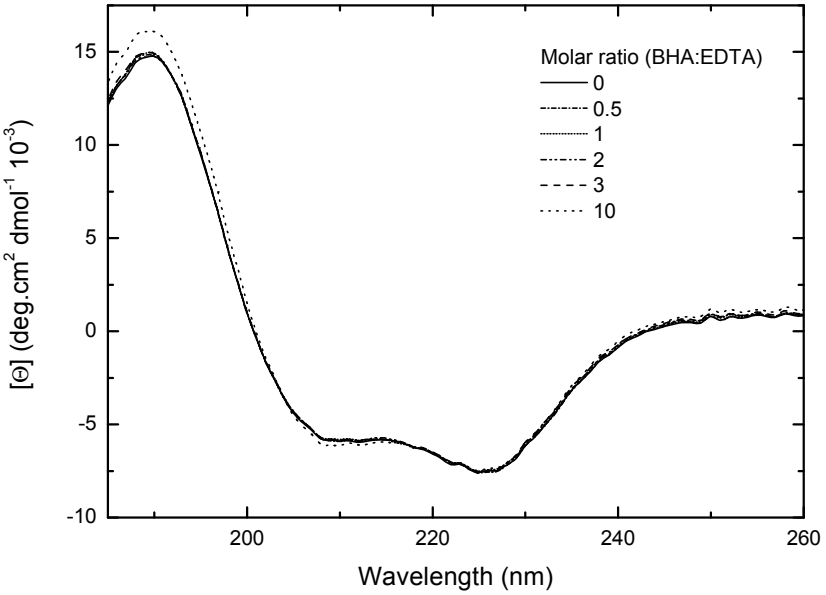

Fig. 4.3: EDTA titration of 3.4 μM BHA followed by CD in the far-UV region at 25°C in 10 mM borate, pH 8.0 buffer. The molar ratios (BHA:EDTA) are shown in the legend.

4.4.2 DSC

The thermal stability of BHA was investigated using DSC. Without added calcium ions, an apparent T_m of 92°C at a scan rate of 1.5 °C/min. is observed (see scan 8 in Fig. 4.4). The denaturation is irreversible, which is clearly illustrated by performing a rescan, where no significant peaks in the thermogram are observed. In order to further examine the reversibility of the BHA denaturation process we performed repeated scans where the final temperature was gradually increased (see

Fig. 4.4). From the resulting thermograms, it is evident that the process is almost completely reversible up to 80°C at a scan rate of 1.5 °C/min.

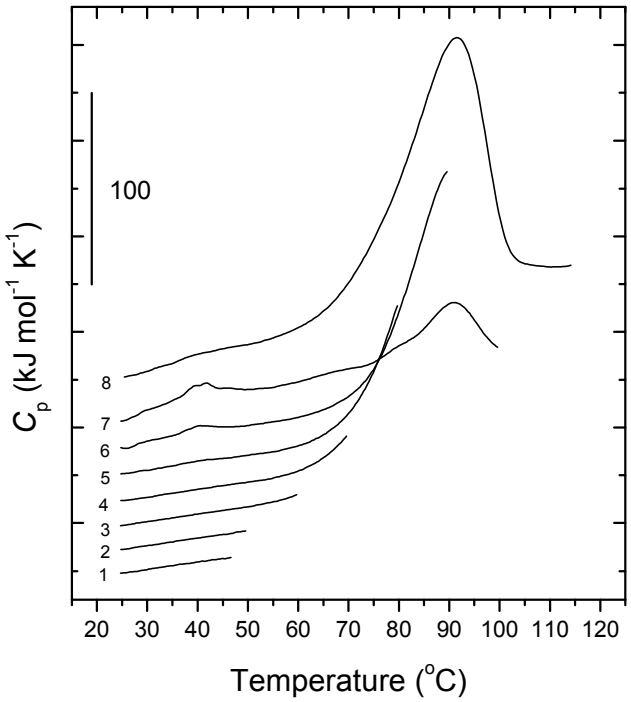

Fig. 4.4: DSC thermogram of 26 μM BHA denaturation in 20 mM borate, pH 8.0 buffer. Scans 1-7 represent thermograms from repeated heating and subsequent cooling. The scans were stopped at 46 (1), 50 (2), 60 (3), 70 (4), 80 (5), 90 (6) and 100°C (7). Scan 8 is a full scan up to 115°C. Almost complete reversibility is observed up to 80°C. All experiments were performed at a scan rate of 1.5 °C min^{-1}.

Decreasing the scan rate results in a lower apparent T_m value. Thus, decreasing the scan rate from 1.5 °C/min to 0.5 °C/min resulted in a 6°C lower apparent T_m value (see Fig. 4.5). Scan rate dependence is a typical hallmark of kinetically controlled processes [29-31] which suggests that an irreversible step takes place during denaturation of BHA. Previous differential scanning calorimetric investigations of the thermal unfolding of *Bacillus* α-amylases have applied models based on equilibrium thermodynamics despite the fact that the amylases unfolded irreversibly. Feller *et al.* have deconvoluted the thermograms of BAA and BLA according to a model for reversible two-state unfolding of three cooperative domains [32]. This analysis was carried out under the assumption that the

irreversible process did not impair the calorimetric trace. Similar deconvolution of calorimetric traces from BAA and BLA has been used by Fitter *et al.* [33]. The Authors justified their approach by the minor scan rate dependence of the apparent T_m. The significant scan rate dependence in the case of BHA does not justify the application of models based on reversibility in the analysis of the thermograms. Therefore, a deconvolution of the BHA thermograms was carried out according to models for kinetically controlled protein denaturation.

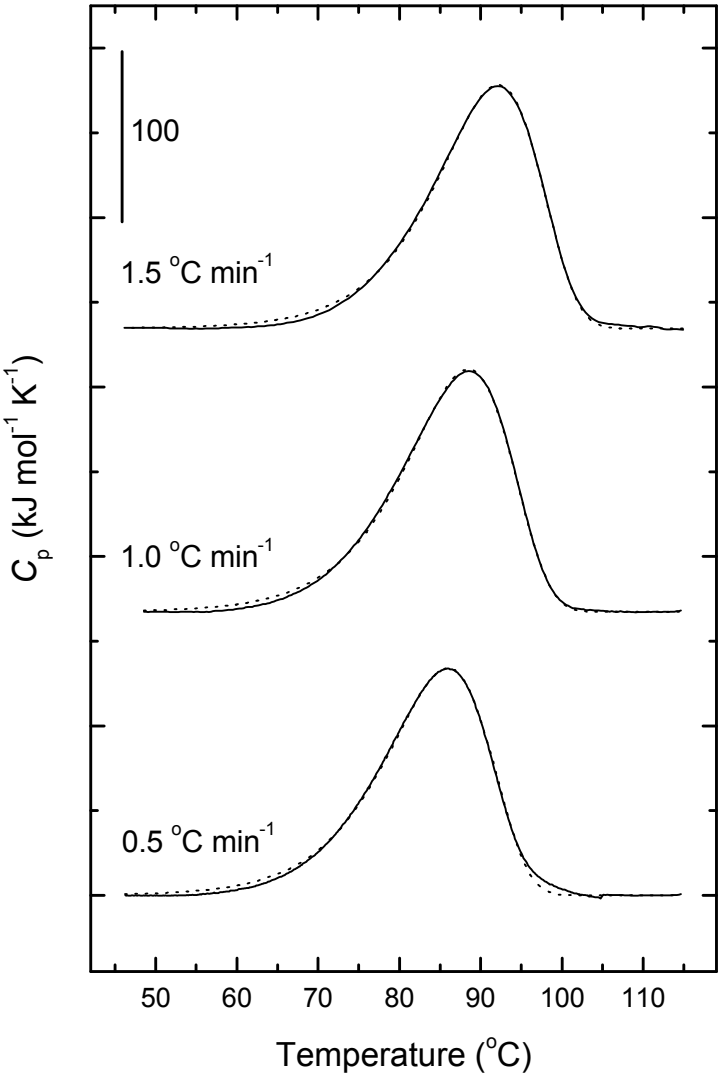

Fig. 4.5: Denaturation of 26 μM BHA in 20 mM borate, pH 8.0 buffer at scan rates from 0.5 – 1.5 °C min^{-1}. Solid lines are DSC thermograms obtained experimentally, after baseline subtraction, and dashed lines are the result of fitting to a one-step irreversible model (Eq. (3)).

Irreversible denaturation of a protein is suggested to involve at least two steps according to the Lumry & Eyring model [34]. The first step is a reversible unfolding of the native, catalytically active enzyme (N). This is followed by an irreversible change of the denatured protein (D) into an irreversible inactivated state (I) that cannot fold back into the native state:

$$N \underset{k_2}{\overset{k_1}{\leftrightarrow}} D \overset{k_3}{\rightarrow} I \tag{12}$$

A special case of the Lumry & Eyring model is when $k_3 >> k_2$ where most of the D molecules will be converted to I as an alternative to refolding back into the native state. In this case, the denaturation process can be regarded as a one-step process following first-order kinetics:

$$N \overset{k}{\rightarrow} I \tag{13}$$

Rigorous procedures to analyze thermograms according to the above model have previously been developed [25;30]. The excess heat capacity can be described as [35]:

$$C_p^{ex} = \frac{\Delta H\, E_A}{R T_m{}^2} \exp\left(\frac{\Delta H\,(T - T_m)}{R T_m^2}\right) \times \exp\left\{-\exp\left(\frac{\Delta H\,(T - T_m)}{R T_m^2}\right)\right\} \tag{14}$$

Thus, it is possible to obtain the denaturation enthalpy (ΔH), activation energy (E_A) and T_m by fitting the thermograms to Eq. (14). The obtained parameters are presented in Table 4.1. Average values of 2443 kJ/mol and 88.9 °C is obtained for ΔH and T_m, respectively. ΔH and T_m values of 2038 kJ/mol and 85.7 °C for BAA and 2686 kJ/mol and 102.5 °C for BLA have been reported previously [32]. Similar T_m values but lower ΔH values, 1412 kJ/mol and 1521 kJ/mol for BAA and BLA respectively, have been reported by Fitter er al. [33]. This difference in ΔH values is somewhat surprising since both studies were performed in the presence of 1 mM $CaCl_2$ and at similar pH (respectively 7.2 and 7.4).

Table 4.1: Denaturation temperature, enthalpy and activation energy of irreversible denaturation of BHA in Borate buffer pH 8.0 (no added calcium)

Scanrate (°C min^{-1})	T_m [#] (°C)	ΔH [#] (kJ mol^{-1})	E_A [#] (kJ mol^{-1})	E_A [$] (kJ mol^{-1})	E_A [*] (kJ mol^{-1})	E_A [§] (kJ mol^{-1})	E_A [&] (kJ mol^{-1})
0.5	86.0 ± 0.2	2434 ± 197	173 ± 4	175 ± 4	172 ± 9	179 ± 9	
1.0	88.8 ± 0.5	2468 ± 15	171 ± 5	173 ± 2	162 ± 3	173 ± 1	
1.5	91.7 ± 0.9	2427 ± 149	170 ± 11	169 ± 11	166 ± 13	175 ± 14	
Average	88.9 ± 3	2443 ± 22	172 ± 2	172 ± 3	167 ± 5	176 ± 3	204 ± 32

[#]: determined using Eq.(14)
[$]: determined using Eq.(15)
[*]: determined using Eq.(16)
[§]: determined using Eq.(17)
[&]: determined using Eq.(18)

The thermograms contain kinetic information that allows one to calculate the activation energy of the one-step process in several different ways [25;30;36]: (a) from estimated values of ΔH, the maximum excess C_p value ($C_{p,max}$) and T_m:

$$E_A = \frac{e R T_m^2 C_{p,\max}}{\Delta H} \tag{15}$$

(b) from an Arrhenius plot (ln k vs. $1/T$).

$$\ln\left(\frac{n\, Q_t}{Q_t - Q}\right) = \frac{E_A}{R}\left(\frac{1}{T}\right) + \text{constant} \tag{16}$$

where Q_t is the total heat for the denaturation process and Q is the heat evolved at a given temperature.n is the scan rate. (c) from the temperature dependence of Q:

$$\ln\left(\ln\left[\frac{Q_t}{Q_t - Q}\right]\right) = \frac{E_A}{R}\left(\frac{1}{T_m} + \frac{1}{T}\right) \tag{17}$$

(d) from the scan rate dependence of T_m:

$$\ln\left(\frac{n}{T_m^2}\right) = \text{constant} - \frac{E_A}{R\, T_m} \tag{18}$$

Eqs. (15-18) have been used to calculate E_A and the obtained values are listed in table 4.1. It is clear that there is a sufficient agreement between the E_A values determined using the different methods, thus supporting the validity of the proposed kinetic model outlined in Eq. (13). Only the value obtained using Eq. (18) is somewhat larger compared to the other values and with a higher standard deviation. It should be noted that this value is determined using only a single data point (at T_m) from each DSC curve whereas the other values are determined based on large temperature intervals of the DSC curves. We therefore conclude that the activation energies calculated according to eqs. (15-17) are in accordance with the one-step irreversible description of the BHA denaturation process. In comparison, we have previously determined an activation energy of 101 kJ/mol for partially calcium depleted BHA [37]. This value is considerably lower than the present E_A values (on average 178 kJ/mol, Table 4.1) for the denaturation of BHA with bound calcium ions, and signify the effect of calcium ions on the kinetic stability of BHA.

The effect of calcium ions on the thermal stability of BHA was investigated by DSC scan with added calcium salts. A correlation between added $CaCl_2$ and the apparent T_m is observed (see Fig. 4.6). In the presence of 3 fold excess $CaCl_2$ (3:1 $CaCl_2$:BHA) T_m is increased 4°C from approximately 91 to 95°C. The stabilizing effect is also reflected in a higher ΔH (data not shown), which is expected in case of exothermic ligand binding [38]. Increasing the $CaCl_2$ concentration further to 6 fold excess results in a similar apparent T_m, but also aggregation is observed. This is illustrated by the exothermic heat flow at the end of the denaturation process, and permits estimation of ΔH values. No significant increase in T_m is observed upon addition of 10 fold excess $CaCl_2$, but aggregation is notably enhanced. The T_m values in the presence of 6 and 10 fold excess $CaCl_2$ should be regarded as a minimum values due to aggregation. Similar effects on the thermal stability and aggregation of BHA was observed by addition of excess $CaSO_4$ (data not shown). Khajeh et al. [27] have previously observed that BAA aggregation at 70°C is reduced upon addition of 10 mM $CaCl_2$.

The data confirms the stabilizing effect of calcium ions, but also indicate their role in the aggregation process. It is noticeable that even very low concentrations of calcium ions (corresponding to a BHA:Ca molar ratio of 1:6) have a large effect on the tendency of BHA to aggregate. This indicates that calcium ions are involved in a specific interaction between BHA molecules.

Therefore, we suggest that calcium ions may act as a "bridging" atom between denatured or partially denatured BHA molecules. Aggregation of BHA at high temperatures has also been observed in HEPES buffer in the presence of calcium ions, but heavy aggregation was seen in the presence of only two fold excess calcium ions [37]. From thermograms (Fig. 4.6), where the final part of the C_p - curve is not distorted due to aggregation, it is possible to estimate the change in heat capacity (ΔC_p) upon denaturation of BHA by extrapolating the C_p signal of the native ($C_{p,N}$) and denatured ($C_{p,D}$) state of the protein. An ΔC_p value of 30-35 kJ/(mol K) is obtained as the difference between $C_{p,N}$ and $C_{p,D}$ at T_m. This value is large but similar to values reported for α-amylases from *Alteromonas haloplanctis* (35.4 kJ/(mol K)), BAA (36.0 kJ/(mol K)) and Taka-amylase from *Aspergillus oryzae* (36.4 kJ/(mol K)) [32;39].

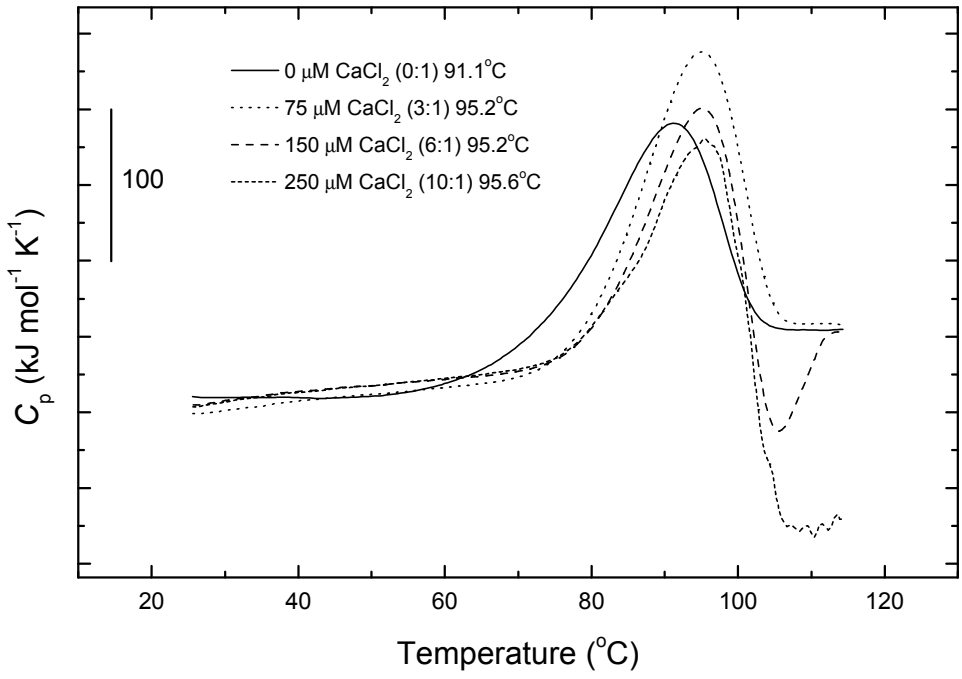

Fig. 4.6: Effect of excess $CaCl_2$ on denaturation of BHA in 20 mM borate, pH 8.0 buffer. The $CaCl_2$ concentration and the corresponding molar ratio (BHA:Ca) is shown in the legend together with the apparent T_m value. At molar ratios of 6 and 10 aggregation is evident as exothermic heat flows at the highest temperatures. A scan rate of 1.5 °C min^{-1} was used in all experiments.

The effect of calcium ions on the stability of BHA was further elucidated by performing DSC scans in the presence of the strong calcium chelator EGTA. Addition of 1 mM EGTA (corresponding to approximately 40 fold excess EGTA) result in considerably reduced thermal stability of BHA (see Fig. 4.7A). Hence, the thermogram shows a large narrow peak with maximum around 50°C. However, it is also possible to observe some minor peaks around 80°C. Significant changes in the thermogram are observed upon reducing the scan rate, and the apparent T_m decreases. Similar experiments in the presence of 10 fold excess EGTA also displayed a large narrow peak around 50°C, but a least two other peaks can be identified (see Fig. 4.7B). One broad peak has maximum around 65°C and another peak is observed at 70°C. Large differences in the thermogram are observed when the scan rate is decreased and apparently the peak around 65°C is reduced whereas the size of the peak at 50°C is increased. The additional transitions in the thermograms obtained in 10 fold, compared to thermograms obtained in 40 fold, excess EGTA suggests that some BHA:Ca complexes become more populated when only 10 fold excess chelator is added. Furthermore, the significant scan rate dependence suggests that the inactivation is governed by kinetic processes.

Deconvolution of the complex thermograms is not straight forward. However, Shnyrov *et al.* [26;40] have developed a successive annealing procedure, that facilitates the identification of completely or partially irreversible thermal transitions in complex thermograms. The rationale of the procedure is to perform an initial DSC scan and use it to predict the number of transitions and their apparent transition temperatures. Secondly, multiple DSC reheating scans on a new sample are performed. In the first run, the sample is heated to a temperature 1-2 °C higher than the predicted transition temperature of the first transition. Then the sample is cooled to the starting temperature. A second scan is performed up to a temperature slightly higher than the predicted second maximum and the sample is cooled to the starting temperature. Subtraction of the curve obtained in the second scan from that of the first scan makes it possible to single out the front of the first transition. By repeating the procedure successively, it is possible to identify temperatures of all the transitions.

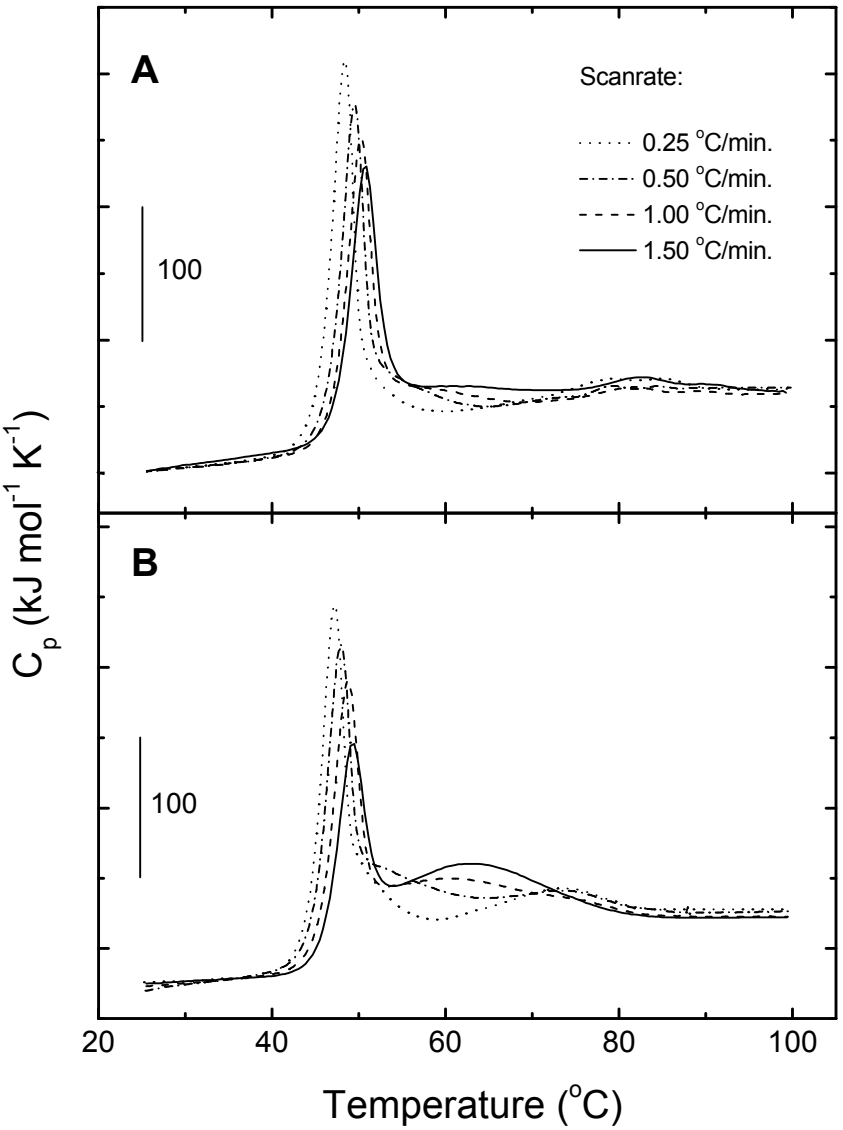

Fig. 4.7: Effect of EGTA on the denaturation of 25 μM BHA in 20 mM borate. pH 8.0 buffer at scan rates from 0.25 – 1.5 °C min^{-1} (see legend). (A) DSC scans in the presence of 1000 μM EGTA. (B) DSC scans in the presence of 250 μM EGTA. A pronounced scan rate dependency is observed in both (A) and (B).

We have applied the successive annealing procedure on BHA in the presence of 10 fold excess EGTA to identify the thermal transitions that contributes to the observed complex thermograms. The result of successive annealing experiments performed at a scan rate of 1.5 °C/min. is illustrated in Fig. 4.8. It is evident that a reversible or partially reversible transition is occurring at 49°C, since the transition can easily be identified in the following reheating scans (Fig. 4.8A). Subtraction of

the successive scans reveals three transitions, with apparent T_m values of respectively 56, 65 and 74°C, which appear to be irreversible (Fig. 4.8B). An analogous successive annealing procedure was performed at a scan rate of 0.5 °C/min. and resulted in similar calorimetric profiles (data not shown). However, the reversible or partially reversible transition occurs at a slightly lower temperature (48°C). The apparent T_m values of the three irreversible transitions decreased to respectively 53, 63 and 72°C at the lower scan rate.

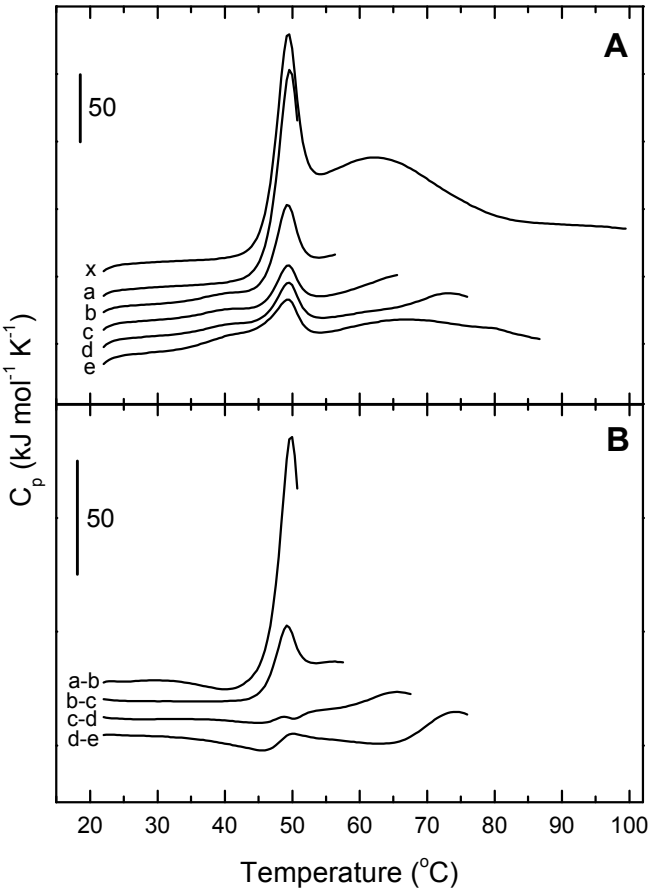

Fig. 4.8: DSC thermogram of 24 μM BHA denaturation in 250 μM EGTA, 20 mM borate, pH 8.0 buffer. (A) DSC scans a-e represent thermograms from repeated heating and subsequent cooling. The scans were stopped at 51 (a), 57 (b), 67 (c), 76 (d) and 87°C (e). Scan x is a full scan up to 115°C. (B) Thermograms obtained by subtraction according to the successive annealing procedure, as described in the text. Thus, the a-b curve is obtained by subtraction of scan b from a. The curves b-c, c-d and d-e have been obtained by similar subtraction. Analysis indicates a reversible or partial reversible transition at about 49°C and 3 irreversible transitions at approximately 56, 65 and 74°C. All experiments were performed at a scan rate of 1.5 °C min^{-1}.

The information from the successive annealing experiments has provided the basis for a crude deconvolution of the thermograms presented in Fig. 4.7B. Thus, we have used the transition temperatures to estimate the heat contribution from each transition process to the total heat of the denaturation process at different scan rates. The thermograms were fitted to a simple model including four Gauss peaks, where the transition temperatures obtained from the annealing experiments were used as fixed parameters during fitting. As illustrated in Fig. 4.9 the multiple Gauss model satisfactorily accounts for the thermogram of BHA in 10 fold excess EGTA at a scan rate of 1.5 °C/min.

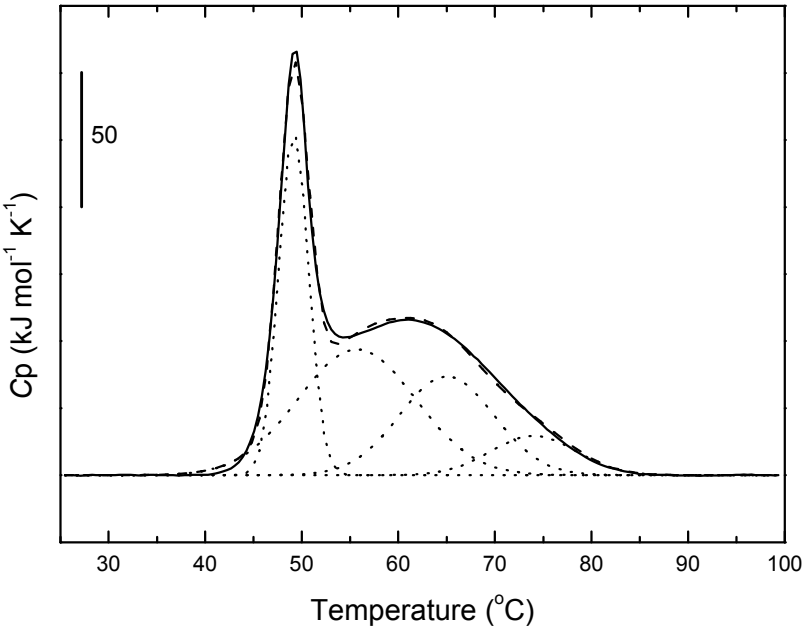

Fig. 4.9: Multiple Gaussian fit of BHA thermogram recorded in the presence of 250 μM EGTA at a scan rate of 1.5 °C min^{-1} (Fig. 4.7A). Deconvolution of the recorded thermogram (solid line), after baseline subtraction, was carried out fitting using a function of 4 Gauss curves (dotted lines). T_m values obtained using successive annealing (Fig. 4.8B) were used as fixed parameters in the fitting process. The cumulative Gauss curve (dashed line) describes the experimental curve satisfactorily. The area under each Gauss curve is listed in Table 4.2 together with the total area under the thermogram.

The area under each Gauss peak was used to estimate of the heat associated with the transitions described above. The area under each Gauss peak should only be regarded as a rough estimate of the heat contribution from the corresponding transition, and that the Gauss deconvolution can not be used to extract molecular

information. This is especially true for the irreversible transitions, where significant distortions of the symmetry of the transition peaks can be expected [25;41]. Similar fitting procedures were applied to the thermograms obtained at scan rates from 0.25 – 1.0 °C/min. Table 4.2 summarizes the estimated heat contributions from each transition and the total heat of denaturation at different scan rates. The total heat of denaturation is approximately 600 kJ/mol lower than the corresponding value obtained without EGTA.

Table 4.2: Estimated heat values of individuel calorimetric transitions of BHA in 10 fold exces EGTA and their apparent transition temperutes.

	Transition 1		Transition 2		Transition 3		Transition 4		
Scanrate °C/min.	Q_1 (kJ mol^{-1})	$T_{max,1}$ (°C)	Q_2 (kJ mol^{-1})	$T_{max,2}$ (°C)	Q_3 (kJ mol^{-1})	$T_{max,3}$ (°C)	Q_4 (kJ mol^{-1})	$T_{max,4}$ (°C)	Q_T (kJ mol^{-1})
0.25	603	47	716	50	94	63	301	72	1714
0.50	584	48	814	53	72	63	278	72	1749
1.00	587	49	821	55	192	64	225	73	1825
1.50	492	49	715	56	453	65	163	74	1823

Fig. 4.10 illustrates the heat contribution from each transition to the total heat of denaturation as a function of scan rate. Apparently, transitions 1, 2 and 4 display a similar scan rate dependence, where the heat contribution is decreased when the scan rate is increased. In contrast, transition 3 shows a reverse scan rate dependence, where the heat contribution is decreased from approximately 25 to 5% at scan rates of respectively 1.5 and 0.25 °C/min. These observations support, as mentioned previously, that kinetic processes are of major importance and that slow equilibrium processes are involved. A simple explanation of the different transition "patterns" observed in the presence of 10 and 40 fold EGTA is that each transition corresponds to denaturation of different BHA:calcium$_X$ populations, where x denotes the number of occupied calcium binding sites. Thus, increasing the EGTA concentration is expected to shift the BHA population towards complexes where fewer calcium binding sites are occupied. This is in agreement with the observation that transitions with the lowest thermal stability become dominant in high concentrations of EGTA (Fig. 4.7).

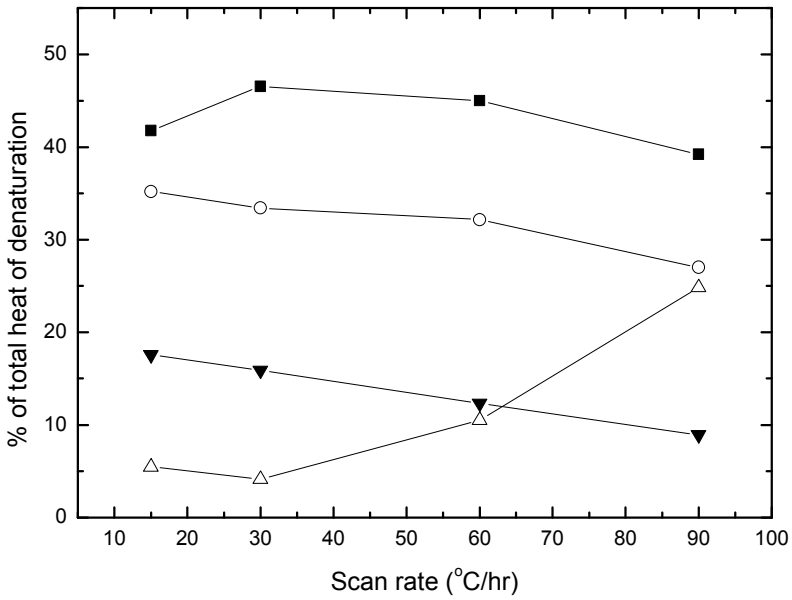

Fig. 4.10: The heat contribution from transition I (open circles), II (filled squares), III (open up triangles) and IV (filled down triangles) to the total heat of denaturation vs. scan rate (Table 4.2). Apparently, the contribution from transition 1, 2 and 4 decreases at higher scan rates. In contrast, transition 4 displays a reverse scan rate dependency.

Previous studies on BAA in excess EGTA have also revealed the significant stabilizing effect of calcium ions. Thus, the apparent T_m is decreased from 86 °C in excess $CaCl_2$ to approximately 40°C in the presence of excess EGTA [32;33]. For BLA the apparent T_m decreased from 103 to 52°C [33]. In line with the present BHA observations, previous DSC experiments with BAA and BLA in excess EGTA revealed that the scan rate has a considerable influence on the apparent T_m values [33]. The observations led the Authors to suggest that an irreversible step during the denaturation process takes place.

4.4.3 A proposed model for BHA denaturation

In search for a mechanistic interpretation of the results, we have included structural observations obtained from homologous *Bacillus* α-amylases. The differences in the three dimensional structures of BLA with and without bound calcium ions provides insight into the role of calcium ions for maintaining the structure of the protein, and in turn the mechanism of the thermal inactivation process. In the

calcium depleted structure significant changes in domain B around the CaI and CaII binding sites are observed, whereas no significant change is observed in the region in proximity to CaIII [10]. These observations have led Machius et al. to propose a disorder-order transition upon calcium binding. The structural observations suggest that it is possible to remove CaIII, but not CaI and CaII, without significant structural changes. A similar disorder-order transition coupled to calcium binding might occur in BHA and could account for the reversible transition, at approximately 49°C, observed in DSC scans of BHA:EDTA solutions (Fig. 4.8). This however, requires that partially calcium depleted BHA is mainly in the folded state below the observed transition temperature. The CD results support this, since only minor changes in the secondary structure of BHA take place upon titration with EDTA up to molar ratios of 10 at room temperature (Fig. 4.3). In addition, we have previously found that titration of BHA with EDTA results in removal of approximately 1.5 calcium ions per BHA molecule [42]. Assuming that BHA contains 3 calcium binding sites the titration results indicate that BHA populations with one and two bound calcium ions are dominant in the presence of moderate excess EGTA. The removal of bound calcium ions does not lead to significant structural changes at temperatures below 40°C and this indicate that partially calcium depleted BHA is mainly in the folded state [37]. Addition of calcium to calcium-free BAA and BLA showed no effect on the catalytic activity at room temperature [33], whereas decreased activity was observed with increasing temperature compared to calcium bound amylase. Therefore Fitter et al. [33] deduced that calcium does not directly effect the catalytic ability but maintains the catalytic activity at higher temperatures due to stabilization of catalytically active structure. These observations are in excellent agreement with the interpretation of the present results as discussed below.

The proposed model for thermal denaturation of BHA and the role of calcium is illustrated in Fig. 4.11 and described below. Based on the preceding discussion we suggest that the reversible transition at 49°C is the reversible unfolding of native BHA with a single calcium site occupied (NCa) into a partially unfolded state (N*Ca), illustrated as transition (I) in Fig. 4.11. The observed irreversible transitions at approximately 53, 63 and 72°C are identified as the result of denaturation of N*Ca, NCa and BHA, with two calcium sites occupied (NCa_2), respectively. In Fig. 4.11 transition II, III and IV correspond to the transitions at 53, 63 and 72°C, respectively. The populations of NCa and NCa_2 are coupled through

a calcium binding equilibrium. These assignments are mainly based on the observed differences between thermograms obtained in 10 and 40 fold excess calcium chelator (Fig. 4.7), where contributions from the transitions at 63 and 72°C become less dominant at high chelator concentration.

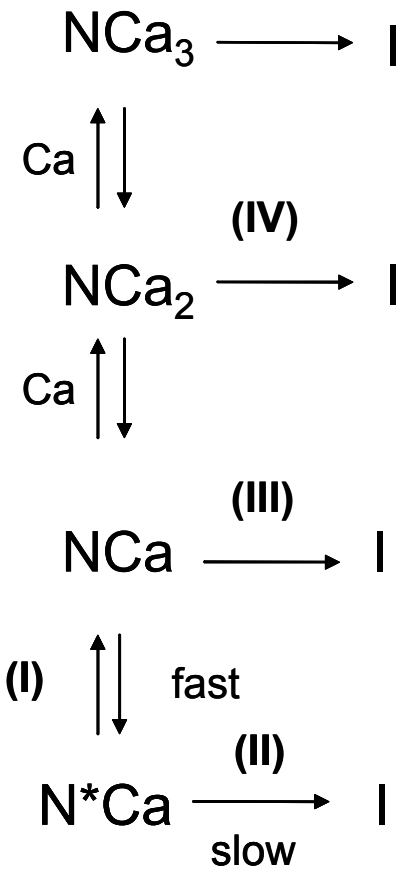

Fig. 4.11: Proposed mechanism for the thermal denaturation of BHA. NCa, NCa_2 and NCa_3 denote different populations of BHA in the native state with 1, 2 and 3 calcium ions bound, respectively. N*Ca denote partially unfolded BHA with a single calcium ion bound. I represent an irreversibly denatured state of BHA. The roman numbers refer to the transitions defined in Table 4.2. Fast and slow refer to the relative rate of transition I and II.

The heat contribution from transition III is increased with the scan rate (Fig. 4.10) as mentioned earlier. This is expected if transition II is a slow process compared to the equilibrium between N*Ca and NCa (transition I). In this case calcium ions released during the irreversible denaturation of N*Ca may shift the equilibrium between N*Ca and NCa towards the last species if the scan rate is high. A previous investigation indicated that irreversible denaturation of partially calcium depleted BHA is a relatively slow process with half-lifes in the order of minutes [37].

Lastly, NCa_2 is in equilibrium with BHA with all calcium sites occupied (NCa_3) which denatures irreversibly at a temperature higher than 80°C (see Fig. 4.2B and 5). Further calcium saturation increases the stability of BHA, but also promotes precipitation of the protein as illustrated in Fig. 4.6.

It is important to point out that the model in Fig. 4.11 is the simplest model that accounts for the thermal denaturation of BHA. In the suggested model, all irreversible transitions are regarded as simple first-order processes. A more realistic description of the irreversible processes includes more steps, in agreement with the Lumry-Eyring model (Eq. (1)). Furthermore, the model does not quantitatively account for the competition between BHA and the chelator for the calcium ions released upon BHA denaturation.

In summary, previous calorimetric studies on α-amylases, typically multi-step reversible models have been applied. However, our data demonstrate that BHA denaturation is kinetically controlled. Therefore, we find that a one-step irreversible model more realistically accounts for the denaturation of BHA. This model should be regarded as a simplification of the actual and more complex denaturation mechanism that possibly involves both reversible and irreversible steps. A plausible explanation of the apparent irreversible denaturation is that refolding is very slow compared to unfolding as discussed by Potekhin & Kovrigin [43]. If this is the case, it is practically impossible to attain equilibrium during the DSC scan, even at very low scan rates. A very slow refolding rate, compared to other *Bacillus* α-amylases, might be characteristic feature of BHA and explain why this α-amylase apparently denatures irreversibly in a one-step process.

The stabilizing effect of calcium is evident from both spectroscopic and calorimetric results. An expected increase in T_m is observed upon addition of excess calcium ions. However, even small amounts of calcium enhance aggregation and indicate a specific role of the metal in the aggregation process. In agreement with previous BAA and BLA observations [32;33], a decrease of about 40°C in the apparent T_m upon addition of excess calcium chelator is observed. The present results support earlier observations [37] that partial stripping of bound calcium ions does not induce major structural changes in BHA at room temperature. Unfolding of BHA in moderate amounts of calcium chelator reveals complex thermograms including both reversible and irreversible transitions, which we have interpreted as unfolding of BHA populations with different degree of calcium

saturated binding sites. Combination of the present observations with structural data on homologous *Bacillus* α-amylases has been utilized to put forward a mechanism for the denaturation of BHA with respect to temperature and calcium activity.

4.5 Acknowledgements

This work was supported by the Danish Academy of Technical Sciences.

4.6 References

1 Vihinen, M. and Mäntsälä, P., Microbial amylolytic enzymes, Crit. Rev. Biochem. Mol. Biol. 24 (1989) 329-418

2 Guzmán-Maldonado, H. and Paredes, L., Amylolytic enzymes and products derived from starch: a review, Crit. Rev. Food. Sci. Nutr. 35 (1995) 373-403

3 Nielsen, J. E. and Borchert, T. V., Protein engineering of bacterial α-amylases, Biochim.Biophys.Acta 1543 (2001) 253-274

4 Kirk, O., Borchert, T. V., and Fuglsang, C. C., Industrial enzyme applications, Curr. Opin. Biotechnol. 13 (2002) 345-351

5 Declerck, N., Machius, M., Joyet, P., Wiegand, G., Huber, R., and Gaillardin, C., Engineering the thermostability of *Bacillus licheniformis* alpha-amylase, Biologica 57 (2002) 203-211

6 Yuuki, T., Nomura, T., Tezuka, H., Tsuboi, A., Yamagata, H., Tsukagoshi, N., and Udaka, S., Complete nucleotide sequence of a gene coding for heat- and pH-stable alpha-amylase of *Bacillus licheniformis*: comparison of the amino acid sequences of three bacterial liquefying alpha-amylases deduced from the DNA sequences, J. Biochem. (Tokyo) 98 (1985) 1147-1156

7 Machius, M., Wiegand, G., and Huber, R., Crystal structure of calcium-depleted *Bacillus licheniformis* alpha-amylase at 2.2 A resolution, J. Mol. Biol. 246 (1995) 545-559

8 Hwang, K. Y., Song, H. K., Chang, C., Lee, J., Lee, S. Y., Kim, K. K., Choe, S., Sweet, R. M., and Suh, S. W., Crystal structure of thermostable alpha-amylase from *Bacillus licheniformis* refined at 1.7 A resolution, Mol. Cells. 7 (1997) 251-258

9 Suvd, D., Fujimoto, Z., Takase, K., Matsumura, M., and Mizuno, H., Crystal structure of *Bacillus stearothermaphilus* alpha- amylase: Possible factors determining the thermostability, J. Biochem. (Tokyo) 129 (2001) 461-468

10 Machius, M., Declerck, N., Huber, R., and Wiegand, G., Activation of *Bacillus licheniformis* alpha-amylase through a disorder - order transition of the substrate-binding site mediated by a calcium-sodium-calcium metal triad, Structure 6 (1998) 281-292

11 Vallee, B. L., Stein, E. A., Sumerwell, W. N., and Fischer, E. H., Metal content of amylases of various origins, J. Biol. Chem. 234 (1959) 2901-2905

12 Violet, M. and Meunier, J. C., Kinetic Study of the irreversible thermal denaturation of *Bacillus licheniformis* alpha amylase, Biochem. J. 263 (1989) 665-670

13 Boel, E., Brady, L., Brzozowski, A. M., Derewenda, Z., Dodson, G. G., Jensen, V. J., Petersen, S. B., Swift, H., Thim, L., and Woldike, H. F., Calcium binding in alpha-amylases: An X-ray diffraction study at 2.1- some resolution of two enzymes from *Aspergillus*, Biochemistry 29 (1990) 6244-6249

14 Levitzki, A. and Steer, M. L., The allosteric activation of mammalian alpha-amylase by chloride, Eur. J. Biochem. 41 (1974) 171-180

15 Declerck, N., Machius, M., Wiegand, G., Huber, R., and Gaillardin, C., Probing structural determinants specifying high thermostability in Bacillus licheniformis alpha-amylase, J. Mol. Biol. 301 (2000) 1041-1057

16 Brzozowski, A. M., Lawson, D. M., Turkenburg, J. P., Bisgaard-Frantzen, H., Svendsen, A., Borchert, T. V., Dauter, Z., Wilson, K. S., and Davies, G. J., Structural analysis of a chimeric bacterial alpha-amylase. High-resolution analysis of native and ligand complexes, Biochemistry 39 (2000) 9099-9107

17 Tomazic, S. J. and Klibanov, A. M., Why is one *Bacillus* alpha-amylase more resistant against irreversible thermoinactivation than another?, J. Biol. Chem. 263 (1988) 3092-3096

18 Tomazic, S. J. and Klibanov, A. M., Mechanisms of irreversible thermal inactivation of *Bacillus* alpha- amylases, J. Biol. Chem. 263 (1988) 3086-3091

19 Lecker, D. N. and Khan, A., Model for inactivation of alpha-amylase in the presence of salts: Theoretical and experimental studies, Biotechnol. Prog. 14 (1998) 621-625

20 Lecker, D. N. and Khan, A., Theoretical and experimental studies of the effects of heat, EDTA, and enzyme concentration on the inactivation rate of alpha-amylase from *Bacillus* sp, Biotechnol. Prog. 12 (1996) 713-717

21 Tanaka, A. and Hoshino, E., Calcium-binding parameter of Bacillus amyloliquefaciens alpha-amylase determined by inactivation kinetics, Biochem. J. 364 (2002) 635-639

22 Bush, D. S., Sticher, L., van Huystee, R., Wagner, D., and Jones, R. L., The calcium requirement for stability and enzymatic activity of two isoforms of barley aleurone alpha-amylase, J. Biol. Chem. 264 (1989) 19392-19398

23 Bisgaard-Frantzen, H., Svendsen, A., Norman, B., Pedersen, S., Kjaerulf, S., Outtrup, H., and Borchert, T. V., Development of industrially important α–amylases, J. Appl. Glycosci. 46 (1999) 199-206

24 Plotnikov, V. V., Brandts, J. M., Lin, L., and Brandts, J. F., A new ultrasensitive scanning calorimeter, Anal. Biochem. 250 (1997) 237-244

25 Sanchez-Ruiz, J. M., Theoretical analysis of Lumry-Eyring models in differential scanning calorimetry, Biophys. J. 61 (1992) 921-935

26 Shnyrov, V. L., Zhadan, G. G., and Akoev, I. G., Calorimetric measurements of the effect of 330-MHz radiofrequency radiation on human erythrocyte ghosts, Bioelectromagnetics 5 (1984) 411-418

27 Khajeh, K., Ranjbar, B., Naderi-Manesh, H., Ebrahim-Habibi, A., and Nemat-Gorgani, M., Chemical modification of bacterial alpha-amylases: changes in tertiary structures and the effect of additional calcium, Biochim. Biophys. Acta 1548 (2001) 229-237

28 Oh, H. S., Kim, K. H., Suh, S. W., and Choi, M., Spectroscopic and electrophoretic studies on structural stability of alpha amylase from *Bacillus-amyloliquefaciens*, Korean Biochem. J. 24 (1991) 158-167

29 Lepock, J. R., Ritchie, K. P., Kolios, M. C., Rodahl, A. M., Heinz, K. A., and Kruuv, J., Influence of transition rates and scan rate on kinetic simulations of differential scanning calorimetry profiles of reversible and irreversible protein denaturation, Biochemistry 31 (1992) 12706-12712

30 Sanchez-Ruiz, J. M., Lopez-Lacomba, J. L., Cortijo, M., and Mateo, P. L., Differential scanning calorimetry of the irreversible thermal denaturation of thermolysin, Biochemistry 27 (1988) 1648-1652

31 Galisteo, M. L., Mateo, P. L., and Sanchez-Ruiz, J. M., Kinetic study on the irreversible thermal denaturation of yeast phosphoglycerate kinase, Biochemistry 30 (1991) 2061-2066

32 Feller, G., D'Amico, D., and Gerday, C., Thermodynamic stability of a cold-active alpha-amylase from the Antarctic bacterium *Alteromonas haloplanctis*, Biochemistry 38 (1999) 4613-4619

33 Fitter, J., Herrmann, R., Dencher, N. A., Blume, A., and Hauss, T., Activity and stability of a thermostable alpha-amylase compared to its mesophilic homologue: Mechanisms of thermal adaptation, Biochemistry 40 (2001) 10723-10731

34 Lumry, R. and Eyring, H., Conformation changes of proteins, J. Phys. Chem. 58 (1954) 110-120

35 Sanchez-Ruiz, J. M., Differential scanning calorimetry of proteins, Subcellular Biochemistry 24 (1995) 133-176

36 Conejero-Lara, F., Sanchez-Ruiz, J. M., Mateo, P. L., Burgos, F. J., Vendrell, J., and Avilés, F. X., Differential scanning calorimetric study of carboxypeptidase B, procarboxypeptidase B and its globular activation domain, Eur. J. Biochem. 200 (1991) 663-670

37 Nielsen, A. D., Fuglsang, C. C., and Westh, P., The effect of calcium ions on the irreversible denaturation of a recombinant *Bacillus halmapalus* α-amylase – a calorimetric investigation, Biochem. J. In press (2003)

38 Brandts, J. F. and Lin, L. N., Study of strong to ultratight protein interactions using differential scanning calorimetry, Biochemistry 29 (1990) 6927-6940

39 Fukada, H., Takahashi, K., and Sturtevant, J. M., Differential scanning calorimetric study of the thermal unfolding of Taka-amylase A from *Aspergillus oryzae*, Biochemistry 26 (1987) 4063-4068

40 Shnyrov, V. L. and Mateo, P. L., Thermal transitions in the purple membrane from Halobacterium halobium, Febs Letter 324 (1993) 237-240

41 Milardi, D., Larosa, C., and Grasso, D., Extended theoretical-analysis of irreversible protein thermal unfolding, Biophys. Chem. 52 (1994) 183-189

42 Nielsen, A. D., Fuglsang, C. C., and Westh, P., Isothermal titration calorimetric procedure to determine protein-metal ion binding parameters in the presence of excess metal ion or chelator, Anal.Biochem. 314 (2003) 227-234

43 Potekhin, S. A. and Kovrigin, E. L., Folding under inequilibrium conditions as a possible reason for partial irreversibility of heat-denatured proteins: Computer simulation study, Biophys. Chem. 73 (1998) 241-248

5

Solubility of *Bacillus halmapalus* α-amylase

5.1 Introduction

The preceding chapters have discussed the calcium binding properties and thermal stability of BHA. In this chapter, the focus is shifted to the solubility of BHA. While perhaps not immediately obvious, the two fields are indeed strongly related both from theoretical and practical points of view. Thus, a common problem observed during the earliest ITC experiments with this protein was precipitation in the calorimeter cell. The precipitation resulted in noisy baselines and precluded in most cases the possibility of extracting any reliable information from the thermograms. This observation initiated a screening phase to identify an optimal buffer and protein concentration to avoid precipitation. The main observations from this work were that removing NaCl and lowering the buffer concentration led to decreased precipitation. Eventually it was found that 20 mM HEPES, pH 8.0 buffer was a suitable buffer in which no significant precipitation was observed when a BHA concentration up to ~3.5 mg/mL was used. Initially the same buffer was used in DSC experiments. However, it turned out that HEPES was not optimal for DSC - since aggregation or precipitation was observed upon heating. Instead a 20 mM borate, pH 8.0 buffer proved to be optimal due to minimal aggregation/-precipitation. A common observation in ITC and DSC experiments was that calcium ions increased the tendency of BHA to aggregate/precipitate whereas calcium chelators had the opposite effect.

The above observations only provide a sporadic insight into the apparently complex solubility properties of BHA and call for systematic experiments to address these properties. Based on the observations from ITC, we have carried out experiments to study the effect of mechanical perturbation on BHA precipitation. Furthermore, we have determined the effect of temperature and $CaCl_2$ on the solubility of BHA. In this respect, we define solubility in the conventional thermodynamic way, i.e. as the concentration where a protein solution is in equilibrium with crystals of the protein (Arakawa and Timasheff, 1985). Other definitions of protein solubility exist in the literature. For example if the

concentration is measured before complete equilibrium is reached or if determined in the presence of amorphous precipitate instead of crystals (Schein, 1990). The solubility of proteins depends on various parameters such as salt, temperature, and pH, and the corresponding solubility diagram is multi-dimensional. Typically, solubility diagrams, i.e. phase diagrams, are presented in two dimensions e.g. protein concentration vs. one of the above parameters, with all other parameters held constant. A schematic illustration of a two-dimensional diagram is presented in Fig. 5.1 and discussed in the following. The diagram can be divided into an undersaturated zone where the protein will never crystallize and an oversaturated zone where crystallization can take place. The solubility curve is defined as the equilibrium soluble concentration in the presence of the solid phase, and the nature of the solid phase (amorphous or crystalline, crystallographic packing) must also be specified. In addition, the supersaturated zone can be subdivided into three zones: (a) a metastable zone where the solution is slightly supersaturated and nucleation does not take place unless a crystal seed is added or the solution is mechanically disturbed. (b) a nucleation zone where protein separates from solution in a crystalline form. (c) a precipitation zone where the protein separates from the solution in an amorphous state (Ries-kautt and Ducruix, 1992).

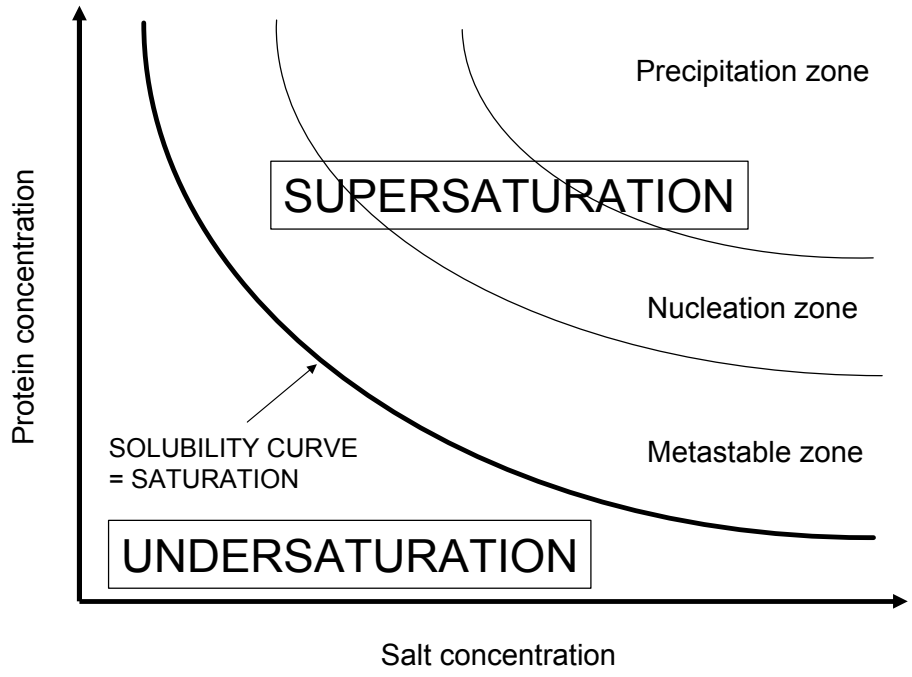

Fig. 5.1: Schematic illustration of a two dimensional solubility diagram where protein and salt concentration are the variables. Redrawn from (Ries-kautt and Ducruix, 1992).

In general, the solubility can be determined either by crystallization of a supersaturated solution or by dissolution of crystals in an undersaturated solution. In both cases, the protein concentration in the liquid phase will converge asymptotically toward the same value when equilibrium is reached, as illustrated in Fig. 5.2. The crystallization/precipitation and dissolution kinetics of proteins are relatively slow which usually makes protein solubility determination a time-consuming task (Howard et al., 1988;Pusey and Munson, 1991). Therefore, the protein must be stable over long time periods and contamination avoided. The difficulties associated with protein crystallization and solubility measurements are probably the main reason for the sparse number of protein solubility diagrams available in the literature. Thus, lysozyme is among the few proteins where a complete phase diagram is currently established (McPherson, 1999).

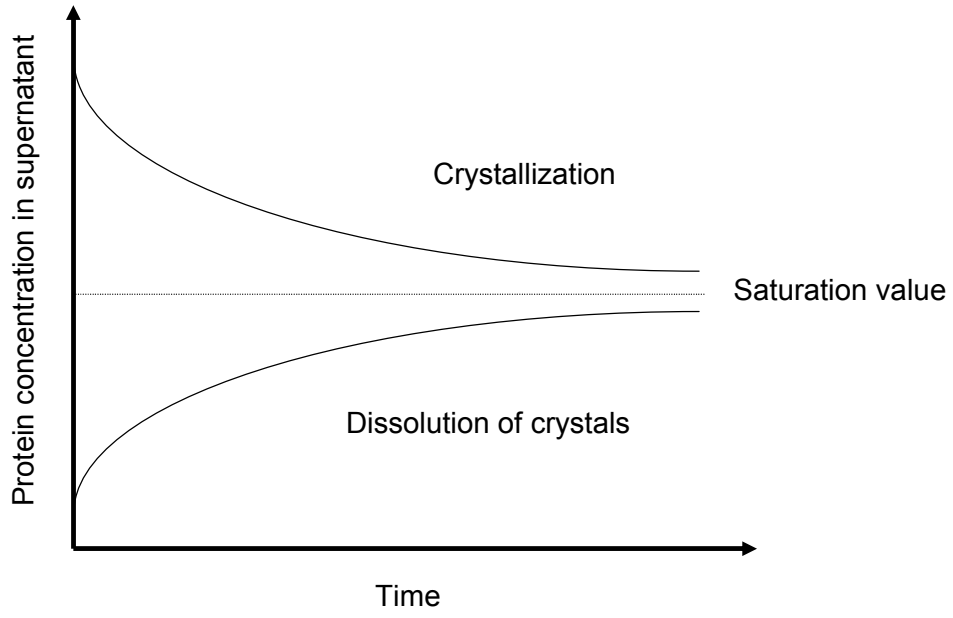

Fig. 5.2: Illustration of the principles used to determine solubility curves. The solubility can be determined either by crystallization of a supersaturated solution or by dissolution of crystals. Near equilibrium, the solubility of using both methods should approach the same saturation value. Redrawn from (Ries-kautt and Ducruix, 1992).

The problems related to determination of solubility diagrams, as discussed above, led to the development of a technique based on protein crystals in columns (Cacioppo et al., 1991;Pusey and Gernert, 1988). This method relies on maximization of the available crystalline surface area and minimization of the

solution volume to be equilibrated (see Fig. 5.3). Thereby, it is possible to obtain fast equilibration times and equilibrium is typically reached in 1-3 days. Using micro-columns as low as milligram quantities of protein crystals are needed (Pusey and Munson, 1991).

The approach in this chapter is mainly empirical compared to the proceeding chapters dealing with thermostability and calcium binding properties of BHA. However, information about the solubility of BHA can be used to obtain a better understanding of the observed aggregation and precipitation during calorimetric experiments. Also, the effect of calcium ions on solubility may be interpreted in terms of BHA-Ca interactions in a somewhat similar way as that applied for the calorimetric binding and stability studies.

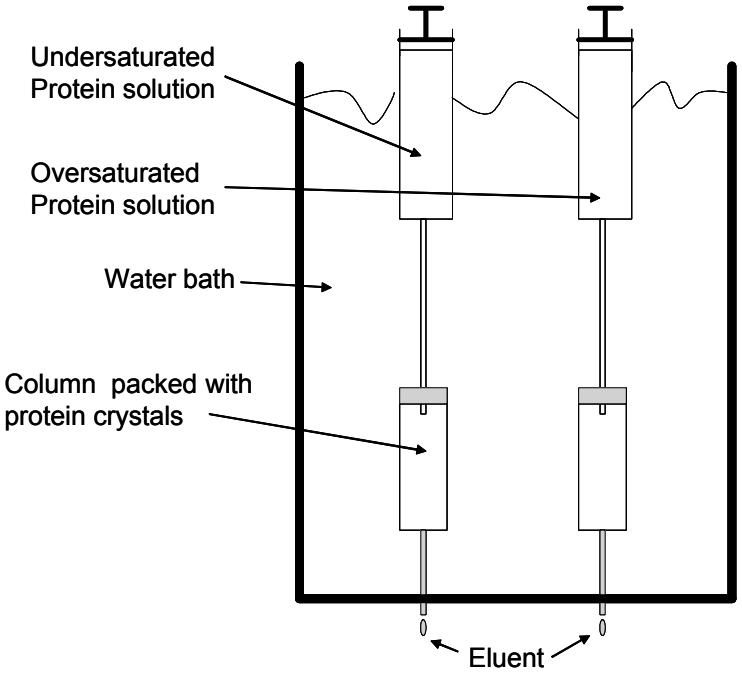

Fig. 5.3: Schematic illustration of the column technique to determine protein solubility. The setup is further discussed in the materials and methods section (5.2.4).

5.2 Materials and methods

5.2.1 Materials

Recombinant BHA was expressed in *Bacillus licheniformis* and purified at Novozymes A/S. The protein was solubilized in milli-Q water by adjusting the pH to ~10.5 with NaOH. Recrystallization was carried by slowly decreasing the pH to ~8 followed by 24-48 h equilibration at 5°C. The crystal slurry was then centrifuged for 30 min. at 11000 RPM and the supernatant discarded. The pellet was kept and further recrystallized 3 times, and a purity >95% was determined by SDS/PAGE. Activity was confirmed using the AMYL α-amylase test kit (Roche, Mannheim, Germany). The assay is based upon formation of p-nitrophenol (PNP) upon α-amylase /α-glucosidase catalyzed cleaving of a blocked PNP-glucose substrate, which can be quantified spectroscopically at 405 nm (Lorentz, 2000). The following chemicals were used: 4-(2-Hydroxyethyl)piperazine-1-ethanesulfonic acid, HEPES (>99.5%, Sigma, St. Louis, MO, USA), calcium chloride, $CaCl_2$ (>99%, Sigma, St. Louis, MO, USA), calcium sulfate, $CaSO_4$ (>99%, Sigma, St. Louis, MO, USA) and calcium acetate, $Ca(CH_3COO)_2$ (>99%, Sigma, St. Louis, MO, USA).

5.2.2 Mechanical stress

The effect of mechanical stress (stirring) on BHA solutions was investigated by turbidity and activity measurements. In a typical experiment, a 10 mL tube containing 4.5 mL 0.5 mg/mL BHA in 20 mM HEPES, 100 mM NaCl, pH 8.0 buffer and a 10 x 3 mm cylindrical stirring bar was placed in a water bath. A constant stirring rate (1300 RPM) and temperature (50°C) was obtained by using Heidolph MR3003 (Heidolph Instruments, Schwabach, Germany) magnetic stirring hotplate with temperature sensor and high precision speed control. As the control experiment another tube, containing an identical BHA solution, was placed in the same water bath, but without a stirring bar. An initial sample was collected at t = 0, and additional samples were collected at specific times during the experiment. The activity in the samples was determined at 25°C using the AMYL α-amylase test kit.

Precipitation in the tubes was determined by visual inspection and by measurements of light transmission at 600 nm.

5.2.3 Protein crystallization

Preliminary crystallization conditions were determined using the Crystal Screen kit from Hampton Research Corp. and crystals were grown in sitting drop Cryschem plates. Batch crystallization of BHA was done by dialysis as described below.
Initially BHA was solubilised in 25 mM HEPES, with 5, 10, 15 and 25 mM $CaCl_2$, buffer by increasing pH to 10.5 with NaOH. The solution passed through a 0.22 μm filter and a protein concentration of 25-50 mg/mL was used. The pH was slowly decreased by dialysis against large volumes of 25 mM HEPES buffer containing 5, 10, 15 or 25 mM $CaCl_2$, at pH 8.0. Crystals were typically formed after 12-24 h dialysis at 37°C. The temperature was slowly decreased to room temperature to minimize the formation of micro-crystals. An estimate of the BHA solubility was obtained by measuring the concentration in the mother liquid. Morphology and size of crystals were determined using microscopy.

5.2.4 Protein solubility

Protein solubility was determined using a micro-column apparatus (Cacioppo et al., 1991;Pusey and Munson, 1991). BHA crystals were packed into 1000 μL columns, with a 1 μm mesh filter attached, as suspensions in the mother liquid until a suitable bed level was reached (~900 μL). The packed columns, mounted in a temperature controlled waterbath, were then equilibrated with BHA solutions made by mixing concentrated protein solution with buffer solution to a final concentration corresponding to the protein concentration in the mother liquid. Equilibration was obtained by passing approximately 10 column volumes of the appropriate protein solution through each column. It was further verified that pH in the eluent was equal to the value of the reservoir. Solubility measurements were initiated after adequate equilibration at a desired temperature. The water bath was kept at the desired temperature for about 48 h prior to the first measurement. Measurements were initiated by replacing the outlet plug of each column with a flow tube. Pressure was applied and the initial ~5 μL eluent was discarded. 15-20 μL samples of eluent collected using a Hamilton syringe and diluted into the

appropriate buffer for protein determination using a J&M Spetropette – TIDAS II (Aalen, Germany). Following sampling, the flow tubes were replaced by outlet plugs and the water bath temperature adjusted 1-3°C. New samples were collected after 24-72 hr equilibration depending on the temperature adjustment. Columns were operated in pairs, with one column having a reservoir of undersaturated solution (typically ~½ of the supersaturated solution) and the other of oversaturated solution of BHA. Thus, the only difference between the reservoir solutions is the concentration of protein. The protein concentration in the under- and oversaturated reservoir solutions was adjusted when the measured values passed below or above the current under- and oversaturated reservoir solution concentrations, respectively. The columns were allowed to equilibrate appropriately upon changes in the reservoir solutions.

5.3 Results

5.3.1 Stirring induced precipitation

Based on the observed precipitation of BHA during the early ITC experiments, as described in the introduction, we tested the effect of stirring on BHA solutions. Experiments were carried out in buffers where heavy precipitation was observed in ITC experiments, e.g. 20 mM HEPES, 100 mM NaCl, pH 8.0. The effect of stirring is clearly illustrated in Fig. 5.4 where a non-stirred and stirred sample is shown. In the stirred sample, heavy precipitation is observed whereas the non-stirred sample remains clear after 24 h.

Fig. 5.5 shows the measured activity vs. time for a stirred and non-stirred sample. In the non-stirred sample almost full activity remains after approximately 21 h at 50°C, whereas only 25% activity remains in the stirred sample. The amount of precipitate in the final samples is illustrated by the light transmission values at 600 nm of 0.01 and 0.52 in the non-stirred and stirred sample, respectively. Preliminary experiments indicated that precipitation could be reduced by lowering the temperature, lowering the salt concentration or addition of non-ionic surfactants.

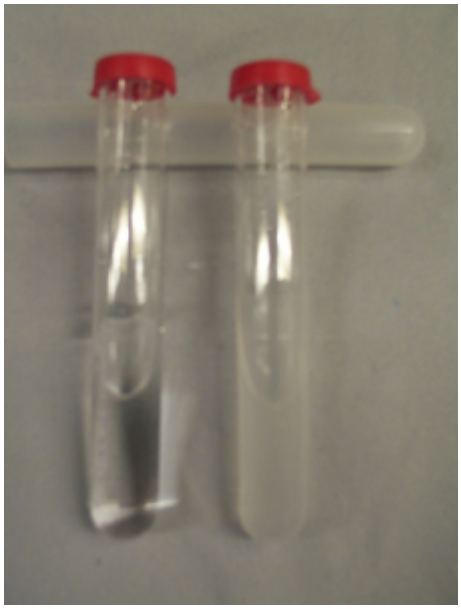

Fig. 5.4: Stirring induced precipitation of 0.5 mg/mL BHA in 20 mM HEPES, 100 mM NaCl, pH 8.0 buffer at 50°C. The left tube contains a non-stirred sample whereas the right tube contains a stirred sample. The picture was taken after 24 h.

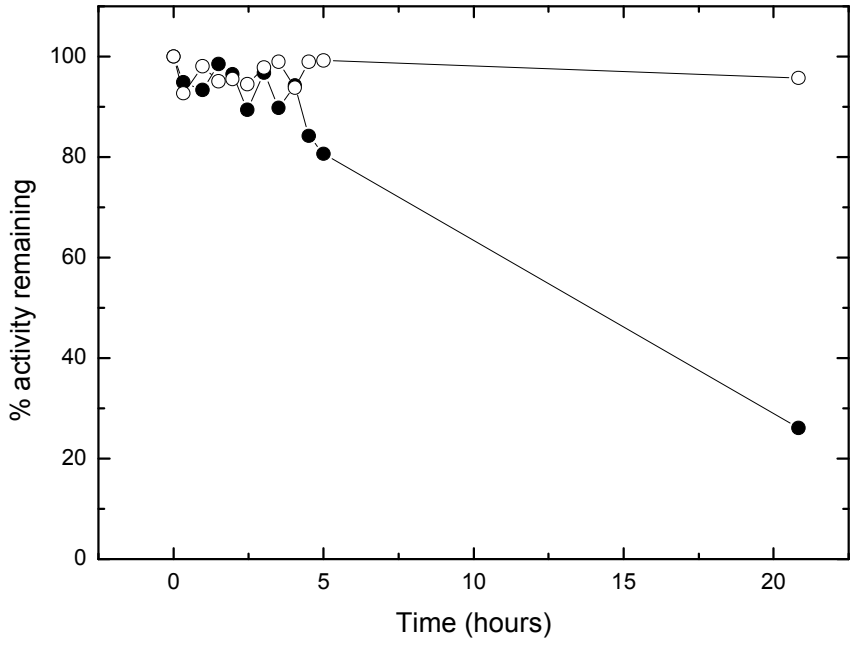

Fig. 5.5: The effect of stirring on the activity of BHA in 0.5 mg/mL BHA in 20 mM HEPES, 100 mM NaCl, pH 8.0 buffer at 50°C. Each data point represents the remaining activity at given times of a non-stirred sample (open circles) and stirred sample (filled circles), respectively.

5.3.2 BHA crystallization

Preliminary screening for crystallization conditions revealed that salt and temperature were among the most important parameters for obtaining suitable crystals for use in the micro-column setup, which requires a crystal size of >10 µm. When batch crystallization, using dialysis, was performed at room temperature, typically mixtures of small rod shaped crystals and amorphous precipitate was observed (Fig. 5.6A). However, when the dialysis was carried out at 37°C large orthorhombic crystals were harvested after 12-24 h (Fig. 5.6B). This procedure even made it possible to obtain large crystals with a maximum length of ~0.7 mm (Fig 5.5C and 5.5D). X-ray analysis indicated that the crystals belonged to the space group P222 (E. Bernhardsdottir & M. van der Woerd, personal communication). Addition of calcium ions in the form of either $CaCl_2$ or $CaSO_4$ apparently increased the rate of crystallization as crystals appeared earlier during dialysis compared to dialysis without added calcium. Attempts to crystallize BHA in the presence of the calcium chelator EDTA failed, indicating that the endogenous bound Ca^{2+} was required for crystallization under these conditions.

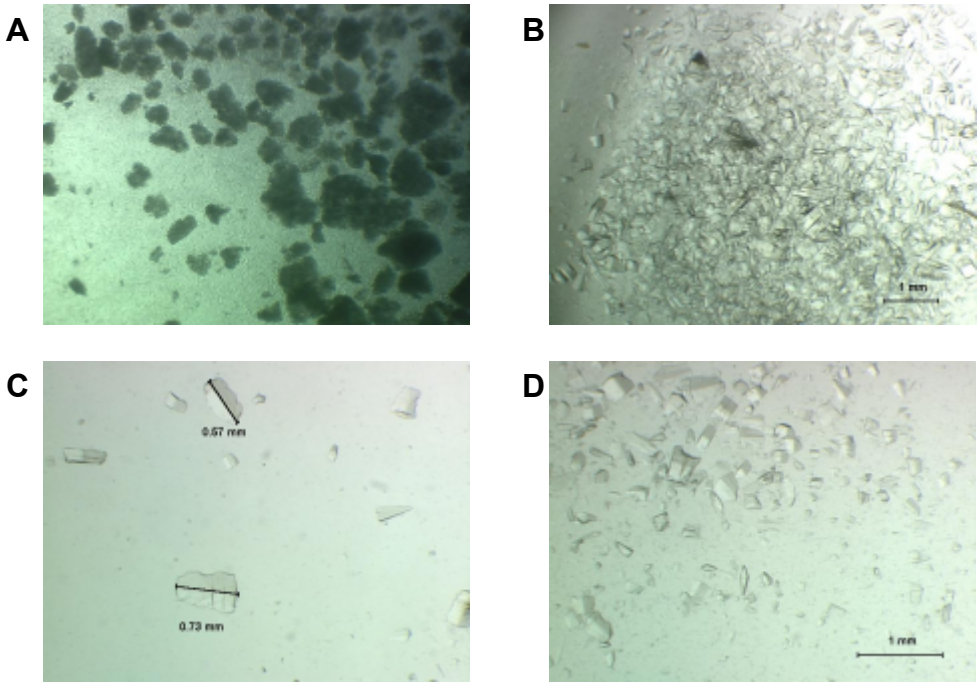

Fig. 5.6: Pictures of BHA crystals and precipitate obtained by macrodialysis in 25 mM HEPES, 15 mM $CaCl_2$, pH 8.0 buffer. (A) Amorphous precipitate and small rod shaped crystals obtained by dialysis at room temperature. (B) Crystals obtained by dialysis at 37°C. (C) and (D) pictures of large crystals obtained at 37°C.

5.3.3 Solubility diagrams

The effect of temperature and $CaCl_2$ on the solubility of BHA was determined using the micro-column technique. In Fig. 5.7 the solubility values obtained by crystallization and dissolution of crystals, in 25 mM HEPES, 10 mM $CaCl_2$, pH 8.0 buffer, is shown. As expected (see Fig. 5.2) the values obtained in the eluent from columns with supersaturated BHA in the reservoir is slightly higher than the corresponding values from columns with undersaturated BHA solution in the reservoir.

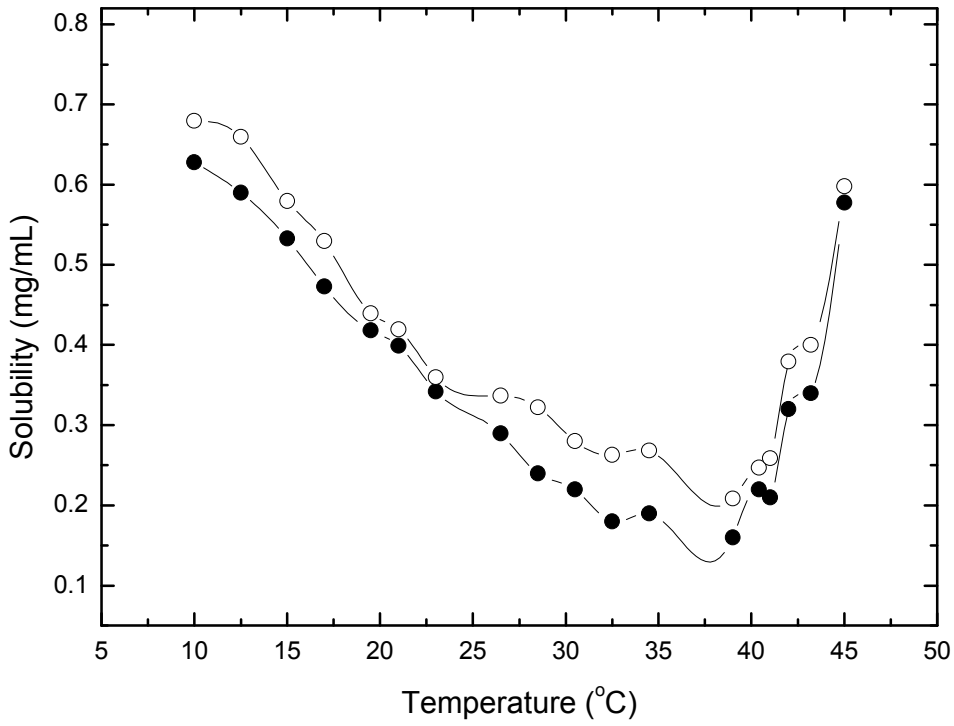

Fig. 5.7: Measured solubility values of BHA in 25 mM HEPES, 10 mM $CaCl_2$, pH 8.0 between 10 and 45°C. Each data point represents the measured solubility at a given temperature in the eluent of columns with either undersaturated (filled circles) or supersaturated BHA solutions (open circles) in the reservoir.

The reasonably small difference between the values obtained from over- and undersaturated columns confirm that equilibrium is nearly reached in the columns. Therefore, we find it justifiable to construct the solubility curve by averaging the curves in Fig. 5.7. The resulting solubility curve is presented in Fig. 5.8 where the average standard deviation is ~11%. Solubility curves in the presence of 5, 15 and

25 mM $CaCl_2$ have been achieved in the same way and are also presented in Fig. 5.8. Retrograde solubility is observed at temperatures below ~30°C whereas normal solubility behavior, i.e. increasing with temperature, is observed at higher temperatures. The lowest solubility, corresponding to ~0.2 mg/mL, is observed in the range from 30-40°C. The solubility increases to 0.6-0.7 mg/mL near the boundaries of the temperature range. Apparently, $CaCl_2$ in the range 5-25 mM has little effect on the solubility of BHA and no systematic correlation can be deduced. Furthermore, the anion of the calcium salt does not seem to have a major effect on the solubility as illustrated in Fig. 5.9 where the solubility diagrams of BHA in 10 mM $CaCl_2$, $CaSO_4$ and CaAc are presented.

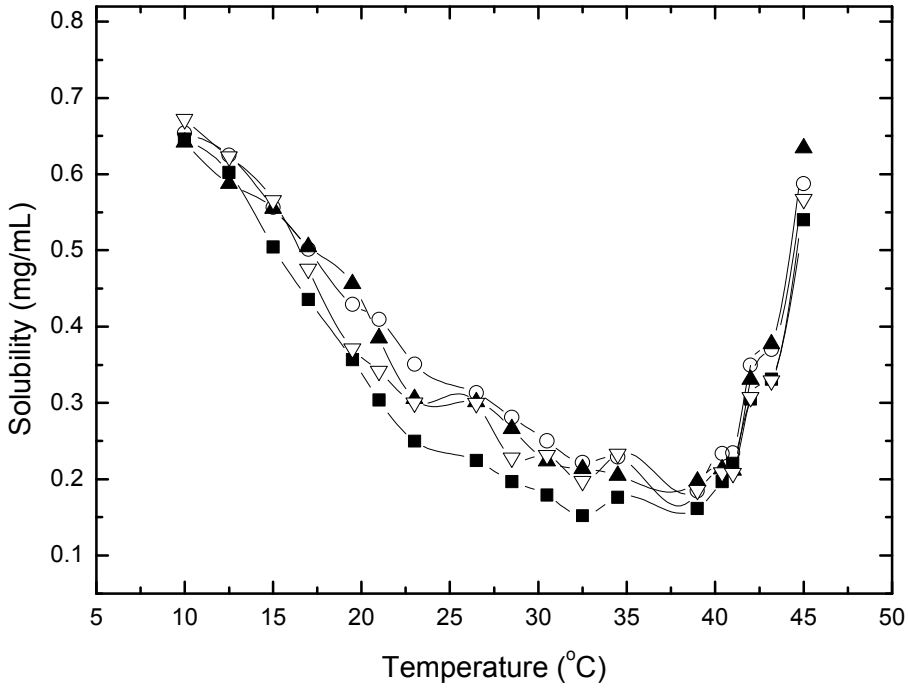

Fig. 5.8: Solubility diagrams of BHA in 25 mM HEPES, pH 8.0 buffer with 5 (filled squares), 10 (open circles), 15 (filled up triangles) and 25 mM $CaCl_2$ (open down triangles). Each solubility curve is obtained by averaging the solubility curves obtained from pairs of under- and supersaturated columns (see Fig. 5.7).

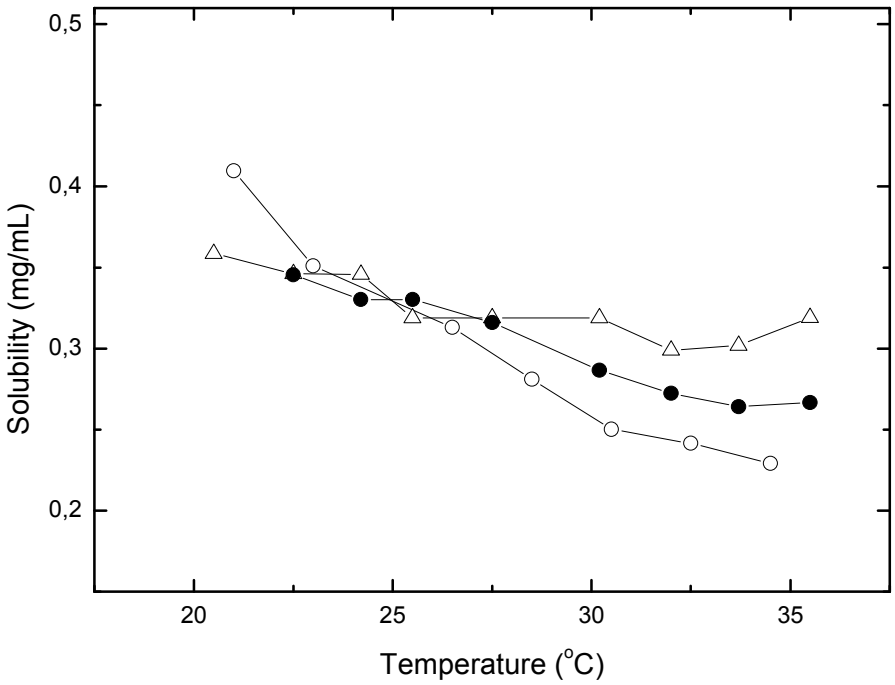

Fig. 5.9: Solubility diagrams of BHA in 25 mM HEPES, pH 8.0 buffer with 10 mM $CaCl_2$ (open circles), $CaSO_4$ (filled circles) and $Ca(CH_3COO)_2$ (open up triangles). The solubility curve is obtained by averaging the solubility curves obtained from pairs of under- and supersaturated columns.

5.4 Discussion

The two main features of the BHA solubility curves are the low solubility and retrograde solubility behavior over the temperature range from 10 to ~30°C. Literature describing the solubility properties of α-amylases is scarce. However, the crystal morphology and solubility of Taka-amylase A have been studied recently (Ninomiya et al., 2001). Amylase crystals were obtained using ammonium sulfate or PEG-8000 as precipitant and several different crystal morphologies were observed, including orthorhombic $P2_12_12_1$ crystals. The solubility of crystals obtained in the presence of ammonium sulfate displayed large temperature dependence, with a solubility of 5 and 120 mg/mL at -1°C and 10°C, respectively. The temperature dependence was significantly smaller for the PEG-form crystals where the solubility varied from ~5 to ~40 mg/mL over the temperature range 3-32°C. A direct comparison of the Taka-amylase A results with the present BHA

data is not feasible as the crystals have been obtained in very different environments, but apparently the solubility of Taka-amylase A is considerably higher than BHA. In addition, no retrograde solubility behavior is observed for Taka-amylase. However, retrograde solubility behavior has been reported for other proteins including concanavalin A (Cacioppo and Pusey, 1992), bovine chymotrypsinogen A (Cacioppo et al., 1991) and horse serum albumin (Rosenberger et al., 1993).

The apparent effect of calcium ions on the crystallization rate is not reflected in the solubility of BHA, since no major decrease in solubility is observed upon increasing the calcium concentration. This suggests that calcium ions promote aggregation of BHA monomers in solution, which increases the tendency to nucleate without significant changing the solubility. In this respect, it is worth mentioning the observations from DSC experiments where even small amounts of $CaCl_2$ increased aggregation of BHA near the denaturation temperature (Nielsen et al., 2003). This led to the suggestion that calcium ions may act as "bridging" atoms between denatured or partially denatured BHA molecules.

The very low solubility observed for BHA provides a plausible explanation of the observed stirring induced precipitation, since the protein concentration used in the experiments is close to values obtained from the solubility diagrams. Hence, BHA may be slightly supersaturated and in the metastable zone (Fig. 5.1) where mechanical disturbances can induce nucleation. If that is the case one might expect the precipitate to be (micro)crystalline rather than amorphous precipitate, but this was not further investigated. However, it is important to note that the stirring experiments were performed in the presence of 100 mM NaCl and at 50°C, where the actual solubility is not known. The reduced precipitation upon removal of NaCl or addition of non-ionic surfactants indicates that hydrophobic interactions are involved. In this respect it is interesting to note that the parent organism, *Bacillus halmapalus*, is very salt intolerant and no growth has been observed in the presence of 5% NaCl (Nielsen et al., 1995). However, it is not known if the low salt tolerance of the recombinant *Bacillus halmapalus* α-amylase used in the present study originates from the parent organism. Irreversible inactivation due to stirring induced aggregation and precipitation has previously been reported for lysozyme (Caussette et al., 1997;Colombie et al., 2000). Aggregation was observed at concentrations as low as 0.1 mg/mL (in water at 25°C), which is far below the expected solubility of the protein (Cacioppo et al., 1991). Thus, mechanical

disturbance of supersaturated solutions does not provide a likely explanation for the observed aggregation. Instead it was suggested that stirring increased collisions between inactive and active molecules which induce inactivation of the latter and leads to aggregation (Colombie et al., 2000).

In summary, it was found that the solubility of BHA is very low. One implication of the low solubility is that even a 1 mg/mL solution of BHA is possibly supersaturated. Therefore, the observed stirring induced precipitation is most likely the result of mechanical disturbance of a metastable BHA solution. Added calcium ions did not seem to have a major effect on the solubility. However, they apparently enhance the rate of crystallization, possibly by promoting bridging interactions between BHA monomers. In order to fully understand the effect of calcium ions on the solubility of BHA further experimental information is needed. Thus, the calcium concentration range used in this study (5-25 mM) must be extended to include concentrations of at least one order of magnitude higher. In addition, the solubility diagram of BHA without calcium ions is wanted, but crystallization of BHA under these conditions proved to be difficult.

The solubility in other buffers may be used to address the apparent differences between e.g. HEPES and borate buffer as discussed in the introduction. The apparent differences between the buffers may be associated to their different abilities to interact with calcium ions. Thus, borate is known to form weak complexes with calcium ions (for example, ref. (Simonson et al., 1988)). Future solubility determinations of BHA should also include activity measurements to verify that activity is maintained over the prolonged periods required to obtain solubility curves.

6

Closing remarks

The intention of this final chapter is to highlight and discus topics, which are general to the experimental work of this Thesis. Thermodynamic fingerprinting is the first topic to be discussed in relation to the microcalorimetric methodology used. This is followed by discussion of the effect of calcium ions on stability and solubility properties of BHA. Finally, the denaturation mechanisms presented in chapter 3 and 4 are compared and their applicability discussed.

6.1 Thermodynamic fingerprinting

A central theme in the present Thesis is characterization of proteins by means of thermodynamic "fingerprints". We utilize that heat is either generated or absorbed in every chemical process. Thus, each process has a distinct "fingerprint" that depend on the system and the conditions under which the process takes place. In principle, it is therefore possible to resolve multiple processes in a single experimental trial. This however requires that the fingerprint of each underlying process can be identified and that they are sufficiently different. Calorimetry has several distinct advantages in this context. First, the technique is non-invasive and directly measures the *in vitro* activity without the use of modified substrates, spectral probes etc. Secondly, the unspecific nature of the technique makes it "blind" to the presence of non-reacting compounds (which is rarely the case for spectroscopic methods) and consequently applicable to samples of low purity. Thirdly, the technique is not dependent on the physical form of the sample, i.e. the sample may be liquid, solid or a two-phase combination. The main drawback of microcalorimetry on the other hand is the relatively limited time resolution, compared to e.g. spectroscopic methods, and that the calorimetric data does not provide structural information. Therefore, a molecular interpretation typically requires structural information obtained by other techniques.

The use of the thermodynamic fingerprinting concept and microcalorimetry is clearly illustrated in several chapters in this Thesis. In chapter 2 we make use of the significant differences between the binding enthalpies and affinities of calcium chelators and an α-amylase to characterize the calcium binding properties of a recombinant *Bacillus halmapalus* α-amylase (BHA). Chapter 3 describes the denaturation of BHA upon calcium removal and relies on several different fingerprints. Firstly, the considerable difference in thermal stability between BHA with and without calcium ions, which provide a temperature window where the denaturation can be controlled by the concentration of calcium ions. Secondly, the enthalpic difference between binding of calcium ions and denaturation of BHA, where the processes are exothermic and endothermic, respectively. Furthermore, the kinetics of the processes are very different. In chapter 4 the complex thermograms of BHA in the presence of calcium chelator are the result multiple transitions, where each transition, or fingerprint, originate from a specific population of BHA:Ca complexes.

The potential of the thermodynamic fingerprinting concept in combination with microcalorimetry is also illustrated by the following examples. Connelly et al. (2002) have developed a technology where microcalorimetry is used to identify the activities of proteins of unknown function. The rationale behind the technique is that heat evolved from an enzymatic reaction is generally large compared to non-specific interactions and mixing enthalpies and therefore easy to identify calorimetrically. By injection of potential substrates into crude bacterial lysates any enzymatic turnover is detected. During the purification process, the same procedure is used to identify which fractions, possible containing numerous proteins, contains the enzyme with activity.

Another example is provided by the work of Gaisford *et al.* (1999) on the applicability of microcalorimetry to study complex reaction schemes with consecutive processes. Thus, acid catalyzed hydrolysis of potassium hydroxylamine trisulfonate, a reaction that proceeds as a three-step, consecutive mechanism, was investigated using isothermal microcalorimetry. It was possible to obtain rate constants and enthalpies of each reaction step by fitting the thermograms to a relevant model. Significant differences between the enthalpy changes of each reaction step were observed, corresponding to both endothermic and exothermic processes.

Finally, in a previous microcalorimetric study of the interactions between surfactants and bovine serum albumin (BSA) we found that it is possible, in some cases, to identify both binding and micellization in the same experimental trial. Thus, upon isothermal calorimetric titration of BSA with nonionic surfactants (e.g. hepta(ethylene glycol) monododecyl ether) a biphasic thermogram was obtained corresponding to initial binding of surfactant to the protein followed by formation of surfactant micelles (Nielsen et al., 2000).

Identification and use of thermodynamic fingerprints have a great potential to expand the applicability of microcalorimetric methods in analysis of complex or multi-component systems. The applicability is limited by the availability of relevant procedures and models to extract thermodynamic information. Clearly, further research is necessary to extend the applicability of the concept.

6.2 Calcium – Friend or Foe

Elucidation of the role of calcium ions on the stability and solubility of BHA has been an important scope of this study. Therefore, the most important findings of the preceding chapters are summarized and put into perspective in the following.
Binding of calcium to specific sites on BHA have an immense effect on the thermal stability of the enzyme. This is clearly illustrated by the difference in the apparent denaturation temperature of ~45°C between BHA in the presence of excess calcium chelator or calcium ions. However, calcium does seem to enhance the tendency of BHA to aggregate, since precipitation and the rate of crystallization are increased upon addition of calcium ions. Furthermore, aggregation of BHA near the denaturation temperature is increased upon addition of calcium ions. This suggests that calcium ions may act as a "bridge" between BHA monomers, in a partially unfolded state, and thus provide basis for formation of aggregates. In contrast, no significant effect of calcium ions on the solubility was discovered.

The aggregating effect of calcium is probably only a concern in supersaturated solutions of BHA. In this context, it is relevant to point out that the solubility of BHA is very low under the experimental conditions in this study and therefore even a 1 mg/mL solution is possibly supersaturated. Aggregation due to the presence of calcium ions is not expected to be a problem under application conditions where the enzyme concentrations are typically very low. On the other hand, it might be advantageous to use low concentrations of calcium during

production and purification where highly concentrated BHA solutions may be encountered. This however requires that the temperature is kept low to maintain a stable enzyme.

6.3 Mechanisms of denaturation

At first, the suggested denaturation mechanism in chapter 3 and 4 might appear to contradict each other. It is believed that this is not the case. Instead, the model in chapter 3 should be regarded as a simplified version of the more complex mechanism derived on the basis of a more comprehensive data set in chapter 4. In the first model only two populations of native BHA are considered, i.e. calcium depleted and saturated BHA (probably BHA:Ca_3). In this context BHA is not completely stripped, as indicated by the titration experiments with calcium chelator, but probably contains one bound calcium ion. Therefore, this model should only be applied to systems dominated by BHA with one calcium ion bound or all sites saturated. Obviously the model also applies for a situation where only these two populations exist, but this seem rather unlikely since other BHA:Ca populations is expected to be present. The model presented in chapter 4 encompasses the BHA populations with varying degree of saturated binding sites and the relevant calcium binding equilibriums between the populations. Therefore, this model can be applied to more realistic systems in which different BHA:Ca populations coexist, like in the presence of moderate amounts of calcium chelator.

An advantage of using the simpler model in chapter 3 is that fewer parameters are involved. As a consequence, relatively little information is necessary when the model is needed to e.g. estimate the effect of the calcium concentration on the kinetic stability or how an increased calcium affinity contributes to the stability. A relevant question in this perspective is how the estimated kinetic stability correlates with the actual stability determined by activity measurements. This however has not been tested in present study, but is essential in the further evaluation of the validity of the model and its application to industrial use of α-amylases. Similar estimates of BHA stability in relation to calcium ions and temperature is more complicated when the model in chapter 4 is used, since a lot more parameters are involved and difficult to obtain experimentally.

7

Literature cited

The list only includes references cited in chapters 1, 5 and 6.

Arakawa,T., R.Bhat, and S.N.Timasheff. 1990. Preferential interactions determine protein solubility in three-component solutions: the $MgCl_2$ system. *Biochemistry* 29:1914-1923.

Arakawa,T. and S.N.Timasheff. 1985. Theory of protein solubility. *Methods Enzymol.* 114:49-77.

Baldwin,R.L. 1996. How hofmeister ion interactions affect protein stability. *Biophys. J.* 71:2056-2063.

Bertoldo,C. and G.Antranikian. 2001. Amylolytic enzymes from hyperthermophiles. *Methods Enzymol.* 330:269-289.

Bisgaard-Frantzen,H., A.Svendsen, B.Norman, S.Pedersen, S.Kjaerulf, H.Outtrup, and T.V.Borchert. 1999. Development of industrially important α–amylases. *J. Appl. Glycosci.* 46:199-206.

Boel,E., L.Brady, A.M.Brzozowski, Z.Derewenda, G.G.Dodson, V.J.Jensen, S.B.Petersen, H.Swift, L.Thim, and H.F.Woldike. 1990. Calcium binding in alpha-amylases: An X-ray diffraction study at 2.1- some resolution of two enzymes from *Aspergillus*. *Biochemistry* 29:6244-6249.

Braxton,S. and J.A.Wells. 1992. Incorporation of a stabilizing Ca(2+)-binding loop into subtilisin BPN'. *Biochemistry* 31:7796-7801.

Brzozowski,A.M., D.M.Lawson, J.P.Turkenburg, H.Bisgaard-Frantzen, A.Svendsen, T.V.Borchert, Z.Dauter, K.S.Wilson, and G.J.Davies. 2000. Structural analysis of a chimeric bacterial alpha-amylase. High-resolution analysis of native and ligand complexes. *Biochemistry* 39:9099-9107.

Bush,D.S., L.Sticher, R.van Huystee, D.Wagner, and R.L.Jones. 1989. The calcium requirement for stability and enzymatic activity of two isoforms of *barley aleurone* alpha-amylase. *J. Biol. Chem.* 264:19392-19398.

Cacioppo,E., S.Munson, and M.L.Pusey. 1991. Protein solubilities determined by a rapid technique and modification of that technique to a micromethod. *J. Cryst. Growth* 110:66-71.

Cacioppo,E. and M.L.Pusey. 1992. The effects of acid treatment and calcium ions on the solubility of concanavalin A. *J. Cryst. Growth* 122:208-212.

Caussette,M., H.Planche, S.Delepine, P.Monsan, A.Gaunand, and B.Lindet. 1997. The self catalytic enzyme inactivation induced by solvent stirring: A new example of protein conformational change induction. *Protein Eng.* 10:1235-1240.

Colombie,S., A.Gaunand, M.Rinaudo, and B.Lindet. 2000. Irreversible lysozyme inactivation and aggregation induced by stirring: kinetic study and aggregates characterisation. *Biotechnol. Lett.* 22:277-283.

Connelly, G. P., Connelly, P. R., Bruzzese, F. J., Ali, J. A., and Faerman, C. 2002 Employing isothermal titration calorimetry to identify novel targets for drug discovery. 85th CSC Conference & Exhibition. Vancouver, June 1-5.

Declerck,N., M.Machius, P.Joyet, G.Wiegand, R.Huber, and C.Gaillardin. 2002. Engineering the thermostability of *Bacillus licheniformis* alpha-amylase. *Biologica* 57:203-211.

Declerck,N., M.Machius, G.Wiegand, R.Huber, and C.Gaillardin. 2000. Probing structural determinants specifying high thermostability in *Bacillus licheniformis* alpha-amylase. *J. Mol. Biol.* 301:1041-1057.

Gaisford,S., A.K.Hills, A.E.Beezer, and J.C.Mitchell. 1999. Thermodynamic and kinetic analysis of isothermal microcalorimetric data: applications to consecutive reaction schemes. *Thermochim. Acta* 328:39-45.

Guzmán-Maldonado,H. and L.Paredes. 1995. Amylolytic enzymes and products derived from starch: a review. *Crit. Rev. Food. Sci. Nutr.* 35:373-403.

Hendrix,T., Y.V.Griko, and P.L.Privalov. 2000. A calorimetric study of the influence of calcium on the stability of bovine alpha-lactalbumin. *Biophys. Chem.* 84:27-34.

Howard,S.B., P.J.Twigg, J.K.Baird, and E.J.Meehan. 1988. The solubility of hen egg-white lysozyme. *J. Cryst. Growth* 90:94-104.

Hwang,K.Y., H.K.Song, C.Chang, J.Lee, S.Y.Lee, K.K.Kim, S.Choe, R.M.Sweet, and S.W.Suh. 1997. Crystal structure of thermostable alpha-amylase from *Bacillus licheniformis* refined at 1.7 A resolution. *Mol. Cells* 7:251-258.

Kirk,O., T.V.Borchert, and C.C.Fuglsang. 2002. Industrial enzyme applications. *Curr. Opin. Biotechnol.* 13:345-351.

Kuroki,R., Y.Taniyama, C.Seko, H.Nakamura, M.Kikuchi, and M.Ikehara. 1989. Design and creation of a Ca^{2+} binding site in human lysozyme to enhance structural stability. *Proc. Natl. Acad. Sci. U S A* 86:6903-6907.

Kuroki,R. and K.Yutani. 1998. Structural and thermodynamic responses of mutations at a Ca^{2+} binding site engineered into human lysozyme. *J. Biol. Chem.* 273:34310-34315.

Lecker,D.N. and A.Khan. 1996. Theoretical and experimental studies of the effects of heat, EDTA, and enzyme concentration on the inactivation rate of alpha-amylase from *Bacillus* sp. *Biotechnol. Prog.* 12:713-717.

Lecker,D.N. and A.Khan. 1998. Model for inactivation of alpha-amylase in the presence of salts: Theoretical and experimental studies. *Biotechnol. Prog.* 14:621-625.

Levitzki,A. and M.L.Steer. 1974. The allosteric activation of mammalian alpha-amylase by chloride. *Eur J Biochem* 41:171-180.

Lorentz,K. 2000. Routine alpha-amylase assay using protected 4-nitrophenyl- 1,4-alpha-D-maltoheptaoside and a novel alpha-glucosidase. *Clin. Chem.* 46:644-649.

Machius,M., N.Declerck, R.Huber, and G.Wiegand. 1998. Activation of *Bacillus licheniformis* alpha-amylase through a disorder - order transition of the substrate-binding site mediated by a calcium-sodium-calcium metal triad. *Structure (London)* 6:281-292.

Machius,M., G.Wiegand, and R.Huber. 1995. Crystal structure of calcium-depleted *Bacillus licheniformis* alpha-amylase at 2.2 A resolution. *J. Mol. Biol.* 246:545-559.

Marrs,B., S.Delagrave, and D.Murphy. 1999. Novel approaches for discovering industrial enzymes. *Curr. Opin. Microbiol.* 2:241-245.

McPherson,A. 1999. Some physical and energetic principles. *In* Crystallization of biological macromolecules. Cold Spring Harbor Laboratory Press, New York. 127-158.

Muheim,A., R.J.Todd, D.R.Casimiro, H.B.Gray, and F.H.Arnold. 1993. Ruthenium-mediated protein cross-linking and stabilization. *J. Am. Chem. Soc.* 115:5312-5313.

Muller,H.N. and A.Skerra. 1994. Grafting of a high-affinity Zn(II)-binding site on the beta- barrel of retinol-binding protein results in enhanced folding stability and enables simplified purification. *Biochemistry* 33:14126-14135.

Niehaus,F., C.Bertoldo, M.Kaehler, and G.Antranikian. 1999. Extremophiles as a source of novel enzymes for industrial application. *App. Microbiol. Biotechnol.* 51:711-729.

Nielsen,A.D., K.Borch, and P.Westh. 2000. Thermochemistry of the specific binding of C12 surfactants to bovine serum albumin. *Biochim. Biophys. Acta* 1479:321-331.

Nielsen,A.D., M.L.Pusey, C.C.Fuglsang, and P.Westh. 2003. A proposed mechanism for the thermal denaturation of a recombinant *Bacillus halmapalus* -amylase – the effect of calcium ions. *Biochim. Biophys. Acta* Submitted.

Nielsen,P., D.Fritze, and F.G.Priest. 1995. Phenetic diversity of alkaliphilic *Bacillus* strains: Proposal for nine new species. *Microbiology* 141:1745-1761.

Ninomiya,K., T.Yamamoto, T.Oheda, K.Sato, G.Sazaki, and Y.Matsuura. 2001. Morphology and solubility of multiple crystal forms of Taka- amylase A. *J. Cryst. Growth* 222:311-316.

Pusey,M.L. and K.Gernert. 1988. A method for rapid liquid-solid phase solubility measurements using the protein lysozyme. *J. Cryst. Growth* 88:419-424.

Pusey,M.L. and S.Munson. 1991. Micro-apparatus for rapid determination of protein solubilities. *J. Cryst. Growth* 113:385-389.

Ries-kautt,M. and A.Ducruix. 1992. Phase diagrams. *In* Crystallization of nucleic acids and proteins: a pratical approach. A.Ducruix and R.Giegé, editors. Oxford University Press, Oxford. 195-218.

Rosenberger,F., S.B.Howard, J.W.Sowers, and T.A.Nyce. 1993. Temperature-dependence of protein solubility - determination and application to crystallization in x-ray capillaries. *J. Cryst. Growth* 129:1-12.

Schein,C.H. 1990. Solubility as a function of protein structure and solvent components. *Biotechnology (N Y)* 8:308-317.

Simonson,J.M., R.N.Roy, D.Mrad, P.Lord, L.N.Roy, and D.A.Johnson. 1988. The thermodynamics of aqueous borate solutions .2. mixtures of boric-acid with calcium or magnesium borate and chloride. *J. Solution Chem.* 17:435-446.

Suvd,D., Z.Fujimoto, K.Takase, M.Matsumura, and H.Mizuno. 2001. Crystal structure of *Bacillus stearothermaphilus* alpha- amylase: Possible factors determining the thermostability. *J Biochem (Tokyo)* 129:461-468.

Tanaka,A. and E.Hoshino. 2002. Calcium-binding parameter of *Bacillus amyloliquefaciens* alpha-amylase determined by inactivation kinetics. *Biochem. J.* 364:635-639.

Timasheff,S.N. 1998. Control of protein stability and reactions by weakly interacting cosolvents: The simplicity of the complicated. *Adv. Protein Chem.* 51:355-432.

Tomazic,S.J. and A.M.Klibanov. 1988a. Mechanisms of irreversible thermal inactivation of *Bacillus* alpha- amylases. *J. Biol. Chem.* 263:3086-3091.

Tomazic,S.J. and A.M.Klibanov. 1988b. Why is one *Bacillus* alpha-amylase more resistant against irreversible thermoinactivation than another? *J. Biol. Chem.* 263:3092-3096.

Vallee,B.L., E.A.Stein, W.N.Sumerwell, and E.H.Fischer. 1959. Metal content of amylases of various origins. *J. Biol. Chem.* 234:2901-2905 .

van der Maarel,M., B.van der Veen, J.C.Uitdehaag, H.Leemhuis, and L.Dijkhuizen. 2002. Properties and applications of starch-converting enzymes of the alpha-amylase family. *J. Biotechnol.* 94:137-155.

Vihinen,M. and P.Mäntsälä. 1989. Microbial amylolytic enzymes. *Crit Rev Biochem. Mol. Biol.* 24:329-418.

Violet,M. and J.C.Meunier. 1989. Kinetic study of the irreversible thermal denaturation of *Bacillus-licheniformis* alpha amylase. *Biochem. J.* 263:665-670.

Yuuki,T., T.Nomura, H.Tezuka, A.Tsuboi, H.Yamagata, N.Tsukagoshi, and S.Udaka. 1985. Complete nucleotide sequence of a gene coding for heat- and pH-stable alpha-amylase of *Bacillus licheniformis*: comparison of the amino acid sequences of three bacterial liquefying alpha-amylases deduced from the DNA sequences. *J Biochem (Tokyo)* 98:1147-1156.